Doctoral Thesis

Development of a User-Centered Virtual Liver Surgery System for Preoperative Liver Surgery Planning

Xiaopeng Yang

Department of Industrial and Management Engineering

Pohang University of Science and Technology

2014

간해부 수술 계획 지원을 위한
인간공학적 가상 간 수술 시스템 개발

Development of a User-Centered Virtual Liver Surgery System for Preoperative Liver Surgery Planning

Development of a User-Centered Virtual Liver Surgery System for Preoperative Liver Surgery Planning

by

Xiaopeng Yang
Department of Industrial and Management Engineering
(Human Factors and Ergonomics Program)
Pohang University of Science and Technology

A dissertation submitted to the faculty of the Pohang University of Science and Technology in partial fulfillment of the requirements for the degree of Doctor of Philosophy in the department of Industrial and Management Engineering
(Human Factors and Ergonomics Program)

Pohang, Korea
12. 20. 2013
Approved by
Heecheon You (Signature)
Academic Advisor

Development of a User-Centered Virtual Liver Surgery System for Preoperative Liver Surgery Planning

Xiaopeng Yang

The undersigned have examined this dissertation and hereby certify that it is worthy of acceptance for a doctoral degree from POSTECH.

12/20/2013

Committee Chair	Heecheon You	(Seal)
Member	Euiho Suh	(Seal)
Member	Hyunbo Cho	(Seal)
Member	Seungyong Lee	(Seal)
Member	Baik Hwan Cho	(Seal)

DMIE 20081030 Xiaopeng Yang, Development of a User-Centered Virtual Liver Surgery System for Preoperative Liver Surgery Planning, 간해부 수술 계획 지원을 위한 인간공학적 가상 간 수술 시스템, Department of Industrial and Management Engineering (Human Factors and Ergonomics Program), 2014, 82P, Advisor: Heecheon You, Text in English.

ABSTRACT

This study developed a user-centered 3D liver surgery planning system, called *Dr. Liver*, to support liver surgery planning in a clinical environment for safe and rational liver surgery. The currently available virtual surgery systems need to be customized to liver surgery and improved for better usability and time efficiency. This study established use scenarios of *Dr. Liver* through literature review, benchmarking, and interviews with surgeons. The use scenarios consist of high level tasks including liver extraction, vessel extraction, tumor extraction, liver segmentation, and liver surgery planning and low level tasks to accomplish the high level tasks. Based on the use scenarios, detailed user interfaces were designed and image processing algorithms were developed. For better usability, *Dr. Liver* provides various user-friendly features such as procedure status indication and color coding, 3D view indication box and resetting buttons for easier 3D object manipulation, and hotkey menus appearing on the screen to decrease users' cognitive workload.

This study developed a hybrid semi-automatic method to extract the liver from abdominal computerized tomography (CT) images. The proposed hybrid method consists of a customized fast-marching level-set method for detection of an optimal initial liver region from multiple seed points selected by the user and a threshold-based level-set method for extraction of the actual liver region based on the initial liver region. The performance of the hybrid method was compared with those of the 2D region growing method implemented in OsiriX using abdominal CT datasets of 15 patients. The hybrid method showed a significantly higher accuracy in liver extraction (similarity index, SI = 97.6% ± 0.5%; false positive error, FPE = 2.2% ± 0.7%; false negative error, FNE = 2.5% ± 0.8%; average symmetric surface distance, ASD = 1.4 ± 0.5 mm) than the 2D (SI = 94.0% ± 1.9%; FPE = 5.3% ± 1.1%; FNE = 6.5% ± 3.7%; ASD = 6.7 ± 3.8 mm) region growing method. The total liver extraction time per CT dataset of the hybrid method (77 ± 10 sec) is significantly less than the 2D region growing method (575 ± 136 sec). The interaction time per CT dataset between the user and a computer of the hybrid method (28 ± 4 sec) is significantly

shorter than the 2D region growing method (484 ± 126 sec). The proposed hybrid method was found preferred for liver segmentation in preoperative virtual liver surgery planning.

This study developed an interactive method for efficient liver vessel extraction from abdominal CT images. The proposed interactive liver extraction method consists of (1) pre-processing of CT images in which multiple phases of abdominal CT images are denoised, registered, and masked with the extracted liver region, (2) selection of multiple seed points, (3) identification of multiple threshold intervals based on the intensity values of the selected seed points, (4) vessel segmentation with identified threshold intervals using region growing method, (5) display of multiple segmentation results for the user to select an appropriate segmentation result, and (6) interactive editing of the extracted vessel trees if necessary. The performance of the interactive method was accessed by an expert radiologist using 15 abdominal CT datasets. No false positive errors were found in the extracted vessel branches. False negative errors were identified at some distal branches of the vessel tree due to small diameter and low contrast. No connections among the extracted portal vein, hepatic vein, and hepatic artery were found in the 15 segmented datasets. A 7-point Likert scale was used for assessment of suitability for liver surgery planning, '1' for very poor and '7' for very good. The average (± S.D.) score of suitability for liver surgery planning was 6.4 (± 0.7). The interaction time and total vessel extraction time were 33 (± 4) sec and 75 (± 8) sec respectively. The proposed interactive liver extraction method was found suitable for clinical application such as liver surgery planning.

Ergonomic usability tests consisting of a preliminary test and a main test were conducted at different system development stages of *Dr. Liver*. While the preliminary usability test conducted at an early system development stage helped developers to identify potential usability problems of *Dr. Liver* and produce recommendations to resolve the problems, the main usability test verified the improvement of the usability of *Dr. Liver*. The usability of *Dr. Liver* was evaluated using a comprehensive set of performance (completion time, similarity index, false positive error, false negative error, number of mouse clicks, and number of keystrokes) and preference (usefulness, ease of use, learnability, informativeness, clarity, tolerance, and overall satisfaction) measures. Ten male medical doctors (aged from 30s to 60s; experienced in liver anatomy and liver surgery) from five different medical centers participated in the main usability test, consisting of five test modules. The system received a high score of satisfaction (mean = 6.2, S.D. = 0.7) as measured using a 7-point Likert scale throughout the five test modules. The present study will help practitioners evaluate the usability of a system and identify potential usability problems in a systematic manner.

TABLE OF CONTENTS

LIST OF FIGURES

LIST OF TABLES

Chapter 1. INTRODUCTION

1.1. Problem Statement

A 3D virtual liver surgery (VLS) planning system can provide surgeons with an effective tool for safe and rational surgery. The safety of major liver resection can be predicted by relative residual liver volume (%RLV), the ratio of residual to total functional liver volume (TFLV = entire liver volume – tumor volume). For example, Schindl et al. (2005) identified that postoperative serious hepatic dysfunction is likely to occur if %RLV < 26.6% based on an ROC analysis for 104 patients with normal synthetic liver function. Ferrero et al. (2007) also reported that hepatectomy can be considered safe if %RLV > 26.5% for patients with healthy liver and %RLV >31% for those with impaired liver function based on an analysis of 119 cases. A rational surgery, which requires the determination of the proper location, orientation, and shape of a cutting plane on the liver, can be planned by localizing a tumor(s) in relation to the three liver vascular trees (portal vein, hepatic vein, and hepatic artery). To support a safe and rational liver surgery, as shown in Figure 1.1, a 3D VLS planning system needs to provide not only visual information of the location and size of a tumor, the structure of the liver vasculature, and the segments of the liver, but also quantitative information of the volumes of the liver, remnant, and/or graft (Debarba et al., 2010; Reitinger et al., 2006; Sorantin et al., 2008).

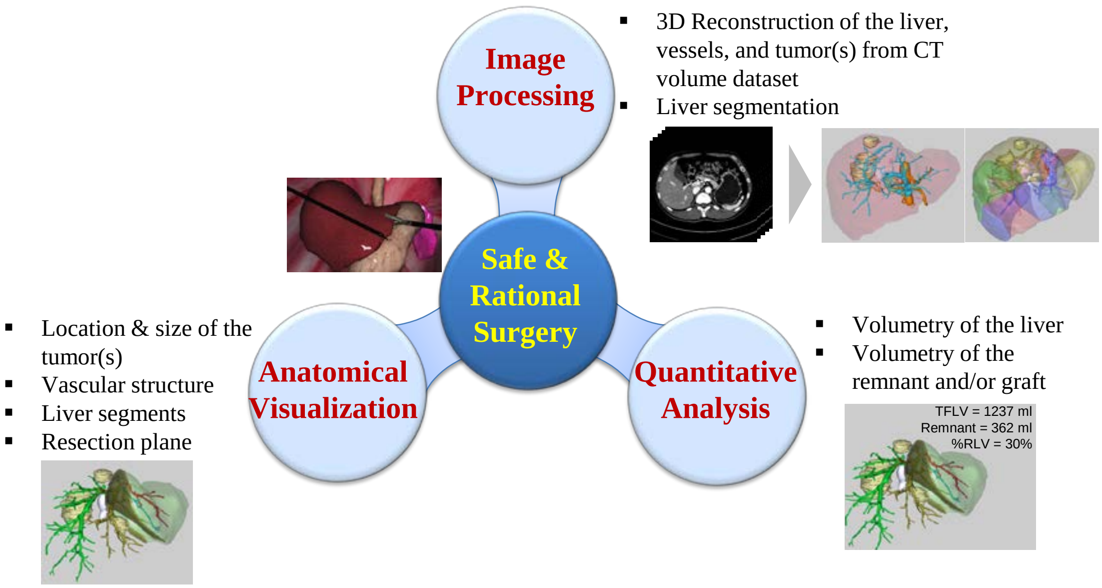

Figure 1.1. Information provided by a liver surgery planning system for safe and rational surgery

Most existing virtual surgery systems such as Rapidia (Infinitt Co., Ltd, South Korea), Voxar 3D (TOSHIBA Co., Japan), Syngovia (SIEMENS Co., Germany), and OsriX (Pixmeo Co., Switzerland) do not provide functions specialized to liver surgery planning. Thus, these generic virtual surgery systems have a significantly limited utility to surgeons for pre-operative liver surgery planning. For example, the manual or semi-automatic liver extraction of a generic virtual surgery system is quite cumbersome and time demanding (> 30 min.) to the user. Furthermore, functions of identification of liver segments and planning of liver surgery are not provided in the generic virtual surgery systems.

Several specialized systems to liver surgery such as LiverAnalyzer™ (MeVis Medical Solutions AG, Germany) and Synapse Vincent™ (FUJIFILM Co., Japan) have been developed, but their user interfaces and algorithms need to be improved for better usability and time efficiency. LiverAnalyzer is not for sale, but is known to have capabilities of segmentation of the liver, vessels, biliary system, and tumors, volumetry of the remnant and/or graft, evaluation of vascular territories, and surgery planning. Only a distant web service is available for LiverAnalyzer—CT images are sent to Mevis Medical Solutions AG and then a liver analysis report is delivered within one day or two depending on the selected payment option. The liver analysis report is viewed by LiverViewer, provided by the company free of charge; however, LiverViewer shows only analysis results without presenting CT images so that surgeons have difficulty to cross-check the accuracy of the analysis results. In contrast, Synapse Vincent is for sale and supports liver extraction, vessel analysis, liver segmentation, volumetry, and surgery planning. However, some user interfaces and algorithms of Synapse Vincent such as those for liver extraction and vessel extraction from CT images are cumbersome to use. For example, the region growing method used by Synapse Vincent for liver extraction often extracts adjacent tissues and/or organs along with the liver, which leads to intensive manual editing to remove the parts inaccurately extracted.

The LV of a patient can be estimated by regression and image processing approaches, which have their own strengths and weaknesses in terms of ease of use, efficiency, and accuracy. The regression method uses a regression equation which explains the statistical relationship between LV and anthropometric dimensions such as height and weight for LV estimation (Heinemann et al., 1999; Urata et al., 1995; Yu et al., 2004). The regression method is simple and easy to use, but sacrifices accuracy in LV estimation. Yu et al. (2004) reported that the standard deviation of LV estimation error ranged from 275.4 to 289.4 ml when various LV regression equations were applied to 652 Korean cases. On the other hand, the image processing approach measures a patient's LV with liver images extracted from the patient's abdominal CT images by using image processing software such as Rapidia (Infinitt Co., Ltd., South Korea), Voxar 3D (Toshiba Co., Japan), Syngovia (Siemens Co., Germany), and OsiriX (Pixmeo Co., Switzerland). The image processing approach is more time demanding for liver extraction but more accurate in LV estimation than the regression approach.

Various automatic and semi-automatic methods have been developed to improve the performance of the image processing approach in liver extraction in terms of time efficiency and accuracy. Automatic liver extraction methods identify the boundary of the liver using a morphological image processing method (Jiang and Cheng, 2009) or a histogram analysis of CT image intensity data (Ruskó et al., 2007; Massoptier and Casciaro, 2008). However, the automatic methods commonly sacrifice the accuracy of liver extraction because their algorithm cannot completely distinguish the liver from the neighboring organs due to the similarity of image intensity between the organs (Lee et al., 2007). Ruskó et al. (2007) reported that their automatic liver extraction method based on a histogram analysis resulted in an average overlap accuracy of 89.3% with an average processing time of 56 sec per CT dataset with a thickness of 1 to 3 mm on a computer with an Intel Pentium 4 CPU 3GHz processor. Li et al. (2012) proposed an automatic liver segmentation method using probabilistic atlas and reported an average overlap accuracy of 92.9% for low-contrast CT images. On the other hand, semi-automatic methods consist of interactive identification of seed points or regions and extraction of the liver boundary from the selected seed points or regions (Dawant et al., 2007; Hermoye et al., 2005). Dawant et al. (2007) proposed a semi-automatic liver extraction method which took 10 min for manual extraction of the liver on 20 to 30 CT slices seleced with an approximately equal interal from a CT dataset and 10 min for extraction of the rest of the liver using a level-set method and an interpolation method on a computer with a Pentium D 3.2 GHz processor and 2GB of memory, resulting in an average overlap accuracy of 90.2% for 10 CT datasets with a thickness of 1 to 3 mm.

Analysis of liver blood vessels including their structures, diameters, and variations is of vital interest for preoperative liver surgery planning. The complex liver anatomy structures consisting of pipeline systems of hepatic artery, portal vein, hepatic vein, and bile duct and their variations result in the complexity, difficulty, and risk of liver surgery. A comprehensive surgery plan should be prepared in consideration of vascular structures and anatomical relationship between the lesion and the adjacent vasculature to ensure a safe and rational liver resection (Meinzer et al., 2002; Radtke et al., 2007; Satou et al., 2007).

Conventional vessel extraction approches are grouped into semi-automatic and fully automatic methods. Semi-automatic extraction methods segment the targeted structures starting from selected seed points or regions by iteratively adding adjacent structures that satisfy certain segmentation criteria. Selle et al. (2002) applied a region growing method to segment liver vessels with automatically adjusted thresholds, but their method has difficuties in segmenting small vessels (Esneault et al., 2010). Yi and Ra (2003) proposed a locally adaptive region growing method to segment vessel trees, in which locally adaptive analysis was repeatedly performed throughout the whole image to idenfity small vessels and therefore not efficient. Lorigo et al. (2001) applied a level-set method to vessel segmentation with an initialization and a speed function. Fully automatic methods segment the targeted structures based on statistical histogram analysis or local shape descriptors such as tube detection filters without a requirement of an initialization. Soler et al. (2001) estimated thresholds based on the intensity histogram to extract vessels with a morphological closing step and then remove false branches by analyzing the skeletonized vessl structures. Eidheim et al. (2004) used a matched filter to enhance vessel structures and then the generic algorithm for globally searching the most likely vasculatures. Their method took one hour to finish vessel extraction and thus inefficient. The conventional semi-automatic and fully automatic methods have difficulties in dealing with local disturbances such as low contrast or connected structures with similar intensity values (Bauer et al., 2010). To overcome the limitations of the conventional methods, Esneault et al. (2010) applied Boykov's graph cuts alrorithm to segment liver vessels, claiming that the portal vein and hepatic vein were naturally separated well in their experiments. Bauer et al. (2010) proposed a two-step mehtod to separate and segment interwoven tubular tree structures, identification of tubular object and grouping different tree structres followed by graph cuts for segmentation. However, the efficiency of their method was not evaluated which is important in practical clinical application such as liver surgery planning.

1.2. Research Objectives

The present study is aimed at (1) development of a user-centered virtual liver surgery system, (2) development and evaluation of a hybrid liver extraction method, (3) development of an interactive vessel extraction method, and (4) usability testing of the virtual liver surgery system (Figure 1.2).

The first objective of this study (Figure 1.3) is aimed at developing a user-centered 3D virtual liver surgery planning system, called *Dr. Liver*. The proposed system provides user interfaces and algorithms specialized in liver surgery for surgeons to obtain information necessary for preoperative liver surgery planning within a reasonable time (< 30 min) by using intuitive and user-friendly interfaces. A use scenario for *Dr. Liver* was established. User interfaces with novel features such as a procedural diagram and a procedure status color coding scheme were designed. Novel algorithms were developed and implemented into *Dr. Liver*.

The second objective of this study is aimed at developing a semi-automatic liver extraction method for better accuracy and time efficiency. This sutdy proposed a hybrid liver extraction method which optimally incorporates a customized fast marching level-set method and a threshold-based level-set method to maximize the accuracy and time efficiency of liver extraction from abdominal CT

Development of a user-centered virtual liver surgery system

(1) Use scenario development
(2) User interface design
(3) Image processing algorithms development and implementation

↓

Development and evaluation of a hybrid liver extraction method

(1) Development of a novel hybrid method for liver extraction which optimally incorporates a customized fast-marching level-set method and a threshold-based level-set method
(2) Performance evaluation of the proposed method

↓

Development of a semi-automatic vessel extraction method

(1) Development of an interactive procedure for liver vessel extraction using region growing method
(2) Performance evaluation of the proposed method

↓

Usability testing of the proposed virtual liver surgery system

(1) Usability testing of the virtual liver surgery planning system using quantitative and qualitative measures

Figure 1.2. Research objectives

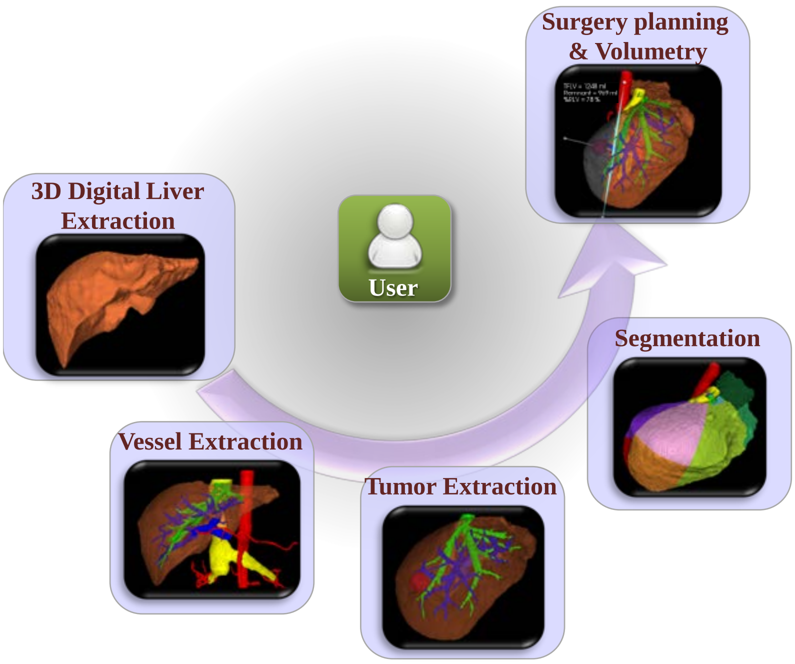

Figure 1.3. Research objective: development of a user-centered virtual liver surgery planning system

images of the portal venous phase. The accuracy and time efficiency of the proposed hybrid semi-automatic method for liver segmentation were compared with those of the 2D region growing method implemented in OsiriX (Pixmeo Co., Switzerland). The liver regions manually extracted by a radiologist using Rapidia (Infinitt Co., Ltd., South Korea) were considered as the gold standard for accuracy evaluation. Furthermore, an onsite evaluation of the proposed hybrid method was performed using the public database provided by the SLiver Grand Challenge of the MICCAI 2007 workshop (Heimann et al., 2009).

The third objective of this study is to develop an interactive vessel extraction method based on a region growing method. Firstly, multiple-phase abdominal CT images were denoised, registered, and masked using the extracted liver region. Secondly, multiple threshold intervals were identified based on the average value and standard deviation of intensity values of selected multiple seed points. Thirdly, multiple vessel trees were extracted based on the identified multiple threshold intervals using a region growing method. Lastly, a user-friendly interface was used for the user to select an appropriately segmented vessel tree among the multiple candidates. The accuracy and time efficiency of the proposed interactive vessel extraction method were evaluated using 15 abdominal CT data sets.

The last objective of this study is to test the usability of the proposed virtual liver surgery planning system. Surgeons from different hospitals, including university hospitals who are experts in liver anatomy and liver surgery were recruited for usability testing. Quantitative measures, including accuracy, task completion time, and number of key and mouse strokes were used for performance evaluation. A 7-scale subjective rating technique was used to indicate the preference of the users to the usability of the proposed virtual liver surgery system.

1.3. Significance of the Study

This study has four significant theoretical and practical aspects. First, the user-centered 3D virtual liver surgery planning system developed in this study can be used for pre-operative surgical planning for liver transplantation and liver tumor resection. The hierarchical user interface developed in the present study based on users' needs and desires provides good usability which facilitates the surgical planning procedure.

Second, the hybrid method for liver extraction proposed in this study overcomes the limitations of the existing liver extraction methods. The new method can generate optimal initial liver regions from multiple seed points selected from four to five CT slices and then propagate the initial liver regions to reach the actual liver boundary. The new method (similarity index, SI = 97.6% ±

0.5%; false positive error, FPE = 2.2% ± 0.7%; false negative error, FNE = 2.5% ± 0.8%; average symmetric surface distance, ASD = 1.4 ± 0.5 mm; Liver extraction time/CT data set = 77 ± 10 sec) achieved higher accuracy and time efficiency than the 2D region growing method (SI = 94.0% ± 1.9%; FPE = 5.3% ± 1.1%; FNE = 6.5% ± 3.7%; ASD = 6.7 ± 3.8 mm; Liver extraction time/CT data set = 575 ± 136 sec).

Third, the novel interactive vessel extraction method proposed in this study avoids the cumbersome repetitions of vessel extraction to find a proper threshold interval in the existing methods by providing multiple threshold intervals identified from selected multiple seed points. In addition, the new method avoids a false extraction of other vessels and organs using masked CT images by the extracted liver region instead of original CT images. The proposed method achieved a satisfactory accuracy (FPE: 0/15 CT data sets; FNE: 2/15 CT data sets; Suitability for liver surgery planning: 6.4 ± 0.7 based on a 7-scale subjective rating technique) and high efficiency (Total vessel extraction time/CT data set = 54 ± 4 sec) in vessel extraction.

Lastly, use of various performance/preference measures, observations, and open suggestions in the usability testing facilitates the identification of potential usability problems of the proposed virtual liver surgery planning system. The usability testing techniques are applicable to any system design and development process to identify potential usability problems.

1.4. Organization of the Dissertation

This dissertation consists of eight chapters. Chapter 1 briefly introduced the background, objectives, and significance of this study. Chapter 2 reviewed previous studies related to the present research including journal articles and commercialized virtual surgery systems. Chapter 3 introduced the development of a user-centered virtual liver surgery system including use scenario identification, customized user interface design, and image processing algorithms development and implementation. Chapter 4 developed and evaluated a hybrid semi-automatic liver extraction method. Chapter 5 developed and evaluated an efficient interactive vessel extraction method. Chapter 6 evaluated the usability of the proposed virtual liver surgery planning system. Chapter 7 addressed a discussion regarding to the contributions and significance of this study. The last chapter concluded with contributions of the present study and further research issues.

Chapter 2. LITERATURE REVIEW

2.1. User-Centered Design

2.1.1. Introduction

User-centered design (UCD) is a term which describes a design process in which users are involved to influence how a design takes shape. The users can be involved during requirements gathering and usability testing. The users can also have a deep impact on the design by being involved as partners with designers through the design process (Abras et al., 2005).

Seven principles of UCD have been suggested by Norman (1988):

1. Use both knowledge in the world and knowledge in the head. By building conceptual models, write manuals that are easily understood and that are written before the design is implemented.
2. Simplify the structure of tasks. Make sure not to overload the short-term memory, or the long-term memory of the user. On average, the user is able to remember five things at a time. Make sure the task in consistent and provide mental aids for easy retrieval of information from long-term memory. Make sure the user has control over the task.
3. Make things visible: bridge the gulfs of Execution and Evaluation. The user should be able to figure out the use of an object by seeing the right buttons or devices for executing an operation.
4. Get the mappings right. One way to make things understandable is to use graphics.
5. Exploit the power of constraints, both natural and artificial, in order to give the user the feel that there is one thing to do.
6. Design for error. Plan for any possible error that can be made, this way the user will be allowed the option of recovery from any possible error made.
7. When all else fails, standardize. Create an international standard if something cannot be designed without arbitrary mappings.

The same basic concepts have been adapted and popularized by Nielsen (1993; 2001) to produce heuristics for usability engineering.

A full exploration of users’ needs and desires is stressed by Norman’s work. The involvement of users in a design lead to more effective, efficient, and safer products and contributed to the acceptance and success of a product (Preece et al., 2002).

2.1.2. Involvement of Users in System Design

Preece et al. (2002) suggested ways to involve users in the design and development of a system (Table 2.1). At the beginning of the design project, tasks and needs analyses are performed to identify users' needs. Design alternatives of simple paper and pencil drawings are developed and evaluated by the users to understand the intended purposes of the system and gain additional information about user needs and expectations. Then at the mid-point of the design cycle prototypes can be developed and tested. This stage is crucial since the evaluation by the users helps identify measurable usability criteria related to the effectiveness, efficiency, safety, usability, learnability, memorability of the system and user's subjective satisfaction with the system. Lastly, at the final stage of the design cycle usability testing is conducted with the refined system to collect quantitative data related to measurable usability criteria and qualitative data related to user satisfaction.

Table 2.1. Involvement of users in system design

Technique	Purpose	Stage of the Design Cycle
Background Interviews and questionnaires	Collecting data related to the needs and expectations of users; evaluation of design alternatives, prototypes and the final artifact	At the beginning of the design project
Sequence of work interviews and questionnaires	Collecting data related to the sequence of work to be performed with the artifact	Early in the design cycle
Focus groups	Include a wide range of stakeholders to discuss issues and requirements	Early in the design cycle
On-site observation	Collecting information concerning the environment in which the artifact will be used	Early in the design cycle
Role Playing, walkthroughs, and simulations	Evaluation of alternative designs and gaining additional information about user needs and expectations; prototype evaluation	Early and mid-point in the design cycle
Usability testing	Collecting quantities data related to measurable usability criteria	Final stage of the design cycle
Interviews and questionnaires	Collecting qualitative data related to user satisfaction with the artifact	Final stage of the design cycle

Source: Preece et al., 2002

2.1.3. Usability Testing

The purposes of usability testing are to (1) improve the product’s usability, (2) involve real users in the testing, (3) give the users real tasks to accomplish, (4) enable testers to observe and record the actions of the participants, and (5) enable testers analyze the data obtained and make changes accordingly (Dumas and Redish, 1993).

Many techniques are employed in usability testing, including: (1) *think aloud* techniques in which the user is asked to articulate all the steps of his / her actions; (2) *videotaping* is valuable to review what the participants did, and to show designers where the problems are in their designs; and (3) *Interviews and user satisfaction questionnaires* enable designers to evaluate the users’ likes and dislikes about the design and gain a deeper understanding of any problems. The tests are conducted with typical users performing typical standardized tasks in a typical task environment to collect data including: (1) time for users to learn a specific function, (2) speed of task performance, (3) type and rate of errors by users, (4) user retention of commands over time, and (5) subjective user satisfaction (Shneiderman, 1998).

2.2. Liver Surgery Planning

2.2.1. Liver Anatomy

The liver is a vital organ which plays a major role in metabolism and has a number of functions in the body, including glycogen storage, decomposition of red blood cells, plasma protein synthesis, hormone production, and detoxification. The liver is located below the diaphragm in the abdominal-pelvic region of the abdomen (Figure 2.1). It also produces bile which aids in digestion.

The liver of a human normally weighs about 1.5 kilograms (Cotran et al., 2005) and is a soft, pinkish-brown, triangular organ. The liver has a right and a left lobe and is connected to two large blood vessels: the hepatic artery and the portal vein which supply blood to the liver. Oxygen is provided from both of the two vessels, while nutrients are provided by the portal vein. The blood leaves the liver through the hepatic vein (Figure 2.2).

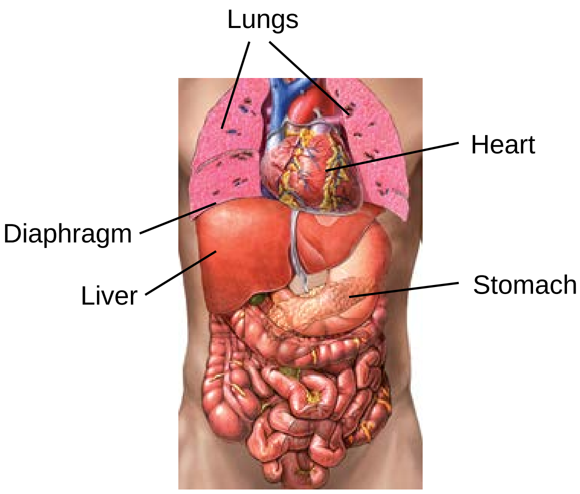

Figure 2.1. Liver location in the human′s body

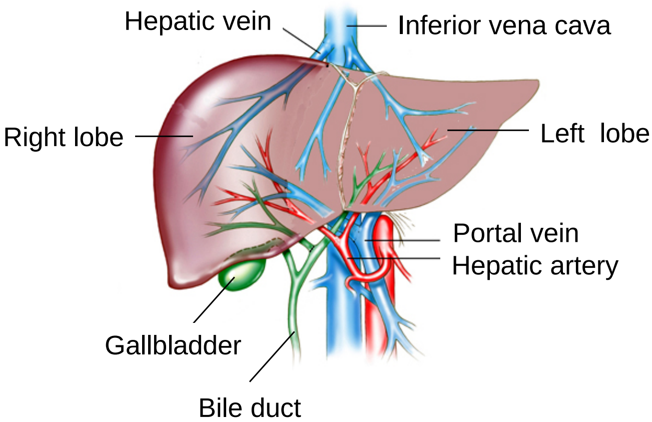

Figure 2.2. Blood flow in the liver

2.2.2. Liver Cancer and Treatment Options

Liver cancer can be classified into two types, primary and secondary. Primary liver cancer indicates that the tumor starts from the liver. Hepatocellular carcinoma (HCC) is the most common form of primary liver cancer. Secondary cancer means that the cancer started somewhere else and spread to the liver.

The treatment of primary cancer is particularly challenging compared to other types of cancer since the treatment not only depends on the size and position of the tumor, but also depends on the stage of the disease, age, overall health, feelings and personal preferences. A surgical resection is the most effective treatment for primary cancer. The resection accounts for tumors which affect up to one liver lobe. If the tumors are larger, liver transplantation is another possible form of treatment.

2.2.3. Medical Imaging Technologies

Medical imaging technologies for observing a patient's internal structure are required for diagnose of liver cancer. In liver surgery, spiral computed tomography (CT) images are mainly used, which forms a volumetric dataset (a series of slices with a certain thickness) of the patient's abdomen.

For liver surgery, contrast agents are used to enhance structures such as blood vessels from the surrounding. A violet fluid such as *iodine* is often injected to enhance portal vein. A CT scan is then performed in different phases to image different vessel branches.

2.2.4. Surgical Resection Strategies Planning

Two surgical resection strategies are clinically used: *anatomical-oriented resections* where liver segments are removed, and *atypical resections* with non-anatomical resection margins. The atypical resection strategy is chosen if the tumor is located at a peripheral section or if healthy liver tissue must be saved for preventing a post-operative liver failure. Otherwise, an anatomical resection is preferred since no main vessels are near segment boundaries, which prevents bleeding during liver surgery.

To make an anatomical resection plan, a pre-operative estimation of liver segment boundaries is required. A standard scheme proposed by Couinaud (1957) divides the liver into 8 segments (Figure 2.3) according to the hepatic vein and portal vein structures.

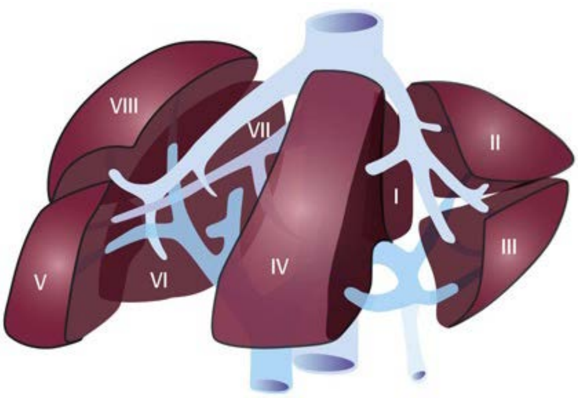

Figure 2.3. The liver divided into 8 segments using the Couinaud's classification scheme

During planning of a liver surgery, the percentage of the remnant liver is crucial since it affects the post-operative liver function and recovery. Schindl et al. (2005) identified that postoperative serious hepatic dysfunction is likely to occur if %RLV < 26.6% based on an ROC analysis for 104 patients with normal synthetic liver function. Ferrero et al. (2007) also reported that hepatectomy can be considered safe if %RLV > 26.5% for patients with healthy liver and %RLV >31% for those with impaired liver function based on an analysis of 119 cases.

2.3. Virtual Surgery Systems

2.3.1. Generic Surgery Systems

Generic surgery systems such as Rapidia (Infinitt Co., Ltd, South Korea), Voxar 3D (TOSHIBA Co., Japan), Syngovia (SIEMENS Co., Germany), and OsriX (Pixmeo Co., Switzerland) do not provide functions specialized for liver surgery planning. Only generic functions such as visualization, volume rendering (Figure 2.4), manual contour drawing, and simple region growing method for contour extraction (Figure 2.5) are provided. The manual contour drawing and simple region growing method to extract the liver, vessels, and tumors are cumbersome and time demanding (> 30 min for liver extraction) to the user. Functions of identification of liver segments and planning of liver surgery are not provided in the generic virtual surgery systems. Thus these generic virtual liver surgery systems have a significantly limited utility to surgeons for pre-operative liver surgery planning.

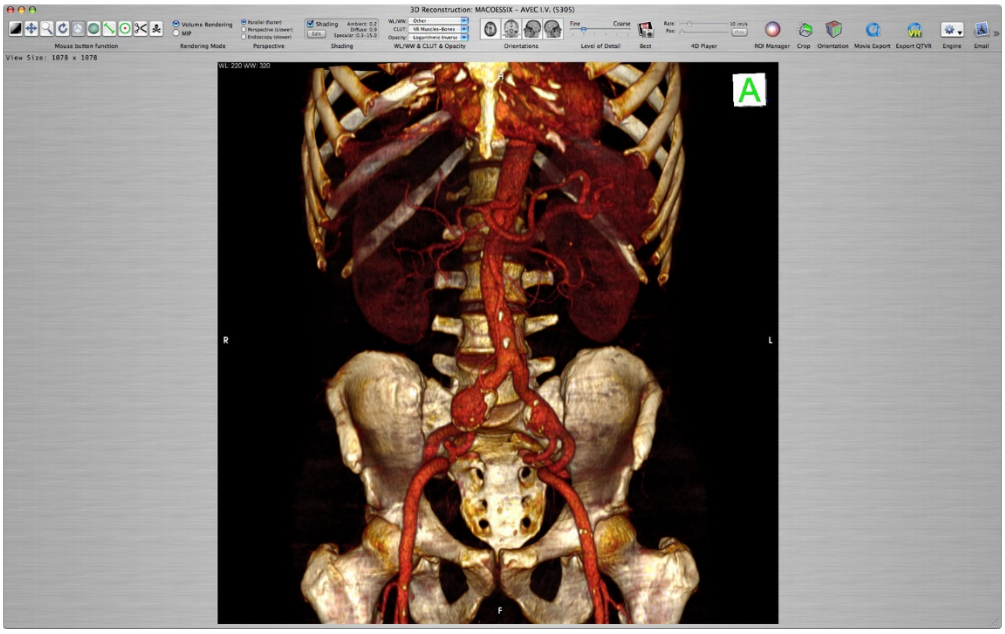

Figure 2.4. Volume rendering function in OsiriX

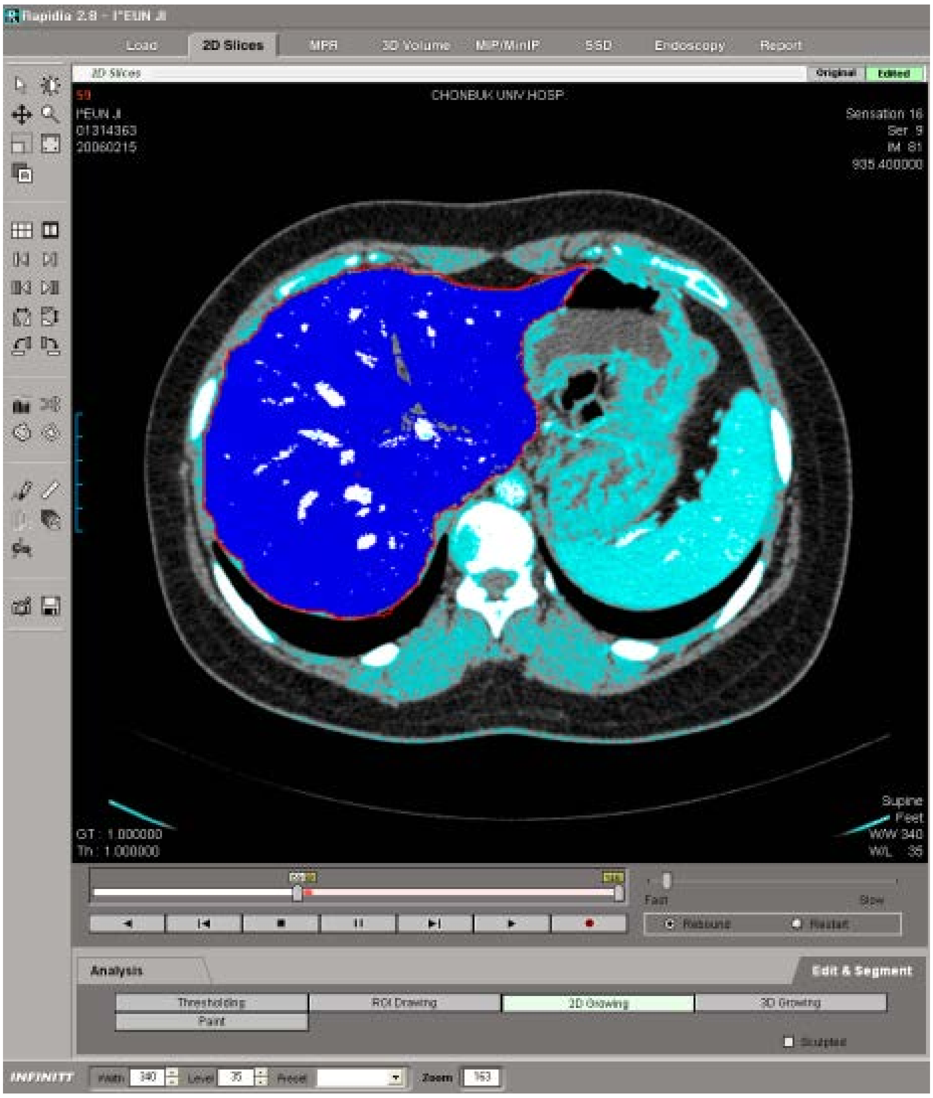

Figure 2.5. An example of liver extraction using a region growing method by Rapidia

2.3.2. Specialized Virtual Liver Surgery Planning Systems

Several specialized systems to virtual liver surgery planning such as LiverAnalyzer™ (MeVis Medical Solutions AG, Germany), Synapse Vincent™ (FUJIFILM Co., Japan), and mint Liver™ (Mint Medical GmbH, Germany) have been developed, but their user interfaces and algorithms need to be improved for better usability and time efficiency.

LiverAnalyzer is known to have capabilities of segmentation of the liver and its veins, arteries, bile system, and tumors, volumetric information on donors and donees for living liver transplantation, individual calculation of the volume based on different sections of the vascular system, risk analysis for oncological resections with respect to safety margins, and preparation of virtual resection proposals based on the patient's anatomy, but is not for sale. Only a distant web service is available for LiverAnalyzer—CT images are sent to Mevis Medical Solutions AG and then a liver analysis report is delivered within one or two days depending on selected payment option. The liver analysis report is viewed by LiverViewer (Figure 2.6), provided free of charge by the company; however, LiverViewer shows only analysis results without presenting CT images so that surgeons have difficulty to cross-check the accuracy of the analysis results. The liver analysis results cannot be adjusted either since no editing functions are provided by LiverViewer.

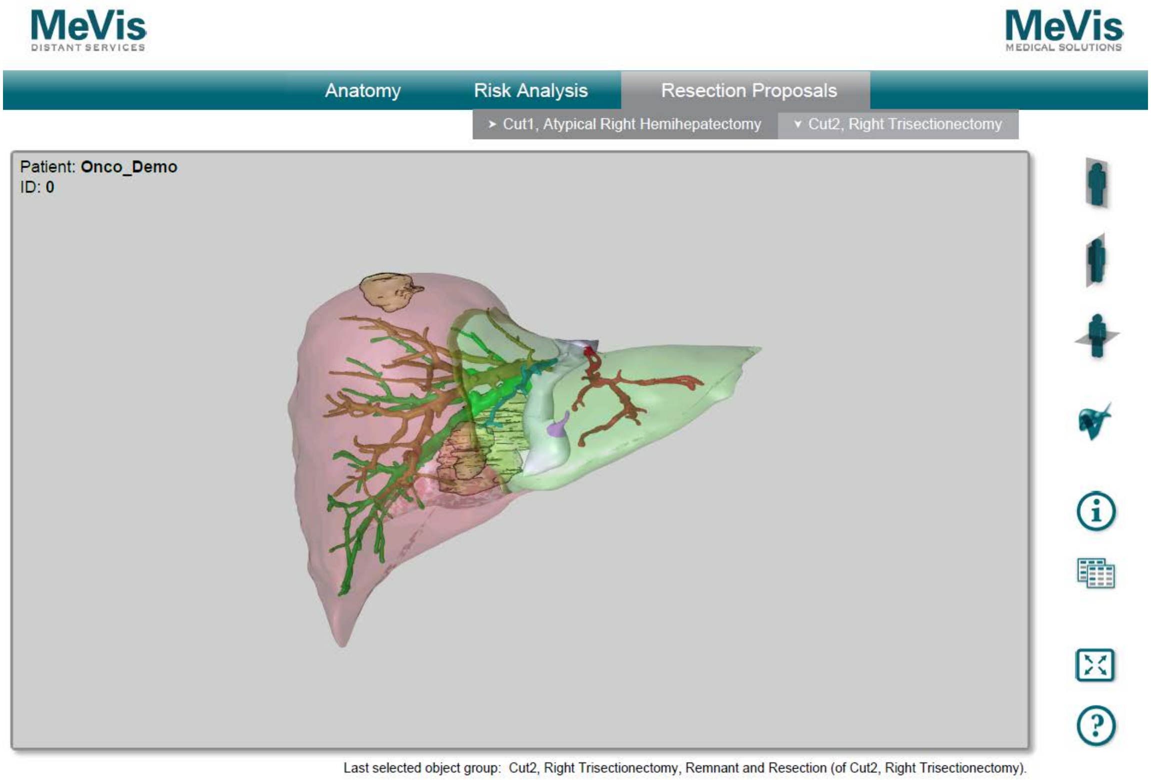

Figure 2.6. Liver analysis report viewed by LiverViewer

Synapse Vincent (Figure 2.7) is for sale and supports liver extraction, vessel analysis, liver segmentation, volumetry, and surgery planning. However, some user interfaces and algorithms of Synapse Vincent such as those for liver extraction and vessel extraction from CT images are cumbersome to use. For example, the region growing method used by Synapse Vincent for liver extraction often extracts adjacent tissues and/or organs along with the liver, which leads to intensive manual editing to remove parts falsely extracted.

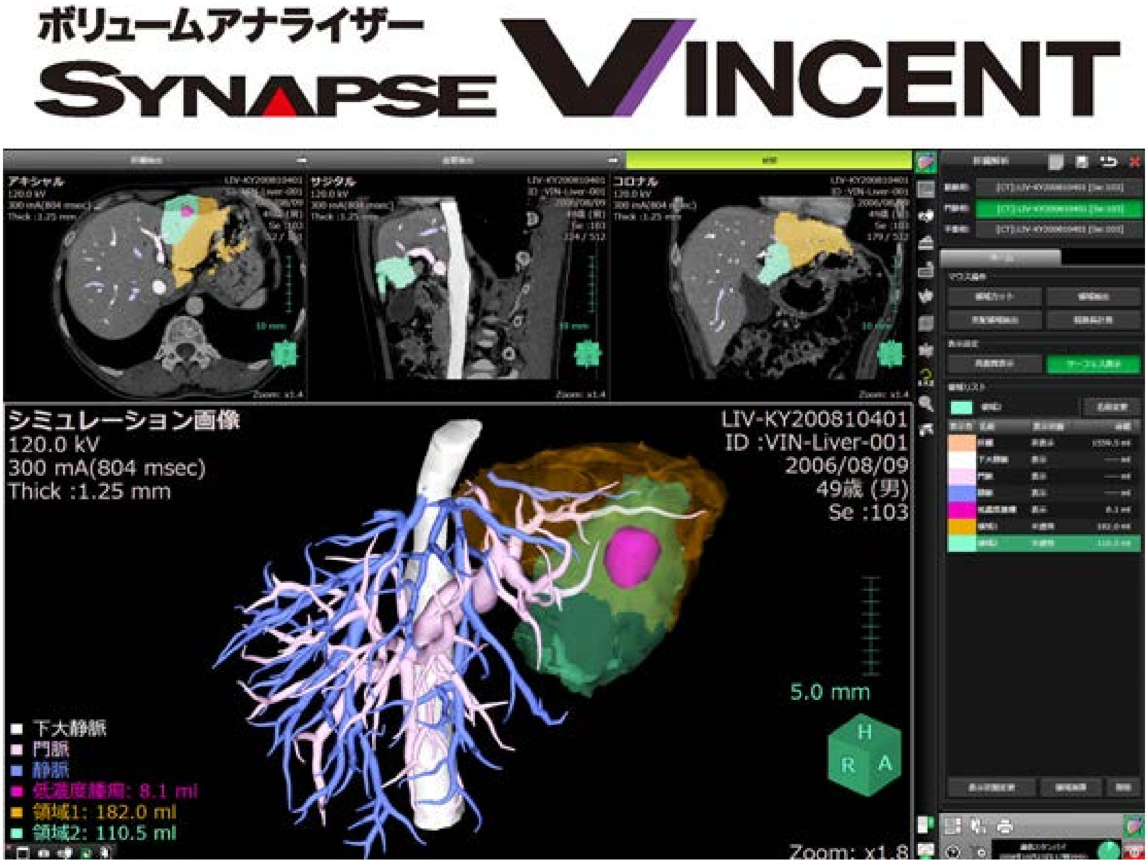

Figure 2.7. Liver surgery planning by Synapse Vincent

Mint Liver (Figure 2.8), corporately developed by Mint Medical GmbH and German Cancer Research Center, provides (1) detailed analysis and visualization of a patient's anatomy, (2) fully automated liver analysis for high quality visualization and volumetric analysis, and (3) risk analysis and assessment of resection strategies for an optimal treatment plan. However, the accuracy and time efficiency of the fully automatic liver extraction method are doubtable. The fully automatic liver extraction methods commonly sacrifice the accuracy in liver extraction because their algorithms cannot completely discriminate the liver from the neighboring organs due to the similarity in image intensity between the organs (Lee et al., 2007).

Figure 2.8. Workflow of mint Liver

2.4. Liver Extraction Methods

2.4.1. Fully Automatic Liver Extraction Methods

Various fully automatic methods have been developed which automatically identify the liver boundaries using statistical models or mathematical morphology. However, the automatic methods sacrifice the accuracy and time efficiency in liver extraction due to the difficulty in discriminating the liver from the neighboring organs automatically because of the similarity in image intensity between the organs (Lee et al., 2007). Jiang and Cheng (2009) proposed a complex automatic liver extraction procedure in which the mathematical morphology was applied to separate the liver from others using the erosion and dilation operations. The average computation time of Jiang and Cheng's method was about 9 sec per slice and an average precision of 94.6% was reported. In their study, some less extracted areas existed at the top of the left lobe of the liver (labeled with left arrow in Figure 2.9) and some over extracted areas existed in the middle of the liver (labeled with right arrow in Figure 2.9).

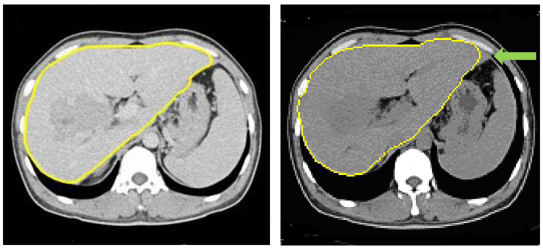

(a) (b)

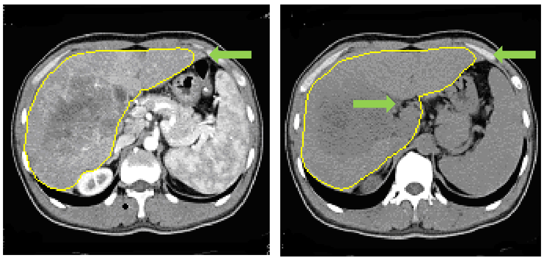

(c) (d)

Figure 2.9. Liver extraction results reported adapted from Jiang and Cheng (2009)

Massoptier and Casciaro (2008) applied statistical method to separat the liver from others since the intensity of the liver region has minimal standard deviation compared to other regions. A volume overlap of 94.2% was reported with an average processing time of 11.4 sec per slice. Ruskó et al. (2007) proposed another fully automatic liver extraction procedure in which a seed region inside the liver was automatically identified based on the histogram analysis. Then erosion operation was used to delete small regions. After that the liver was separated from the heart by means of connecting the bottom of the left and right lung lobes with a surface. Then an advanced region-growing method was used to extract the liver. The results reported by Ruskó et al. showed that the automatic method achieved high accuracy in a relatively easy case (top of Figure 2.10) and low accuracy in a relatively difficult case (bottom of Figure 2.10).

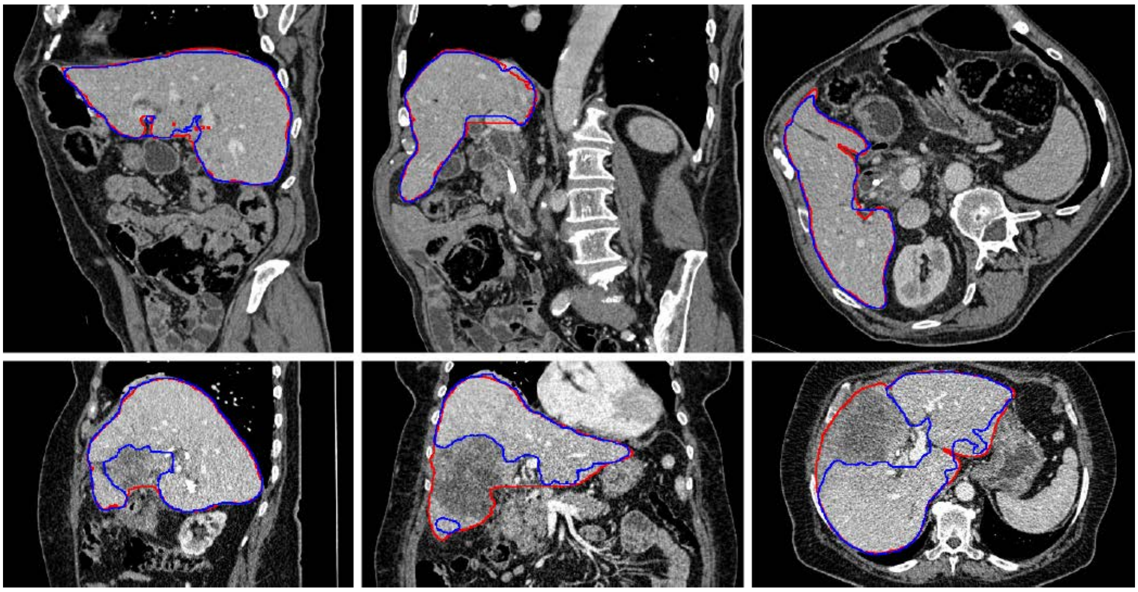

Figure 2.10. Liver extraction results adapted from Ruskó et al. (2007): a relatively easy case (top) and a relatively difficult case (bottom). The outline of the reference standard is in red, and the outline of the results by Ruskó et al. is in blue

2.4.2. Semi-Automatic Liver Extraction Methods

For more accurate and efficient liver extraction, semi-automatic methods have been developed which extract the liver from interactively identified seed points, seed regions, and initial liver regions using various image processing algorithms such as region growing and level-set methods. Dawant et al. (2007) proposed a semi-automatic liver extraction method in which liver contours were manually delineated on a number of slices and then interpolation was used to extract liver contours on the other slices. The method proposed by Dawant et al. is limited by tedious manual delineation of initial liver contours (10 min required). Eventhough the method worked in extracting the liver without tumors (top of Figure 2.11), it had poor performance in extacting the liver with large tumors (bottom of Figure 2.11).

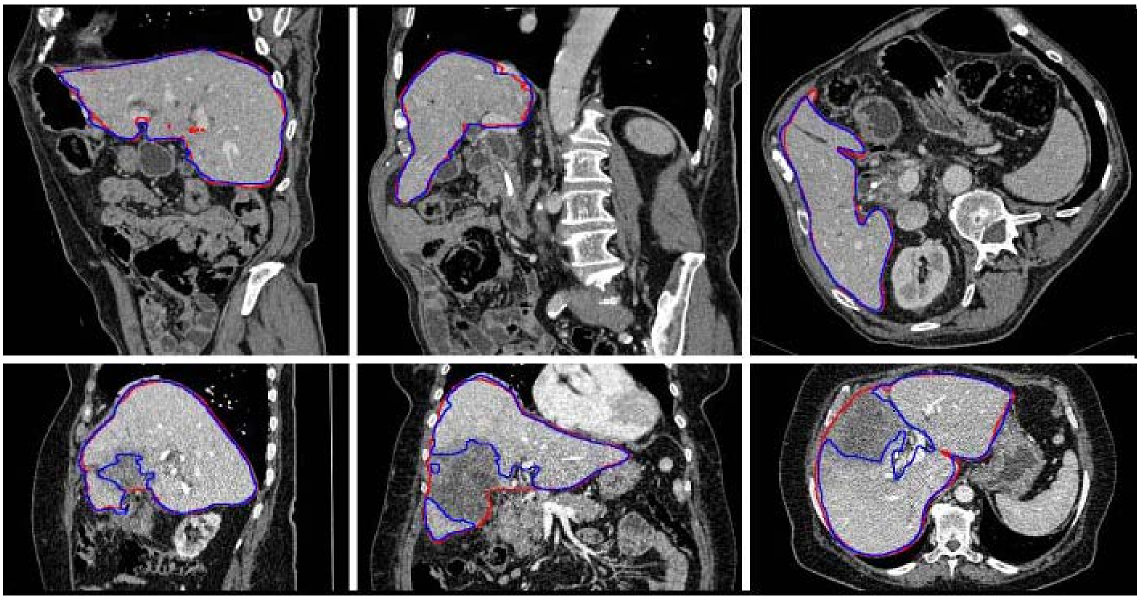

Figure 2.11. Liver extraction results adapted from Dawant et al. (2007): a relatively easy case (top) and a relatively difficult case (bottom). The outline of the reference standard is in red, and the outline of the results by Dawant et al. is in blue

Hermoye et al. (2005)'s semi-automatic method consisted of (1) placing initial circle(s) on each image slice, (2) extracting the liver based on geometric deformable models and the level-set technique, and (3) inspecting and possibly manually modifying the contours obtained with the extraction algorithm. The method required a 5-min interaction period to address initial circles, which could be cumbersome to a user. Pan and Dawant (2001) have proposed a new speed function for level-set propagation from an initilized small circle in each slice. Again, the initialization of small circles in each slice is time demanding. Their method sacrificed time efficiency but achieved a relatively high accuracy (overlap ratio: 95.8%).

2.5. Liver Vessel Extraction Methods

2.5.1. Fully Automatic Liver Vessel Extraction Methods

Fully automatic liver vessel extraction methods segment the liver vessels based on statistical histogram analysis or local shape descriptors such as tube detection filters without a requirement of an initialization. However, the fully automatic methods have difficulties in extracting portal vein and hepatic vein seperately since the intensity values of the two vessels are similar to each other. Algorithms of seperating the extracted portal vein and hepatic vein are therefore needed which sacrifices time efficiency of the fully automatic methods. The fully automatic methods usually miss vessel branches with low contrast or extract lesions with vessels together if the vessels and lesions are connected. Soler et al. (2001) proposed a fully automatic method to initially extract liver vesels through thresholding estimated by intensity histogram analysis, remove any false positve and false negtive errors, and separate portal vein, hepatic vein, and hepatic artery based on geometrical and topological properties of the resulting skeleton structures of the extracted vessels. The authors claimed that the automatically extracted portal vein was exactly the same as a manually extracted one by a radiologist without providing any further proofs. They reported that their automatic method took 15 min to extract the vessels. Eidheim et al. (2004) used a matched filter to enhance vessel structures and then the generic algorithm for globally searching the most likely vasculatures. The quality of their results was not systematically verified. Their method took one hour to finish vessel extraction on a morden personal computer and thus inefficient. Esneault et al. (2010) applied a 3-D geometrical moment-based detector to localize the center of the vessel, its diameter, and local direction and then delivers the final segmentation using Boykov's graph cuts alrorithm. As shown in Figure 2.12 adapted from Esneault et al., the extracted hepatic vein and portal vein seem incomplete. The computation process of their method took 10 to 100 sec on a 1.6 GHz Xeon, 4 G RAM PC. Bauer et al. (2010) proposed a two-step method to separate and segment interwoven tubular tree structures, identification of tubular object and grouping different tree structures followed by graph cuts for segmentation. Their method showed relatively high accuracy (FPE: 0%; FNE: 0.26%). However, the efficiency of their method was not evaluated which is important in practical clinical application such as liver surgery planning.

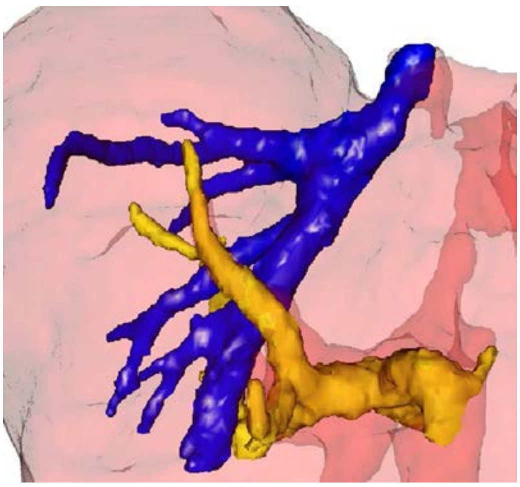

Figure 2.12. Segmented portal (dark blue) and hepatic (yellow) veins adapted from Esneault et al.

2.5.2. Semi-Automatic Liver Vessel Extraction Methods

For more accurate and efficient liver vessel extraction, various semi-automatic methods have been developed to segment liver vessels from an initialization by iteratively adding adjacent voxels that satisfy certain segmentation criteria. Lorigo et al. (2001) applied a level-set method to vessel segmentation with an initialization and a speed function. However, the application of their method to liver vessel extraction was not addressed. Selle et al. (2002) applied a region growing method to segment liver vessels starting from an interactively selected seed point with automatically adjusted thresholds and then interactively separate liver vessels based on skeletonized vascular structures. However, their method has difficulties in segmenting small vessels (Esneault et al., 2010). Yi and Ra (2003) proposed a locally adaptive region growing method to segment vessel trees, in which locally adaptive analysis was repeatedly performed throughout the whole image to identify small vessels. However, their method has not been tested for liver vessel extraction. Shang et al. (2008) applied a traditional region growing method to segment the main branches of the liver vessels from an initial seed and a threshold and then an adaptive region growing method to segment the small branches. As shown in Figure 2.13 adapted from Shang et al., their method achieved better result than the traditional region growing method. However, the efficiency of their method was not evaluated. Huang et al. (2011) proposed a hierarchical region growing method to segment liver vessels from multiple seed points. Their method divided CT images into sub-blocks with a defined size and a homogeneity criterion was established automatically through statistical analysis of the local intensities of the selected seed points. However, their method was not systematically evaluated. As shown in Figure 2.14 adapted from Huang et al., the extracted portal vein and hepatic vein seem incomplete.

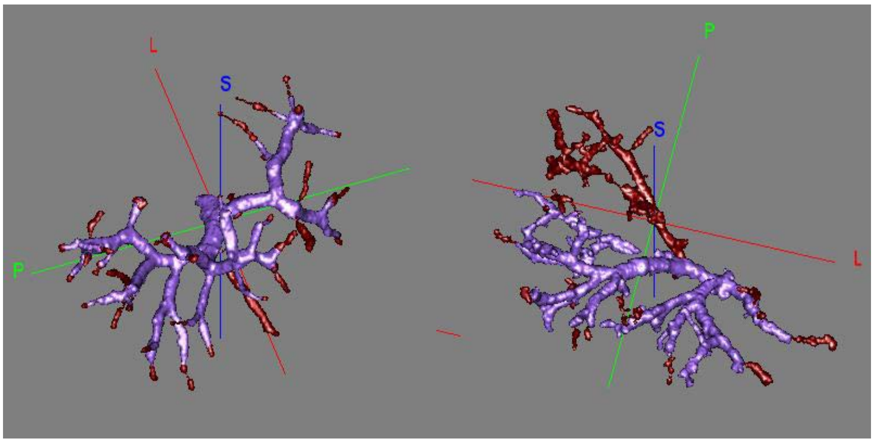

Figure 2.13. Segmented portal (left) and hepatic (right) veins adapted from Shang et al. compared with traditional region growing results (purple)

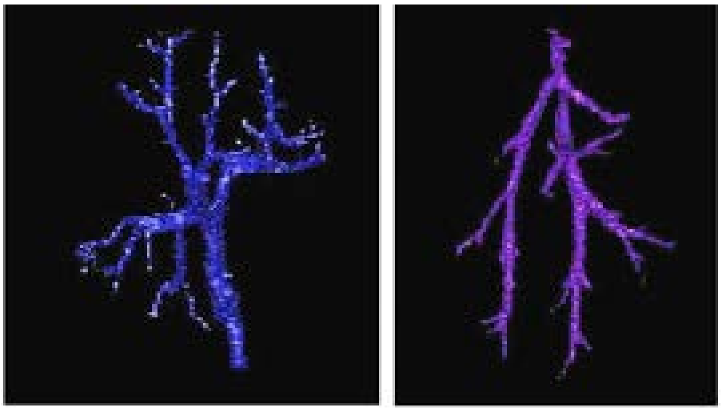

Figure 2.14. Segmented portal (left) and hepatic (right) veins adapted from Huang et al.

Chapter 3. USE SCENARIO AND USER INTERFACE DEVELOPMENT

A use scenario consisting of a five-step process (Figure 3.1) was established for *Dr. Liver* through literature review, benchmarking of virtual surgery systems, and interviews with surgeons: (1) liver extraction, (2) vessel extraction, (3) tumor extraction, (4) liver segmentation, and (5) surgery planning. *Dr. Liver* was designed to provide good usability and accuracy for the surgeon and take an entire processing time of less than 30 min from liver extraction to surgery planning. For each step, detailed sub-steps were determined and then user interfaces were designed. Then, for each sub-step, algorithms were applied or developed to obtain results with an acceptable level of accuracy within a designated duration of time.

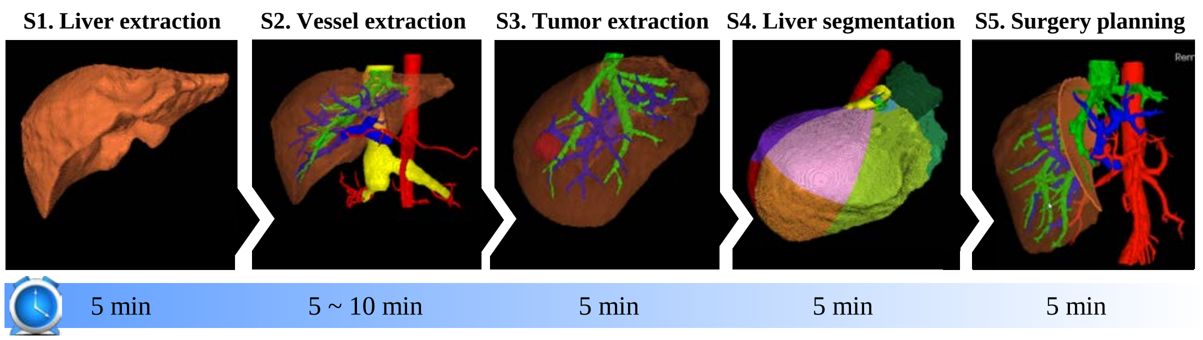

S1.1. Seed point selection	S2.1. Mask the liver	S3.1. Seed point selection	Plane-based	Plane-based
S1.2. Liver extraction	S2.2. Seed point selection	S3.2. Tumor extraction	S4.1.1. Plane generation	S5.1.1. Load files
S1.3. Contour editing	S2.3. Vessel extraction	S3.3. Contour editing	S4.1.2. Confirm segmentation	S5.1.2. Point selection
S1.4. Update & save	S2.4. Contour editing	S3.4. Update & save	S4.1.3. Segment management	S5.1.3. Plane generation
	S2.5. Update & save		Sphere-based	S5.1.4. Volume calculation
			S4.2.1. Load the liver	Segment-based
			S4.2.2. Remove segment	S5.2.1. Load segments
			S4.2.3. Update & save	S5.2.2. Cut by segments
			S4.2.4. Segment management	Sphere-based
				S5.3.1. Load the liver
				S5.3.2. Liver resection
				S5.3.3. Update & save

Figure 3.1. Use scenario of *Dr. Liver*

The customized user interface of *Dr. Liver* (Figure 3.2) was designed to provide surgeons with good usability. Based on the use scenario established for *Dr. Liver*, a hierarchical user interface with two levels was designed as illustrated in Figure 3.3. The design of button size, color, font size, and color is kept consistent for the same hierarchical level. For the high-level tasks, a procedure status indication coding scheme (circle: not conducted; bar in the circle: in progress; cross in the circle:

completed) is employed; for the low-level tasks, a procedure status color coding scheme (grey: completed or not conducted; blue: in progress) is applied. A 3D view indication box and resetting buttons are provided to facilitate 3D object manipulation, as shown in Figure 3.4. Hot key menus (Figure 3.5) are shown on the CT screen for easier accomplishment of various tasks such as seed point selection, zooming in/out, and image translation.

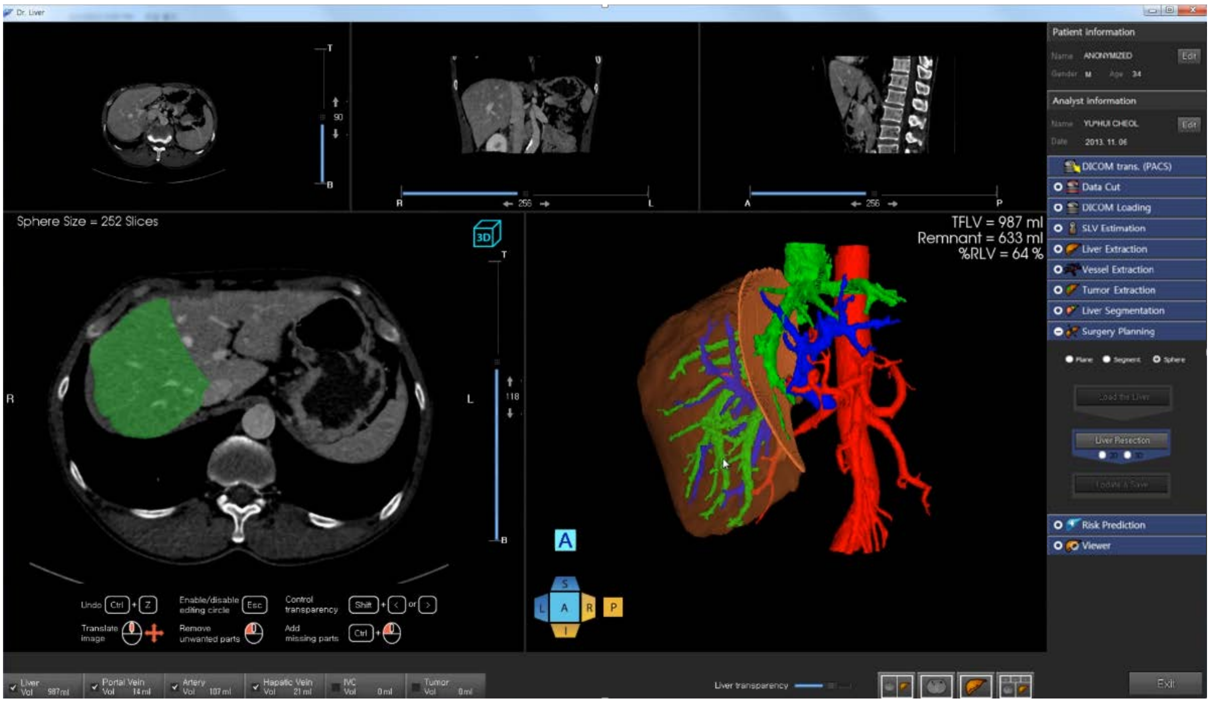

Figure 3.2. The virtual liver surgery planning system *Dr. Liver*

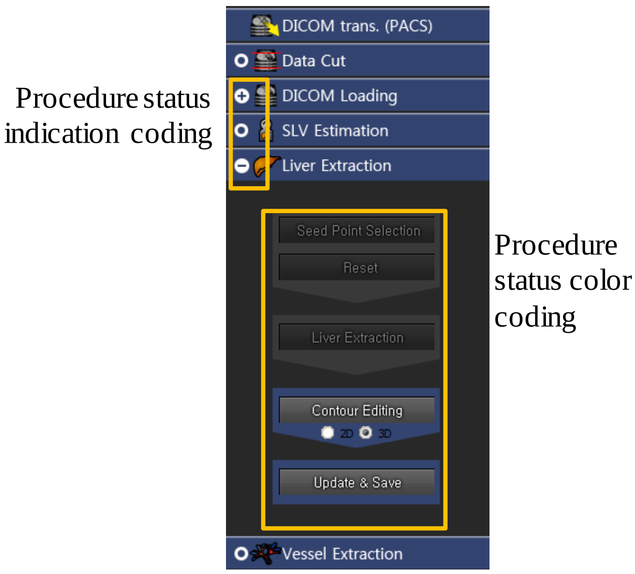

Figure 3.3. A hierarchical user interface of *Dr. Liver*

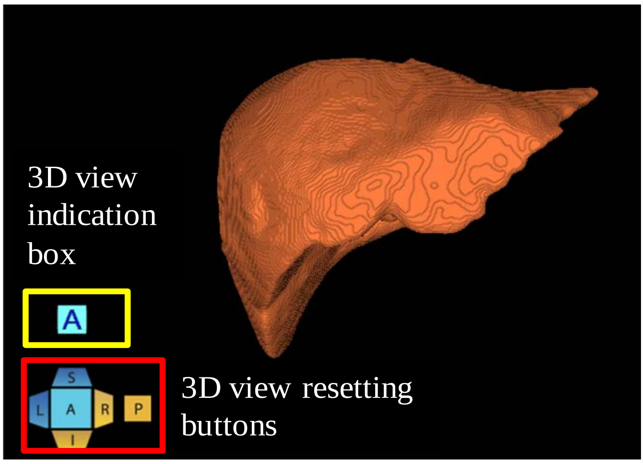

Figure 3.4. 3D view indication box and resetting buttons in *Dr. Liver*

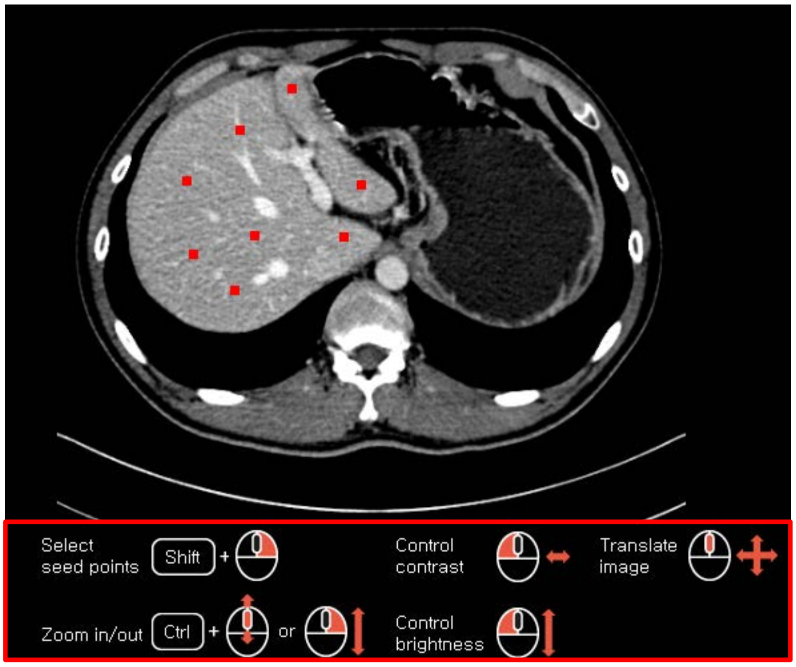

Figure 3.5. Hot key menus shown on the CT screen in *Dr. Liver*

3.1. Liver Extraction Module

The liver is extracted from abdominal CT images by following a four-step procedure (Figure 3.6) using a semi-automatic liver extraction algorithm proposed in the present study: (1) selection of multiple seed points from different CT slices, (2) extraction of the liver, (3) editing of the extracted liver, and (4) updating and saving of the edited liver. In step 1, multiple seed points are interactively selected by the user from different CT slices. In step 2, the liver is automatically extracted from the selected seed points. In step 3, an interactive editing function is provided in which a scalable editing sphere is used to remove a falsely extracted part or add a missing part. Lastly, the edited liver region is updated and saved.

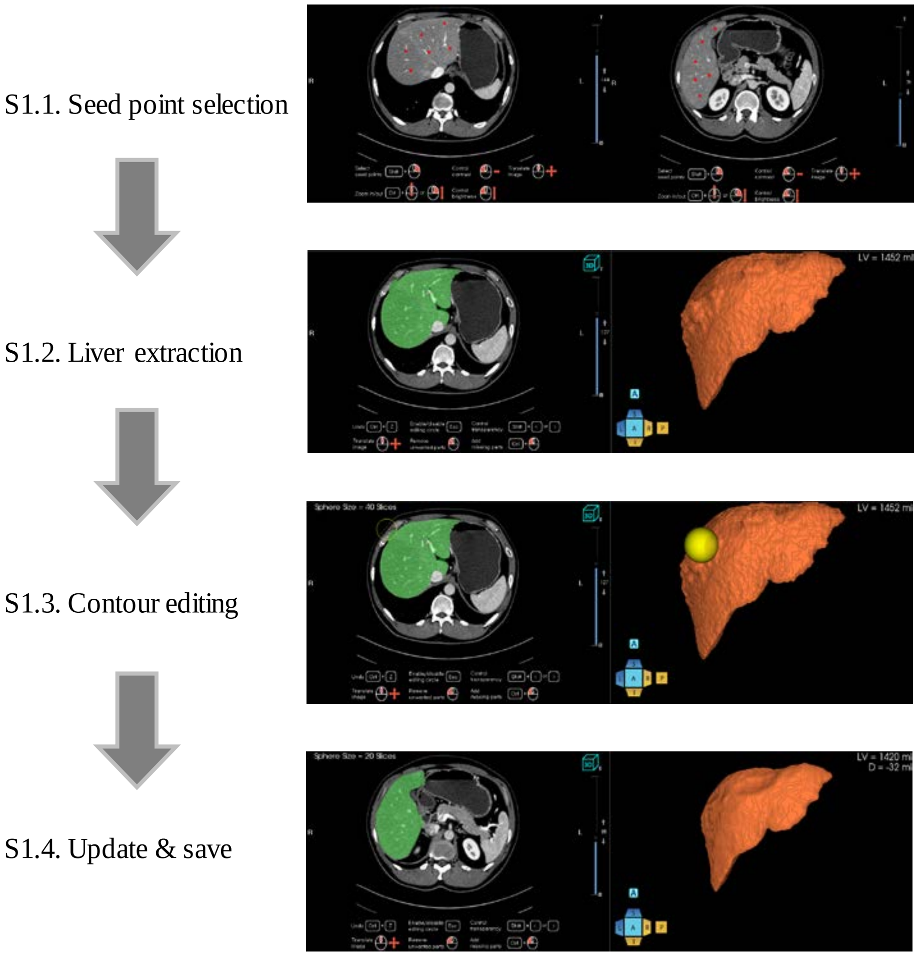

Figure 3.6. Use scenario of liver extraction

The interface of liver extraction module was customized based on the use scenario of liver extraction for good usability (Figure 3.7). For verification of the extracted liver, CT images are overlaid with the extracted liver mask and 3D liver surface model generated from the extracted liver mask is also shown (Figure 3.8). The 2D CT slice window and the 3D liver screen are synchronized to facilitate editing (Figure 3.9).

Figure 3.7. User interface of liver extraction module

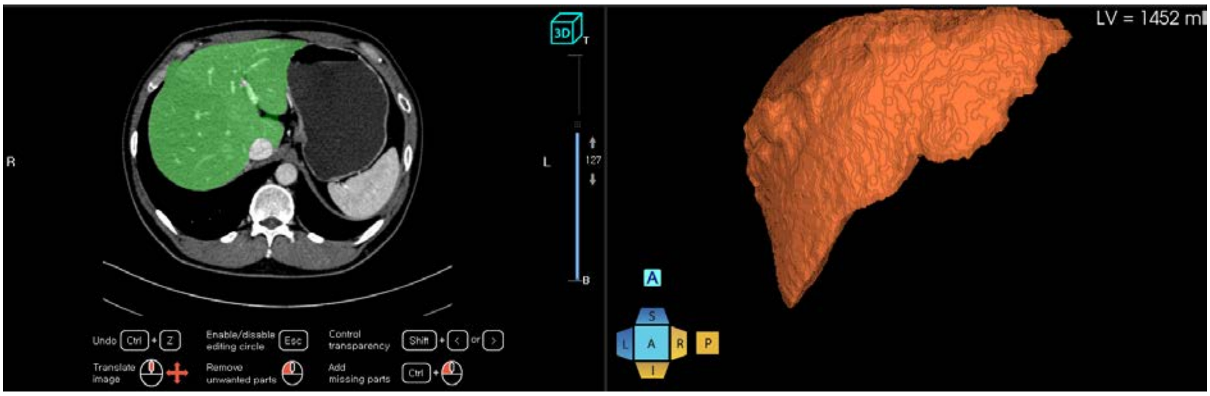

Figure 3.8. Overlaid CT images with liver mask (green) and 3D liver surface model for verification of liver extraction results in *Dr. Liver*

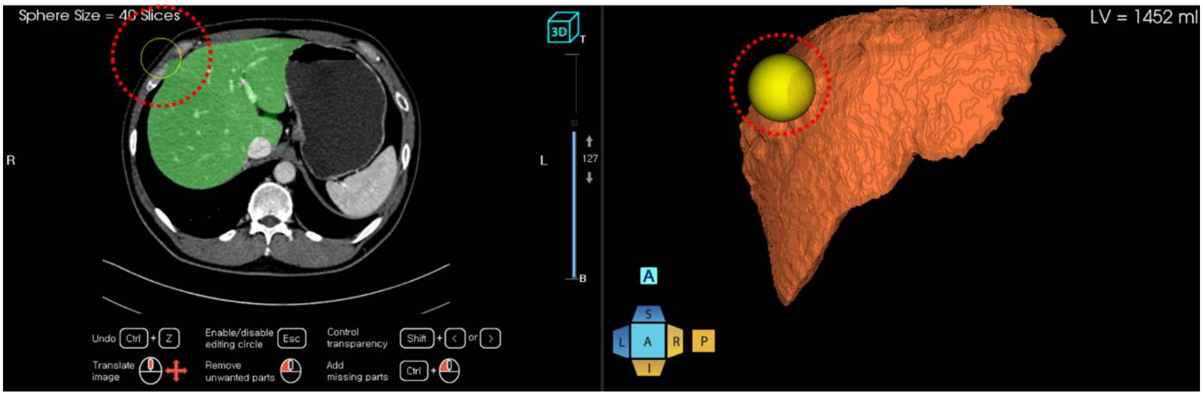

Figure 3.9. Synchronized 2D CT screen and 3D liver screen to facilitate editing of the extracted liver

3.2. Vessel Extraction Module

After liver extraction, the liver vessels are extracted including hepatic artery (HA), portal vein (PV), hepatic vein (HV), and inferior vena cava (IVC). A five-step use scenario (Figure 3.10) was developed for vessel extraction. In step 1, CT images are masked with the extracted liver. Main roots of the vessels are interactively added by the user since they are outside of the extracted liver. In step 2, multiple seed points are interactively selected by the user over the vessel region from different CT slices. In step 3, the vessels are automatically extracted. Multiple candidates of the extracted vessels are shown for the user to select an appropriate result. In step 4, the extracted vessels are interactively edited by the user. In step 5, the editing results are updated and saved.

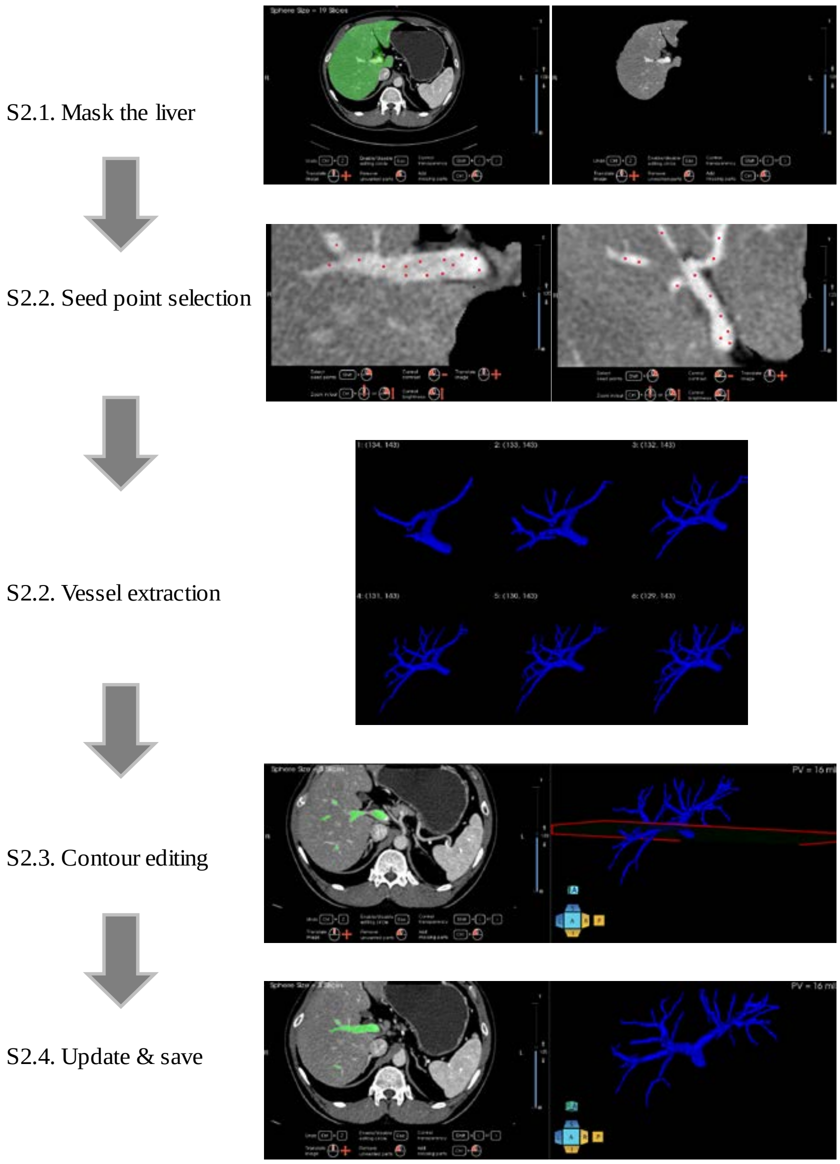

Figure 3.10. Use scenario of vessel extraction

The interface of vessel extraction module was customized based on the use scenario of vessel extraction for good usability (Figure 3.11). Radio buttons were provided for selection of different vessels to be extracted. A user-friendly interface (Figure 3.12) is provided for the user to verify the extracted vessel candidates with multiple 3D vessel surface models and corresponding volume information and select an appropriate result using checkboxes.

Figure 3.11. User interface for vessel extraction module

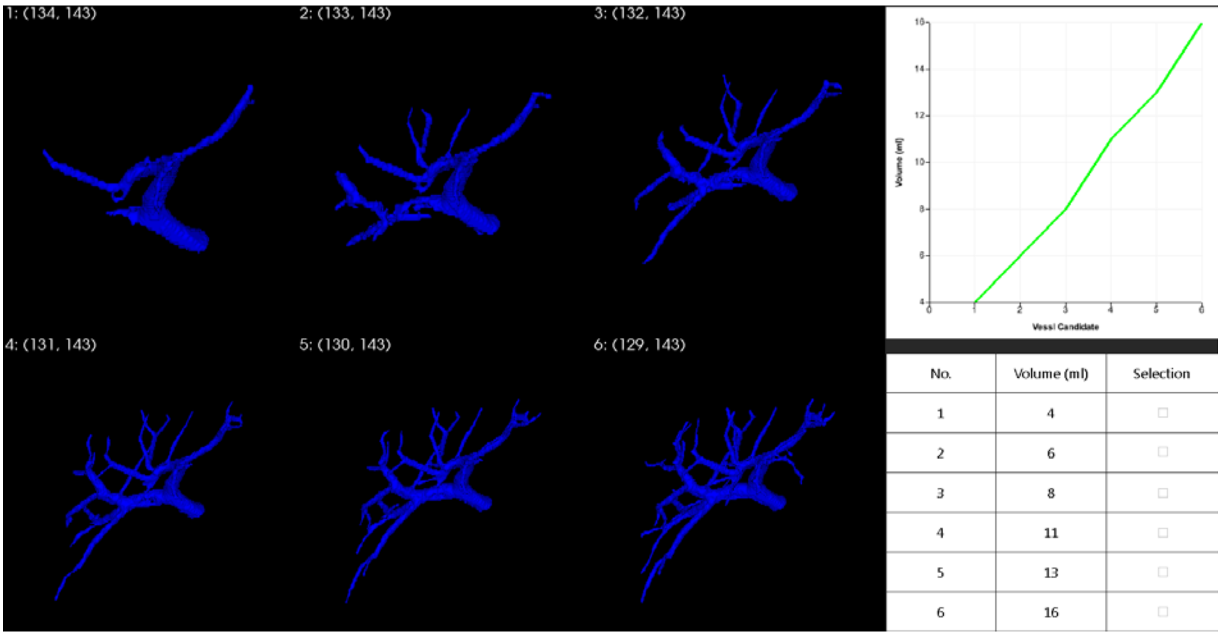

Figure 3.12. An interface for verification of segmented vessels and selection of an appropriate result

3.3. Tumor Extraction Module

After vessel extraction, a tumor(s) is extracted with a four-step use scenario (Figure 3.13): (1) interactive selection of multiple seed points by the user, (2) automatic extraction of the tumor(s), (3) interactive contour editing of the extracted tumor(s), and (4) automatic updating and saving of the editing results.

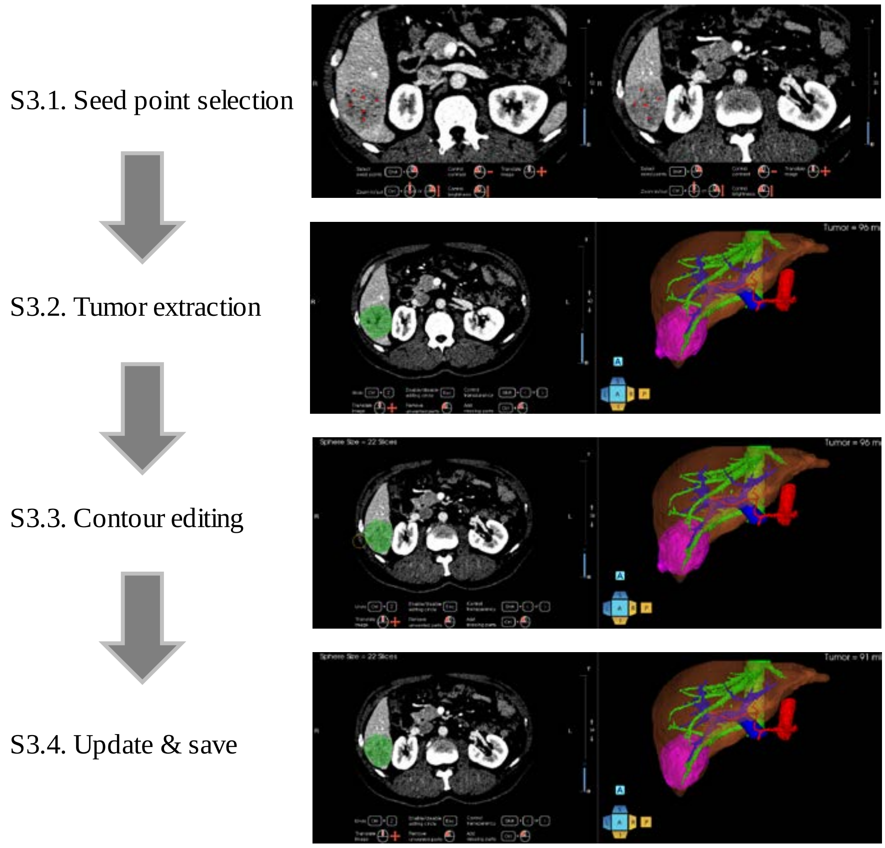

Figure 3.13. Use scenario of tumor extraction

The interface of tumor extraction module was customized based on the tumor extraction procedure for good usability (Figure 3.14). Radio buttons were provided for selection of different CT phases.

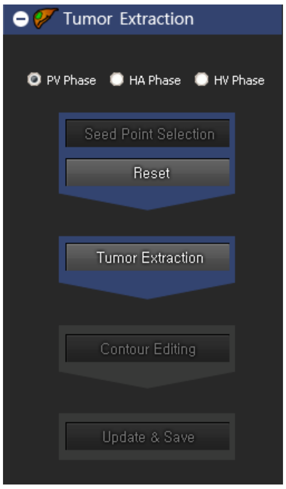

Figure 3.14. User interface for tumor extraction module

3.4. Liver Segmentation Module

Two modules, plane-based and sphere-based are provided for liver segmentation. According to the structures of hepatic and portal veins, the liver can be divided into 8 segments based on the Couinaud model (Couinaud, 1957). A seven-step procedure (Table 3.1) was developed to divide the liver into 8 segments. In step 1, segment 1 was formed by a segmentation sphere. In step 2, the liver is separated into the left and right lobes along the middle hepatic vein. In step 3, the right lobe is separated into anterior and posterior sectors along the right hepatic vein. In step 4, the left lobe is separated into medial and lateral sectors along the left hepatic vein. In step 5, the posterior sector is separated into segments 6 and 7 according to the right portal vein structure. In step 6, the anterior sector is separated into segments 5 and 8 according to the right portal vein structure. In step 7, the lateral sector is separated into segments 2 and 3 according to the left portal vein structure. The liver segmentation can be conducted fully or partially according to the needs of a user.

Plane-Based Segmentation

The use scenario of plane-based liver segmentation (Figure 3.15) consists of a three-step procedure. In step 1, a segmentation plane is automatically generated. Then the liver is interactively segmented by adjusting the orientation and location of the segmentation plane. In step 2, the segmentation result is interactively confirmed according to a pre-assigned color scheme. In step 3, the color and transparency of the liver segments are interactively adjusted according to users’ preferences. Accordingly, a user interface (Figure 3.16) of plane-based liver segmentation was designed. Radio buttons were provided for segmentation of different liver segments. For confirming the liver segmentation results, a popup window (Figure 3.17) was provided for the user to confirm or invert the segmentation results. Another popup window (Figure 3.18) was provided in which the color and transparency of each liver segment can be interactively changed.

Table 3.1. The procedure for dividing the liver into eight segments

Step	Description	Illustration
1	Formation of segment 1	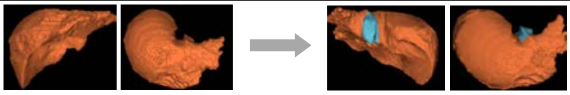
2	Dividing the liver into the left and right lobes	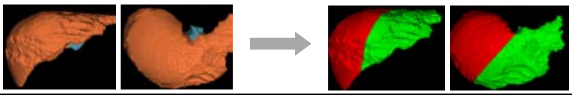
3	Dividing the right lobe into the anterior and posterior sectors	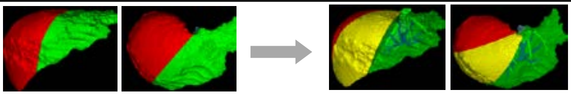
4	Dividing the left lobe into the medial and lateral sectors	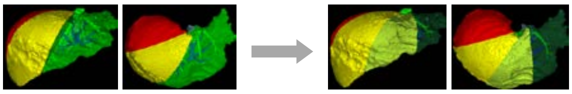
5	Dividing the posterior sector of the right lobe into segments 6 and 7	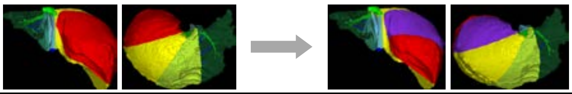
6	Dividing the anterior sector of the right lobe into segments 5 and 8	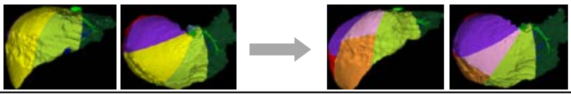
7	Dividing the lateral sector of the left lobe into segments 2 and 3	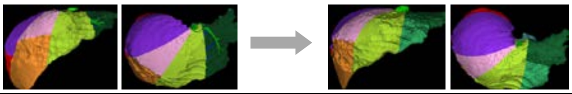

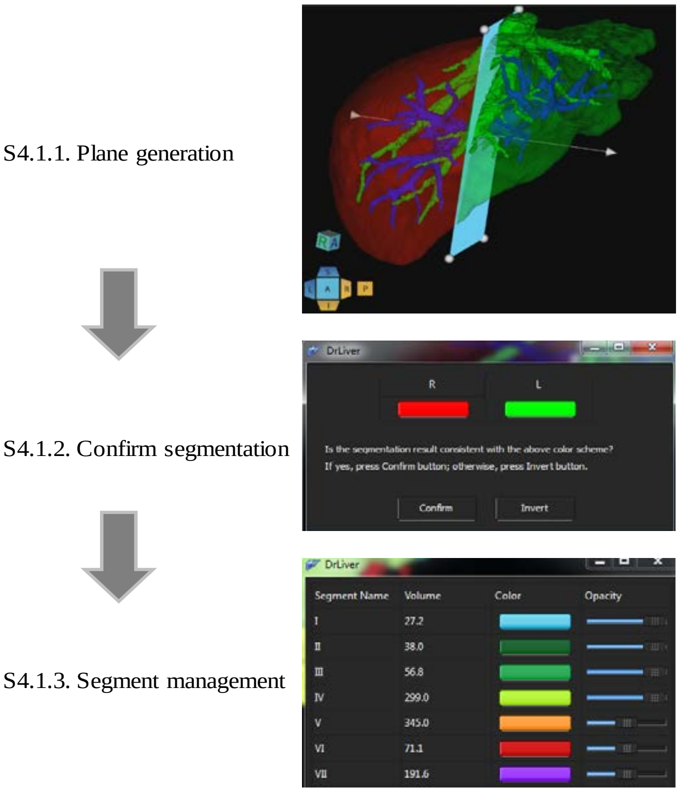

Figure 3.15. Use scenario for plane-based liver segmentation module

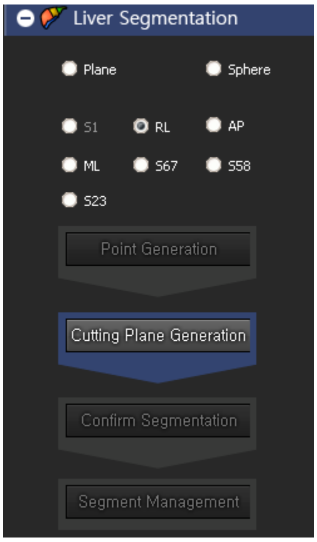

Figure 3.16. User interface of plane-based liver segmentation module

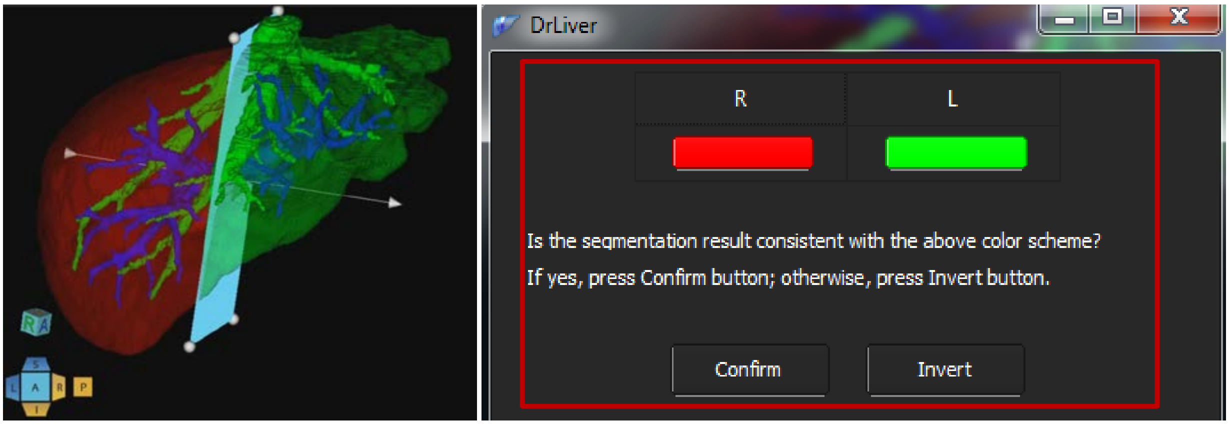

Figure 3.17. Interface for confirmation of plane-based liver segmentation results

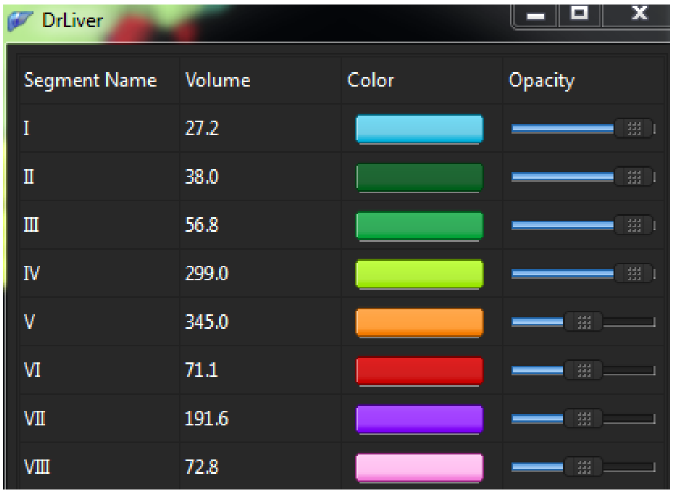

Figure 3.18. Interface for adjusting color and transparency of liver segments

Sphere-Based Segmentation

The use scenario of sphere-based liver segmentation (Figure 3.19) consists of a four-step procedure. In step 1, CT images are automatically overlaid with the liver mask. In step 2, a liver segment is interactively removed. In step 3, the segmentation results are automatically updated and saved. In step 4, the color and transparency of the liver segments are interactively adjusted according to users' preferences. Accordingly, a user interface (Figure 3.20) of sphere-based liver segmentation was designed.

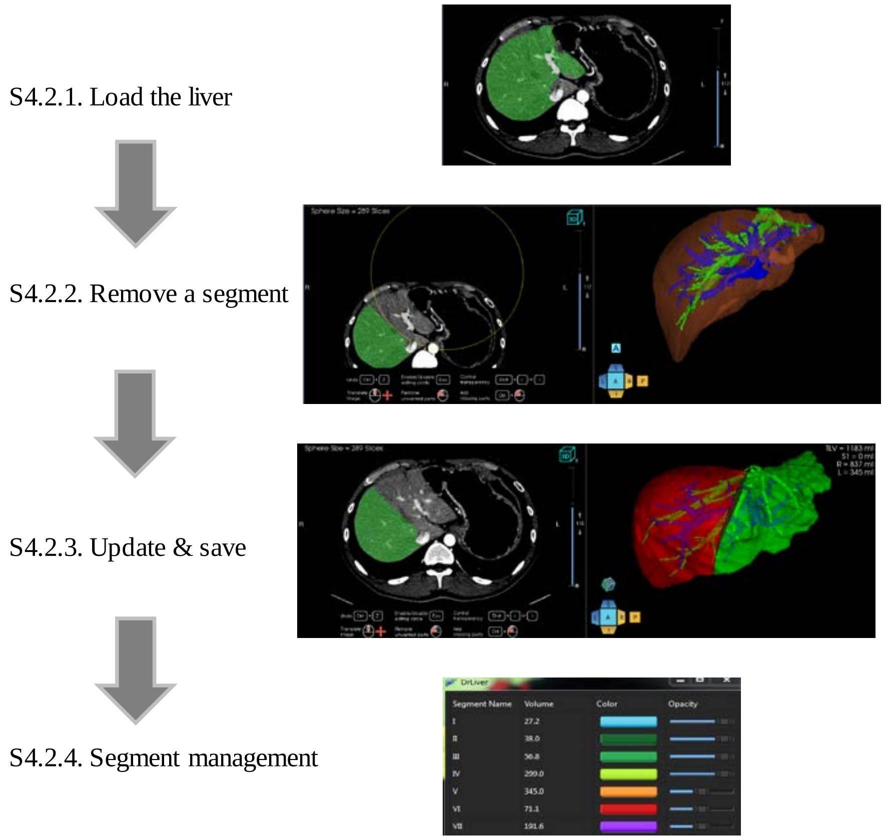

Figure 3.19. Use scenario for sphere-based liver segmentation module

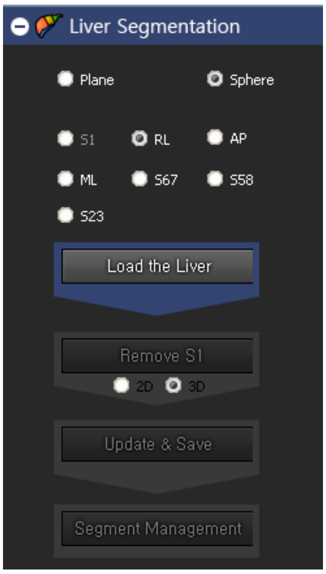

Figure 3.20. User interface of sphere-based liver segmentation module

3.5. Liver Surgery Planning Module

Three modules, plane-based, segment-based, and sphere-based are provided for liver surgery planning.

Plane-based Liver Surgery Planning

Use scenario of the plane-based liver surgery planning module (Figure 3.21) consists of four steps: (1) loading the extracted liver, vessels, and tumor(s), (2) interactive selection of three landmarks for liver resection, (3) interactive liver resection by an adjustable plane generated from the three selected landmarks, and (4) automatic calculation of the total functional liver volume, remnant volume, and %RLV. Accordingly, a four-step user interface (Figure 3.22) was designed.

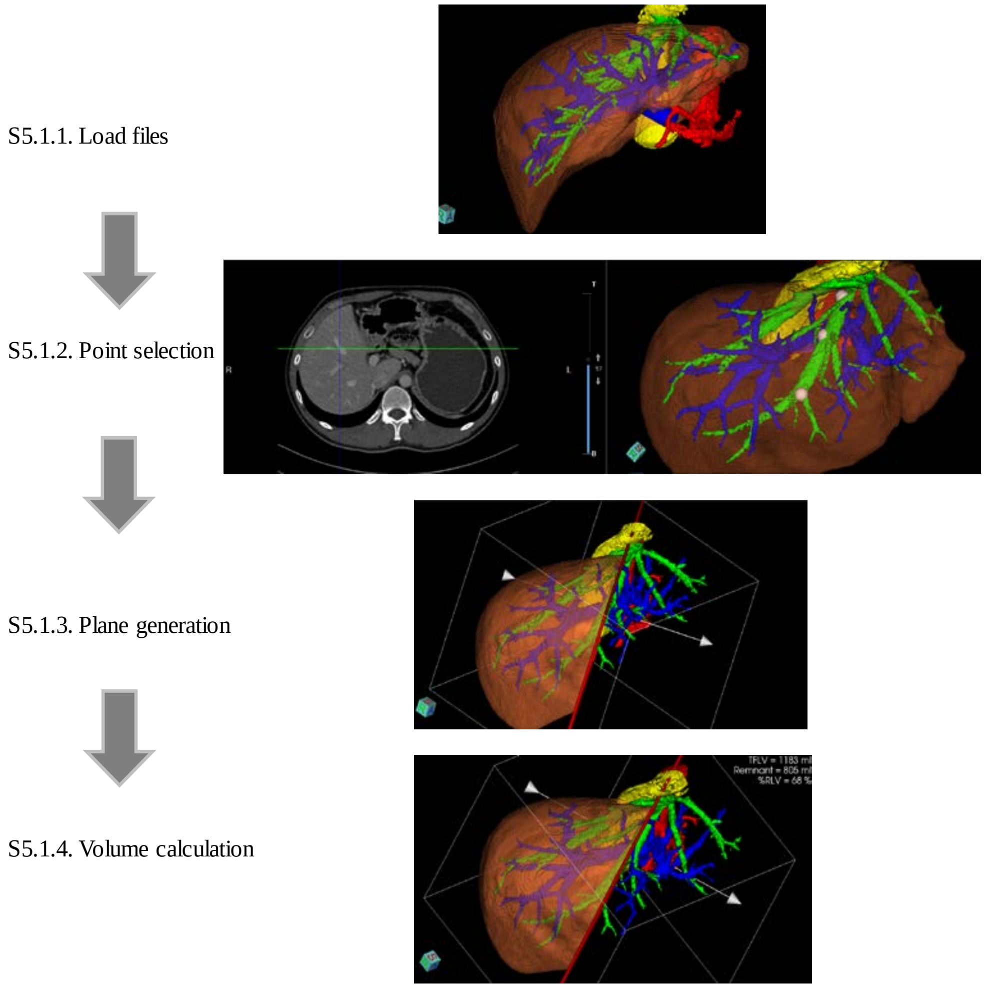

Figure 3.21. Use scenario for plane-based liver surgery planning module

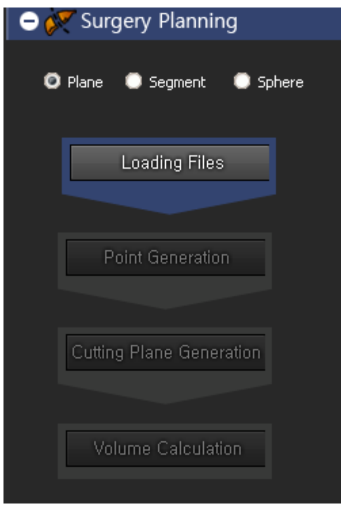

Figure 3.22. User interface for plane-based liver surgery planning module

Segment-based Liver Surgery Planning

Use scenario of the segment-based liver surgery planning module (Figure 3.23) consists of two steps: (1) loading liver segments, vessels, and tumor(s) and (2) interactive liver segments resection and automatic calculation of the total functional liver volume, remnant volume, and %RLV. Accordingly, a two-step user interface (Figure 3.24) was designed. A user interface (Figure 3.25) was provided for interactive liver segments resection using checkboxes. A color scheme was designed for easier recognition of different liver segments by the user.

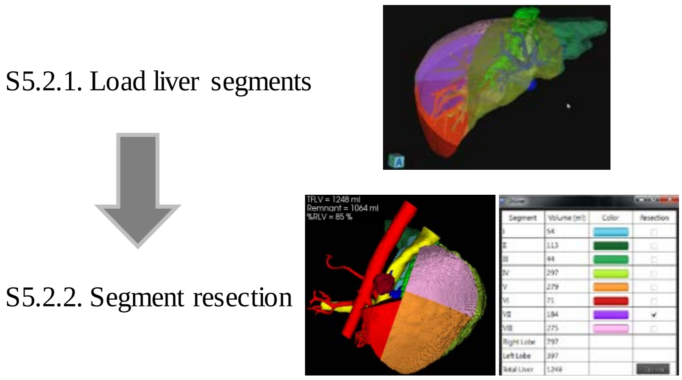

Figure 3.23. Use scenario for segment-based liver surgery planning module

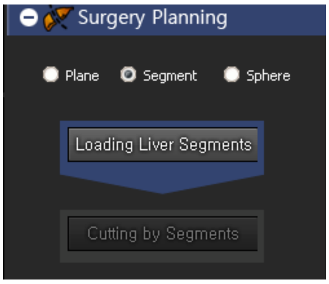

Figure 3.24. User interface for segment-based liver surgery planning module

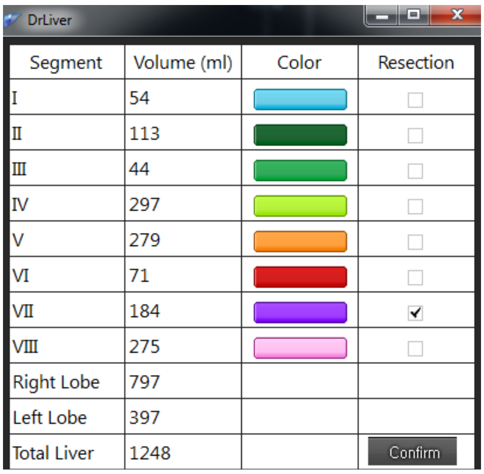

Segment	Volume (ml)	Color	Resection
I	54		☐
II	113		☐
III	44		☐
IV	297		☐
V	279		☐
VI	71		☐
VII	184		☑
VIII	275		☐
Right Lobe	797		
Left Lobe	397		
Total Liver	1248		Confirm

Figure 3.25. User interface for liver segments resection

Sphere-based Liver Surgery Planning

Use scenario of the sphere-based liver surgery planning module (Figure 3.26) consists of three steps: (1) loading the liver mask, vessels, and tumor(s), (2) interactive liver resection using a resection sphere, and (3) automatic updating and saving of the resected results and calculation of the total functional liver volume, remnant volume, and %RLV. Accordingly, a three-step user interface (Figure 3.27) was designed.

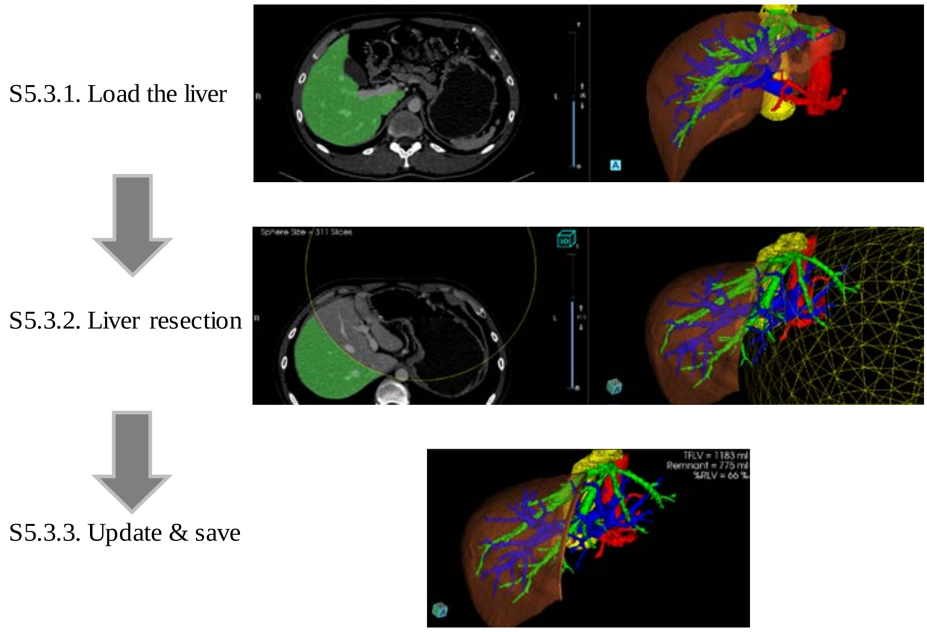

Figure 3.26. Use scenario for sphere-based liver surgery planning module

Figure 3.27. User interface for sphere-based liver surgery planning module

Chapter 4. DEVELOPMENT AND EVALUATION OF A HYBRID SEMI-AUTOMATIC LIVER SEGMENTATION METHOD

4.1. Hybrid Liver Extraction Method Development

A hybrid semi-automatic method which incorporates a fast-marching level-set method (Sethian, 1996) and a threshold-based level-set method (Lefohn et al., 2003; Hsu et al., 2010) was developed in the present study. The proposed hybrid liver segmentation method consists of five steps: (1) pre-processing of CT images, (2) selection of multiple seed points, (3) formation of an initial liver region, (4) extraction of the liver region based on the initial liver region, and (5) post-processing of the extracted liver region.

4.1.1. Preprocessing of CT images

Abdominal CT images of a patient are denoised (Figure 4.1) in the preprocessing stage. Liver extraction without denoising is difficult since the intensity distribution of the liver is irregular due to noise (Lee et al., 2007). An anisotropic diffusion filter (Perona and Malik, 1990), implemented in ITK (Ibáñez et al., 2005), was employed in the present study to reduce the effect of noise while preserving the boundaries and fine details of the organs and tissues on a CT image. The parameters of the anisotropic diffusion method used in the present study were the number of iterations = 4, time step = 0.125, and conductance parameter = 3 (Ibáñez et al., 2005).

4.1.2. Selection of Multiple Seed Points

Multiple points are selected as seed points over the liver region at different CT slices (Figure 4.2). Four to five slices are chosen with an interval of 40 to 50 slices from a CT volume dataset consisting of 150 to 300 slices with a slice thickness of 1 mm. Multiple seed points are evenly selected over the liver region including the area near the liver boundary for each slice. The number of seed points selected on each slice depends on the size of the area of the liver region (e.g., 10 to 15 points for a large liver region and 2 to 6 points for a small liver region) in each slice. The image intensity distribution information is obtained by selecting multiple seed points and utilized for better liver extraction.

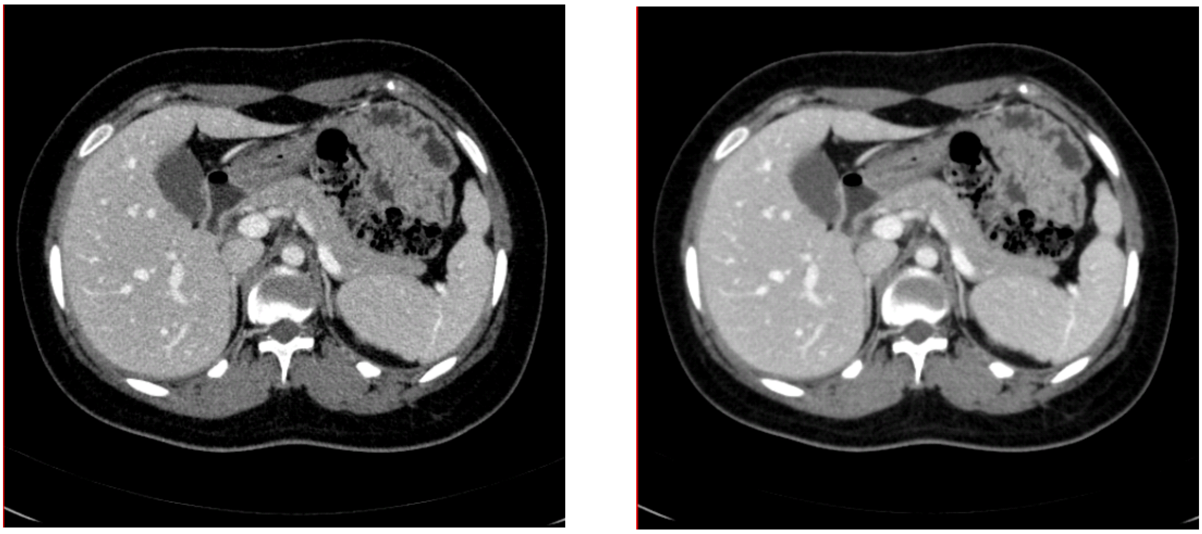

(a) (b)

Figure 4.1. Denoising of a CT image: (a) original and (b) denoised. Slices are displayed with a window of 400 and a level of 70.

4.1.3. Initial Liver Region Formation

A fast-marching level-set method (Sethian, 1996), implemented in ITK (Ibáñez et al., 2005), was customized to form an optimal initial liver region using the intensity information of the selected seed points. The customized fast-marching level-set method consists of four steps (see Figure 4.3): (1) calculation of a CT image gradient magnitude at each voxel, (2) calculation of a contour propagation speed based on the gradient magnitude at each voxel, (3) calculation of an arrival time of the propagation contour at each voxel, and (4) generation of an initial liver region based on calculated arrival times.

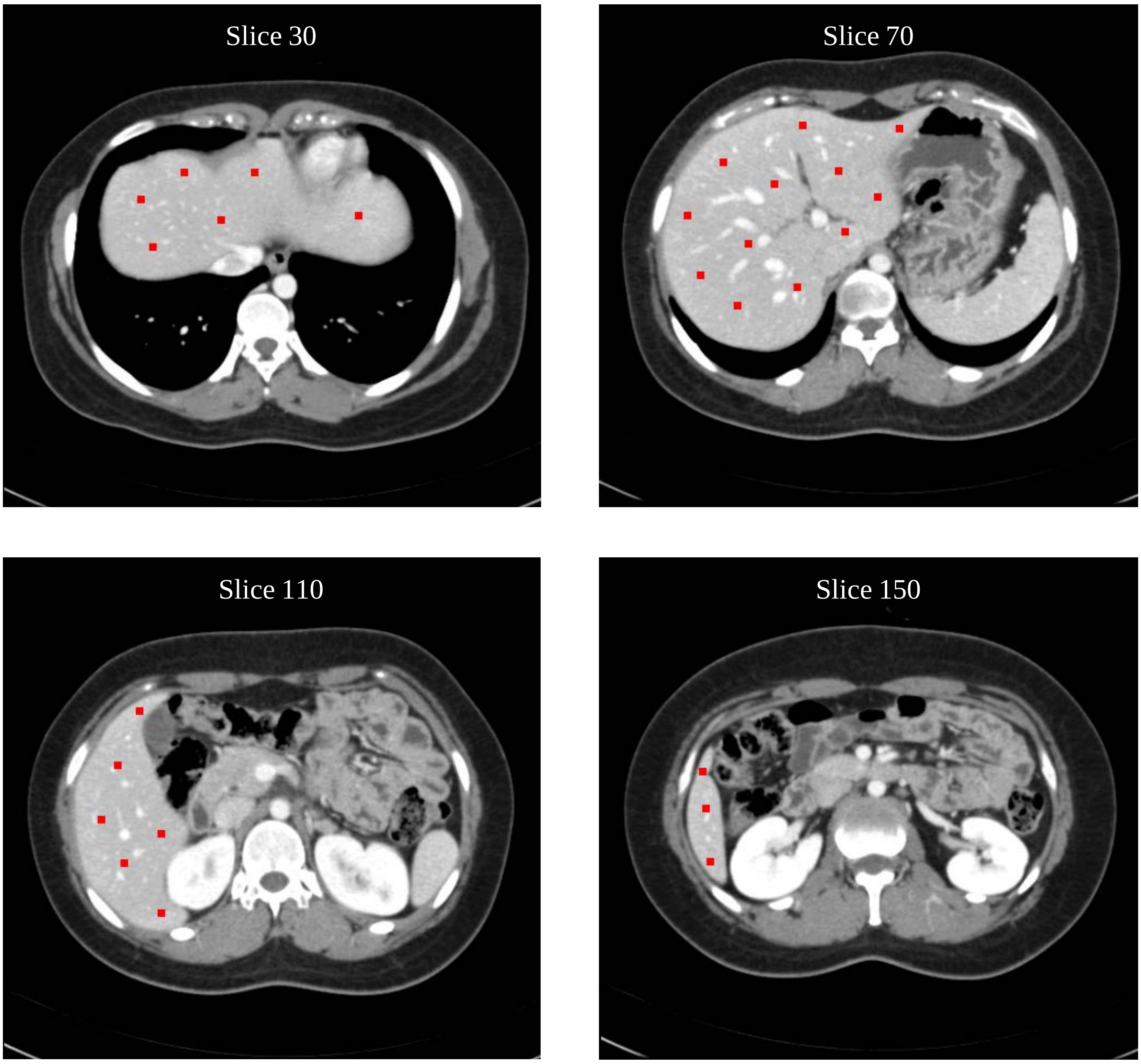

Figure 4.2. Selection of multiple seed points (shown in red dots) for liver extraction. For a CT volume dataset of 184 slices, four slices (30, 70, 110, and 150) with an interval of 40 were selected. The number of seed points selected on each slice depends on the size of the area of the liver region in each slice (e.g., 10 to 15 points for a large liver region and 2 to 6 points for a small liver region).

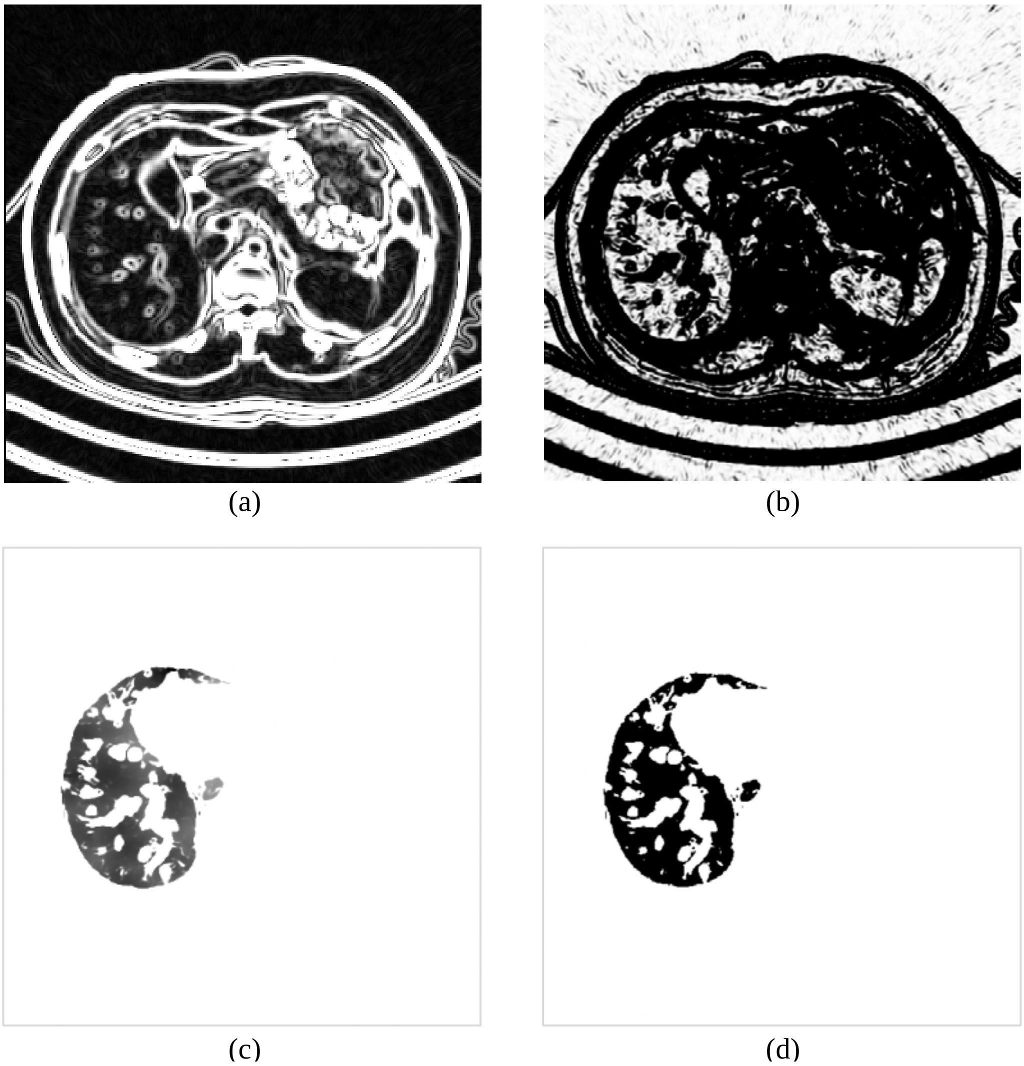

Figure 4.3. Process for an initial liver region formation: (a) calculated image gradient magnitude, (b) calculated contour propagation speed, (c) calculated arrival time of the propagating contour at each voxel, and (d) extracted initial liver region from the calculated arrival time.

First, the gradient magnitudes at the voxels of the CT dataset were calculated by performing a convolution operation with the first derivatives of the Gaussian filter (Deriche, 1990; 1993). Second, the contour propagation speeds were calculated based on the CT image gradient magnitudes using a sigmoid function (Lee et al., 2007):

$$S = \frac{1}{1 + e^{-\left((G-\beta) / \alpha \right)}} \tag{1}$$

where, G = gradient magnitude, and

α and β = parameters which magnify the intensity differences between the liver region and the non-liver region in each CT slice

Third, the arrival times of the propagation contours were calculated by solving the Eikonal equation (Eq. 2) using an upwind finite difference method for approximation to the gradient of arrival time (Sethian, 1996).

$$|\nabla T| S = 1 \qquad (2)$$

where, T = time when a contour passes a voxel, and

S = speed function which controls the propagation velocity of a contour

Lastly, an initial binary liver region was generated based on the calculated arrival times. The voxels with their arrival times in a certain threshold value were considered as the initial liver region.

An exhaustive experiment was conducted to find optimal values for the standard deviation parameter σ of the Gaussian filter, α and β of the sigmoid function, and the threshold for arrival time T, which maximize the accuracy of liver extraction. A total of 12 training CT datasets (thickness: 1 mm) provided by Chonbuk National University Medical School, South Korea, were used in the experiment. The reference segmentation of each CT dataset was manually traced by a radiologist from Chonbuk National University Medical School using Rapidia (Infinitt Co., Ltd., South Korea). The accuracy of liver extraction was assessed using similarity index (SI), the percentage of voxels overlapped between the semi-automatically extracted liver and the manually traced liver (Cabezas et al., 2011; Zijdenbos et al., 1994; Zohios et al., 2012):

$$\mathrm{SI} = 2\frac{|\mathrm{V}_{\text{semi-automatic}} \cap \mathrm{V}_{\text{manual}}|}{|\mathrm{V}_{\text{semi-automatic}}| + |\mathrm{V}_{\text{manual}}|} \times 100\% \qquad (3)$$

where, $\mathrm{V}_{\text{manual}}$ = set of manually extracted voxels, and

$\mathrm{V}_{\text{semi-automatic}}$ = set of semi-automatically extracted voxels

Due to high computation time requirement, the search intervals of parameters were narrowed down to σ = [0.1, 2.0], α = [–0.1, –0.01], β = [0.1, 0.4], and T = [40, 115] through an exhaustive experiment. Then, for each training dataset, similarity index (SI) values were calculated for the combinations of 20 × 10 × 4 × 6 parameter values (σ = 0.1 ~ 2.0 with an interval of 0.1; α = –0.1 ~ –0.01 with an interval of 0.01; β = 0.1 ~ 0.4 with an interval of 0.1; T = 40 ~ 115 with an interval of 15) to find optimal parameter values maximizing SI. As shown in Table 4.1, the average (± S.D.) optimal parameter values in the fast-marching level set method using the training datasets were σ = 1.3 (± 0.2), α = –0.05 (± 0.01), β = 0.3 (± 0.1), and $T = 85$ (± 11) where similarity index (SI) = 98.6% (± 0.4).

Table 4.1. Optimal parameter values in the fast-marching level-set method for initial liver region formation based on 12 training data sets provided by Chonbuk National University Medical School

Training Case	σ	α	β	*T*	SI (%)
1	1.2	-0.04	0.3	85	98.8
2	1.1	-0.05	0.3	70	98.6
3	1.3	-0.04	0.4	100	98.2
4	1.2	-0.06	0.3	85	99.3
5	1.3	-0.03	0.3	85	98.4
6	1.4	-0.04	0.2	85	98.4
7	1.3	-0.05	0.4	100	97.8
8	1.1	-0.05	0.3	85	98.7
9	1.4	-0.06	0.3	85	98.8
10	1.3	-0.04	0.2	100	99.1
11	1.2	-0.05	0.3	70	98.3
12	1.8	-0.05	0.3	70	98.9
Average	1.3	-0.05	0.3	85	98.6
S.D.	0.2	0.01	0.1	11	0.4

For cross-validation of these optimal parameter values, an experiment was conducted with the same protocol using 20 public training datasets (thickness: 0.7 ~ 5.0 mm; having large tumors in most cases) provided by the SLiver Grand Challenge of MICCAI 2007. As shown in Table 4.2, the average (± S.D.) optimal parameter values using the public training datasets were σ = 1.3 (± 0.2), α = –0.05 (± 0.04), β = 0.3 (± 0.1), and T = 92 (± 27), where SI = 96.9% (± 1.5). These average optimal σ, α, and β were found quite stable, whereas the optimal T was found varying but not significantly different by dataset ($t(27) = –0.98$, $p = .336$).

4.1.4. Liver Extraction Based on the Initial Liver Region

The initial liver region formed in Section 2.3 was propagated by a threshold-based level-set method (Hsu et al., 2010; Lefohn et al., 2003) implemented in ITK (Ibáñez et al., 2005) to obtain a final liver region as shown in Figure 4.4. In the threshold-based level-set method, the evolving contour was embedded as the zero level set of a level-set function $\phi(x, y, z, t)$ (Malladi et al., 1995; Osher and Sethian, 1988). The level-set evolution equation is defined as:

Table 4.2. Optimal parameter values in the fast-marching level-set method for initial liver region formation based on 20 training data sets provided by the MICCAI 2007 workshop

Training Case	σ	α	β	*T*	SI (%)
1	1.8	-0.01	0.3	70	94.9
2	1.5	-0.01	0.2	100	94.5
3	1.2	-0.01	0.2	85	93.9
4	1.4	-0.10	0.4	70	98.6
5	1.1	-0.05	0.4	115	98.2
6	1.3	-0.01	0.1	115	96.2
7	1.2	-0.02	0.2	115	97.4
8	1.4	-0.06	0.2	115	97.0
9	1.2	-0.03	0.4	85	98.3
10	1.2	-0.10	0.3	115	97.8
11	1.2	-0.10	0.4	40	98.1
12	1.2	-0.05	0.3	100	98.6
13	1.0	-0.01	0.3	40	95.8
14	0.9	-0.01	0.1	100	94.1
15	1.2	-0.08	0.2	115	98.4
16	1.9	-0.10	0.1	115	97.9
17	1.3	-0.02	0.1	115	97.0
18	1.3	-0.08	0.4	55	97.9
19	0.9	-0.05	0.4	115	98.0
20	1.1	-0.01	0.2	55	96.2
Average	1.3	-0.05	0.3	92	96.9
S.D.	0.2	0.04	0.1	27	1.5

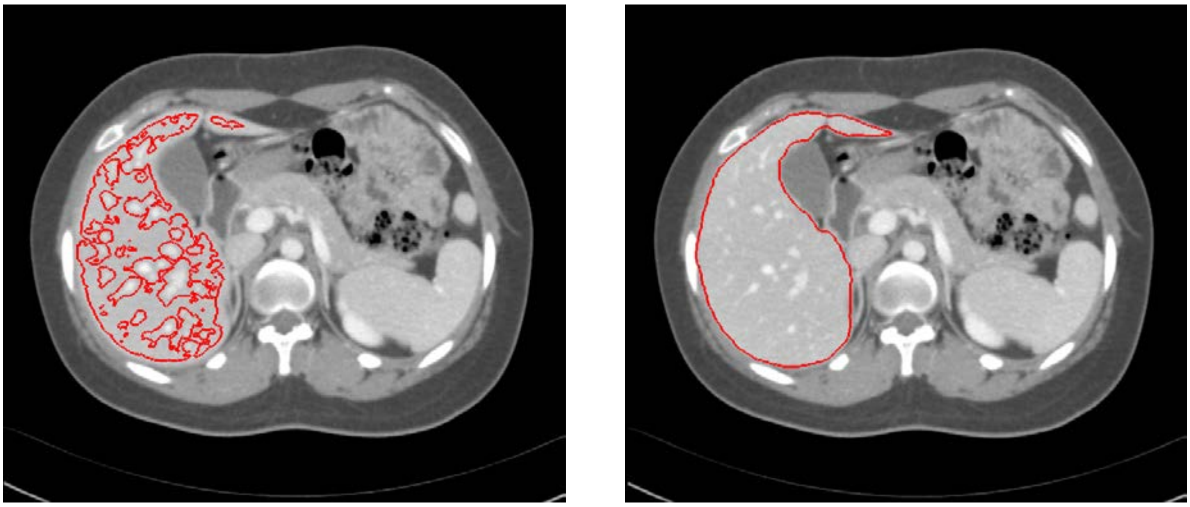

(a) (b)

Figure 4.4. Liver extraction based on an initially detected liver region: (a) initial liver region extracted by a fast-marching level-set method and (b) refined liver region after applying a threshold-based level-set method.

$$\phi_t + F|\nabla\phi| = 0, \quad (4)$$

where, F = speed term, and

$\phi(x, y, z, t = 0)$ = a level-set function embedding the initial liver region formed in Section 4.1.3

The speed term which controls the propagation of the contour is defined as:

$$F = -(\delta D(I) + (1 - \delta)\kappa) \quad (5)$$

$$D(I) = \frac{U - L}{2} - \left| I - \frac{U + L}{2} \right| \quad (6)$$

where, δ = weight ranging 0 to 1 of the curvature κ,

κ = curvature which controls the smoothness of the extracted liver region,

$D(I)$ = propagation term (contour expansion if > 0, and contraction if < 0),

I = image intensity,

L = lower threshold, and

U = upper threshold

The propagation term (shown in Figure 4.5) makes the evolving contour enclose voxels whose intensities are in the threshold interval [L, U] which was defined as [mean – S.D., mean + S.D.] based on the mean value and standard deviation of the intensity values of the selected multiple seed points. The weight δ of the curvature κ was determined as 0.95 (Hsu et al., 2010). For the threshold-based level-set evolution, the number of iterations was fixed as 100 as the stopping criterion (Lee et al., 2007).

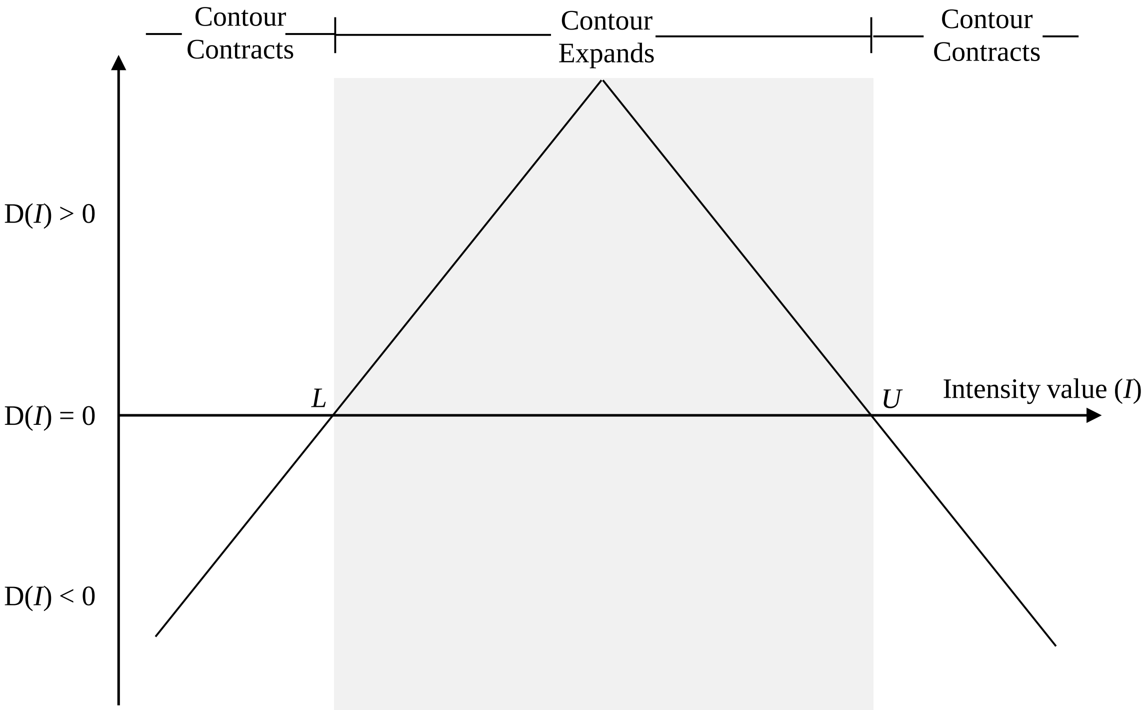

Figure 4.5. The shape of the propagation term D(*I*) for a threshold interval of [*L*, *U*].

4.1.5. Postprocessing of the Extracted Liver

The extracted contour of the liver region was smoothed (Figure 4.6) by a binary median smoothing method (Nodes and Gallagher, 1982), implemented in ITK (Ibáñez et al., 2005). The size of the median smoothing filter was determined as 3 × 3 × 3 (Ibáñez et al., 2005). The binary median smoothing method preserves the liver boundary while smoothing the extracted liver region by assigning a voxel to non-liver region if most of its neighborhood voxels belong to non-liver region, and vice versa.

 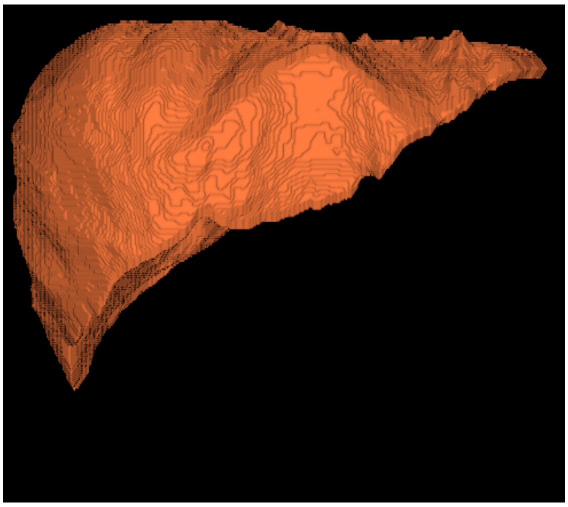

(a) (b)

 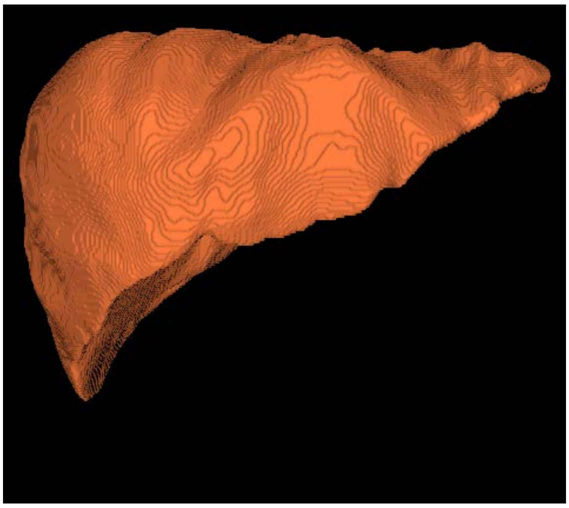

(c) (d)

Figure 4.6. Result of postprocessing: (a) refined liver region before postprocessing, (b) 3D view of refined liver regions before postprocessing, (c) surface-smoothed liver region after postprocessing, and (d) 3D view of postprocessed liver regions.

4.2. Hybrid Liver Segmentation Method Evaluation

4.2.1. Comparison with OsiriX 2D Region Growing Method

Patient Datasets

CT images of 15 patients (4 females and 11 males; average ± SD of age = 36 ± 8; average ± SD of LV = 1377.0 ± 243.6 ml), different from the 12 training datasets, provided by Chonbuk National University Medical School were used for performance evaluation of the hybrid liver extraction method in the present study. Each abdominal CT dataset consisted of 12-bit DICOM images captured from the portal phase with a resolution of 512 × 512 pixels with a thickness of 1 mm. The CT images were obtained with a 16-row multidetector CT scanner (Somatom Sensation 16, Siemens Medical Solutions, Erlangen, Germany). The potential donors fasted for more than 6 hours before CT scanning. CT scanning was performed with a breath hold at the end of inspiration. After obtaining CT images without a contrast medium, 130 mL of iopromide (Ultravist 370; Schering, Berlin, Germany) was administered at a flow rate of 3 ml/sec using a mechanical injector, followed by triphasic CT scanning during the arterial phase (AP), the portal phase (PP), and the delayed phase (DP). With use of the bolus-tracking methods (CARE Bolus, Siemens Medical Solutions), AP scanning was initiated 30 sec after enhancement of the descending aorta reached 100 HU, followed by PP scanning 40 sec after AP scanning and finally DP scanning 100 sec after PP scanning. The scanning and reconstitution parameters were as follows: detector collimation with detector thickness × number of detector rows = 1.5 mm × 16 for unenhanced scanning and 0.75 mm × 16 for enhanced scanning; table feed per gantry rotation = 24 mm for unenhanced scanning and 12 mm for enhanced scanning; gantry rotation time = 0.5 sec; slice thickness = 5 mm for unenhanced scanning and 3 mm for enhanced scanning; and reconstruction interval = 5 mm for unenhanced scanning and 1 mm for enhanced scanning.

Comparison Methods

The hybrid method was compared with the 2D region growing method implemented in OsiriX in terms of accuracy and time efficiency. The hybrid method was implemented in an in-house program run on a desktop PC with 4 GB RAM and 2.67 GHz processor. The OsiriX 2D region growing method extracts the liver in 2D with a seed point interactively selected on each slice by the user. The corresponding threshold interval for region growing is automatically determined by the OsiriX program. A preview function of segmentation results is provided by OsiriX after selecting a seed point. The user can select a seed point at different locations and check segmentation results until a proper segmentation is achieved. In accuracy assessment all the liver regions extracted from the hybrid and OsiriX 2D region growing methods were compared with the corresponding liver region manually traced by a radiologist.

Performance Measures

For evaluation of efficiency, the user interaction time and total liver extraction time were compared between the hybrid and the 2D region growing methods. For evaluation of accuracy, four measures (1) SI (%), (2) false positive error (FPE, %), (3) false negative error (FNE, %), and (4) average symmetric surface distance (ASD, mm) were employed. FPE (Eq. 7) is defined as the ratio of the total number of semi-automatically extracted voxels outside the manually extracted liver region to the total number of manually extracted voxels (Klein et al., 2009). FNE (Eq. 8) is the ratio of the total number of manually extracted voxels outside the extracted liver region to the total number of manually extracted voxels (Klein et al., 2009). Lastly, ASD is the average value of the symmetric surface distance defined as the average of minimal distances between the semi-automatically extracted liver boundary and the manually traced liver boundary, indicating the average magnitude of closeness of the semi-automatically extracted liver boundary to the manually traced liver boundary.

$$FPE = \frac{|V_{\text{semi-automatic}}| - |V_{\text{manual}} \cap V_{\text{semi-automatic}}|}{|V_{\text{manual}}|} \times 100\% \quad (7)$$

where, V_{manual} = set of manually extracted voxels, and

$V_{\text{semi-automatic}}$ = set of semi-automatically extracted voxels

$$FNE = \frac{|V_{\text{manual}}| - |V_{\text{manual}} \cap V_{\text{semi-automatic}}|}{|V_{\text{manual}}|} \times 100\% \quad (8)$$

Statistical Analysis

The paired *t*-test was conducted to find if significant differences exist between the hybrid and 2D region growing methods for the performance measures (total liver extraction time, interaction time, SI, FPE, FNE, and ASD). The statistical testing was performed using Minitab v. 16 at $\alpha = .05$.

Comparison Results

A visual inspection on the liver segmentation results over a patient's CT dataset in Figure 4.7 demonstrates that the hybrid method produces a liver extraction result closer to the golden standard than the 2D region growing method.

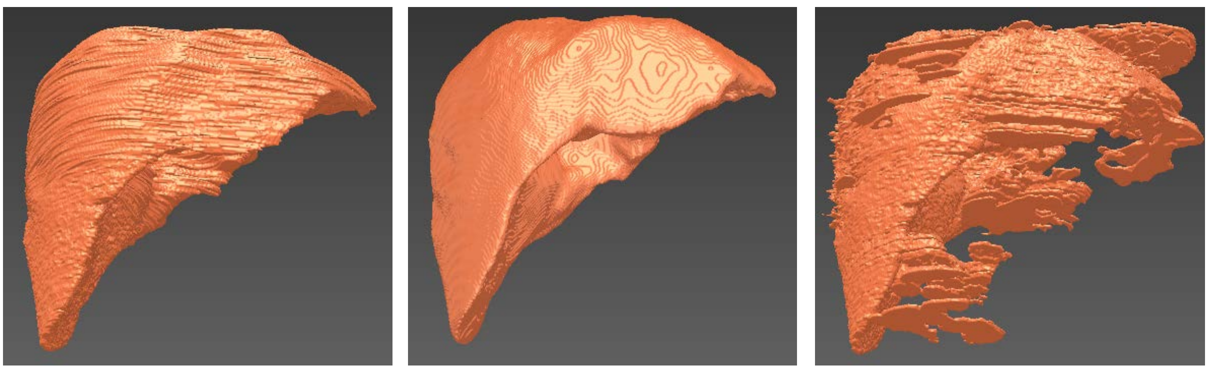

(a) (b) (c)

Figure 4.7. Visual inspection of liver extraction accuracy: (a) golden standard, (b) hybrid method, and (c) 2D region growing method.

The hybrid method was found superior to the 2D region growing method in terms of SI, FPE, FNE, and ASD as shown in Figure 4.8. The average ± SD values of SI of the hybrid and 2D region growing methods were 97.6% ± 0.5% and 94.0% ± 1.9%, respectively (Figure 4.8.a), of which their SI means were significantly different from each other ($t(16) = 6.92$, $p < .001$). The average ± SD values of FPE of the hybrid and 2D region growing methods were 2.2% ± 0.7% and 5.3% ± 1.1%, respectively (Figure 4.8.b), of which their FPE means were significantly different from each other ($t(23) = –9.07$, $p < .001$). The average ± SD values of FNE of the hybrid and 2D region growing were 2.5% ± 0.8% and 6.5% ± 3.7%, respectively (Figure 4.8.c), of which their FNE means were significantly different from each other ($t(15) = –4.19$, $p = .001$). The average ± SD values of ASD of the hybrid and 2D region growing were 1.4 ± 0.5 mm and 6.7 ± 3.8 mm, respectively (Figure 4.8.d), of which their ASD means were significantly different from each other ($t(14) = –5.35$, $p < .001$).

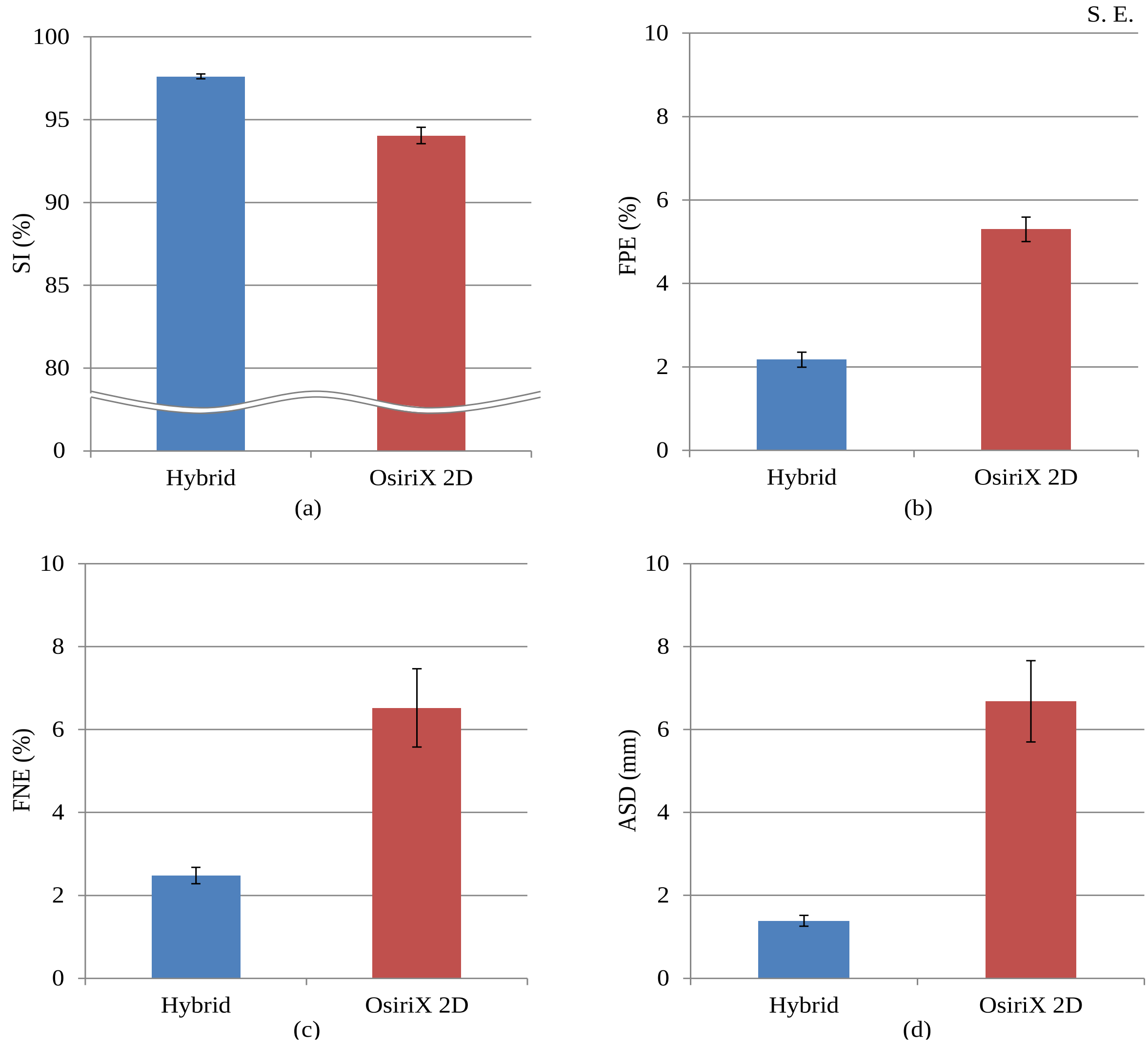

Figure 4.8. Accuracy comparison of the hybrid and OsiriX 2D region growing methods: (a) similarity index (SI), (b) false positive error (FPE), (c) false negative error (FNE), and (d) average symmetric surface distance (ASD).

Lastly, the hybrid method was found quite superior to the 2D region growing method in terms of time efficiency (Figure 4.9). The average (± SD) user interaction times (sec/CT dataset) of the hybrid and 2D region growing methods were 28 (± 4) and 484 (± 126), respectively; the average (± SD) total liver extraction times (sec/CT dataset) of the hybrid and 2D region growing methods were 77 (± 10) and 575 (± 136), respectively. The average user interaction times ($t(14) = -13.97$, $p < .001$) and the average total liver extraction times ($t(14) = -14.20$, $p < .001$) of the two methods were significantly different from each other.

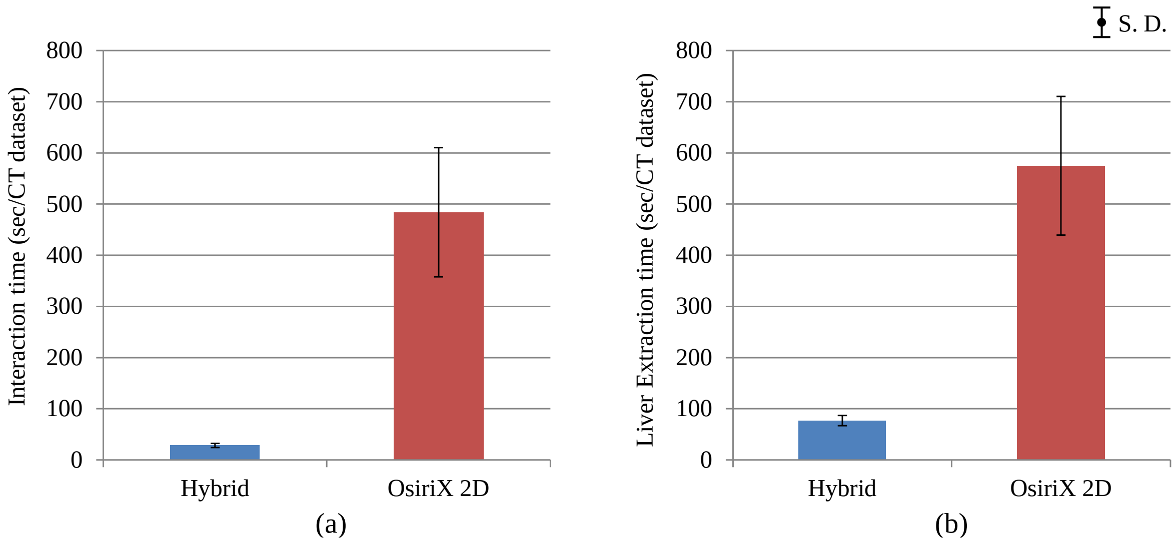

Figure 4.9. Time efficiency comparison of the hybrid and OsiriX 2D region growing methods: (a) interaction time (sec/CT dataset) and (b) total liver extraction time (sec/CT dataset).

4.2.2. Sensitivity Study

To examine the effect of seed point selection on the segmentation results, a sensitivity study was performed for the hybrid method with respect to the number of selected seed points. As shown Figure 4.10, the plotted SI over the number of selected seed points (from 5 to 60 with an interval of 5) increased rapidly as the number of selected seed points increased from 5 to 15. Then the increase of SI slowed down with the number of selected seed points increased from 15 to 30 and lastly the SI became leveled off after the number of selected seed points reached 30. In the liver segmentation experiment with the 15 test datasets in Section 4.2.1, the average (± SD) number of selected seed points for the hybrid method was 40 (± 8). Note that the 2D region growing method is sensitive to seed point selection since the segmentation results were significantly different from each other with seed points selected at different locations.

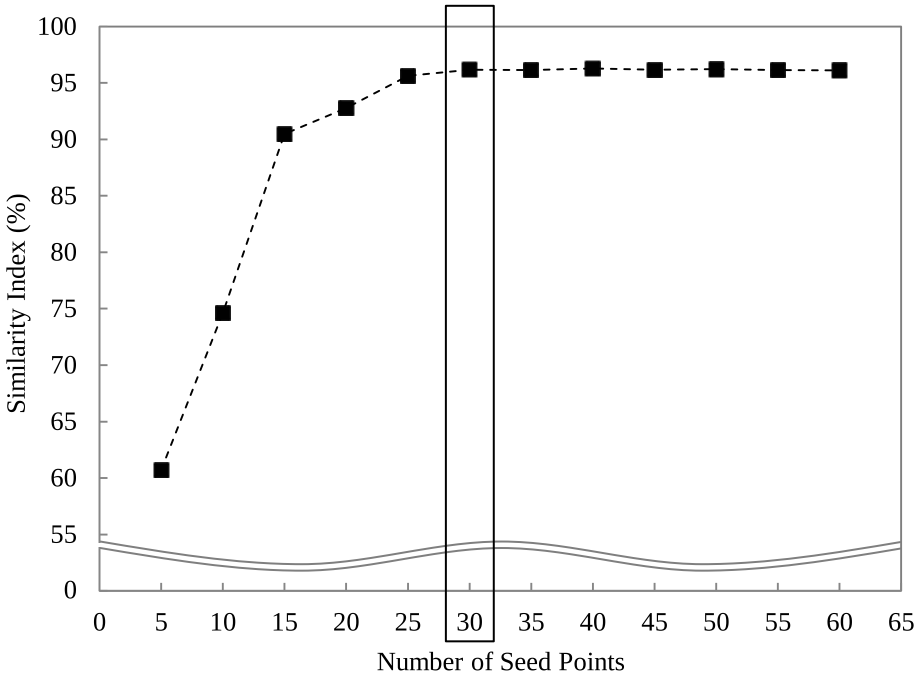

Figure 4.10. Effect of the number of selected seed points on liver segmentation results in terms of similarity index in the hybrid method.

4.2.3. Onsite Evaluation at SLIVER07 of MICCAI 2007 Workshop

The proposed hybrid method was tested using the public liver database consisting of 10 on-site test datasets provided by the SLiver Grand Challenge of MICCAI 2007. The proposed method obtained a score of 78.9. Note that the SLiver Grand Challenge does not consider computation time in performance evaluation of liver segmentation methods. This on-site assessment was performed using five different measures: volumetric overlap error (VOE, %), relative volume difference (RVD, %), ASD (mm), root mean square symmetric surface distance (RMSD, mm), and maximum symmetric surface distance (MSD, mm). Volumetric overlap is defined as the number of voxels in the intersection of the segmented and reference divided by the number of voxels in the union of the segmented and reference (Ghose et al., 2012; Muramatsu et al., 2011). RVD is defined as the difference between the segmented liver volume and the reference liver volume, divided by the reference liver volume (Eq. 10). RMSD is defined as the square root of the average squared distances between the border of the segmented and the reference. Lastly, MSD is defined as the maximum of all border voxel distances.

$$\mathrm{VOE} = \left(1 - \frac{\left|\mathrm{V}_{\mathrm{segmented}} \cap \mathrm{V}_{\mathrm{reference}}\right|}{\left|\mathrm{V}_{\mathrm{segmented}} \cup \mathrm{V}_{\mathrm{reference}}\right|}\right) \times 100\% \qquad (9)$$

where, $V_{segmented}$ = set of segmented voxels, and

$V_{reference}$ = set of reference voxels

$$RVD = \frac{\text{Segmented liver volume} - \text{Reference liver volume}}{\text{Reference liver volume}} \times 100\% \qquad (10)$$

An average (± S.D.) score of 78.9 (± 3.4) was achieved by the proposed hybrid method based on a scoring system that combines the five metrics VOE, RVD, ASD, RMSD, and MSD into a single overall score (Heimann et al., 2009). The negative average value of the RVD (-0.8%) of the hybrid method showed that livers were under-segmented, which is mostly due to exclusion of large branches of the portal vein in liver segmentation as shown in Figure 4.11.

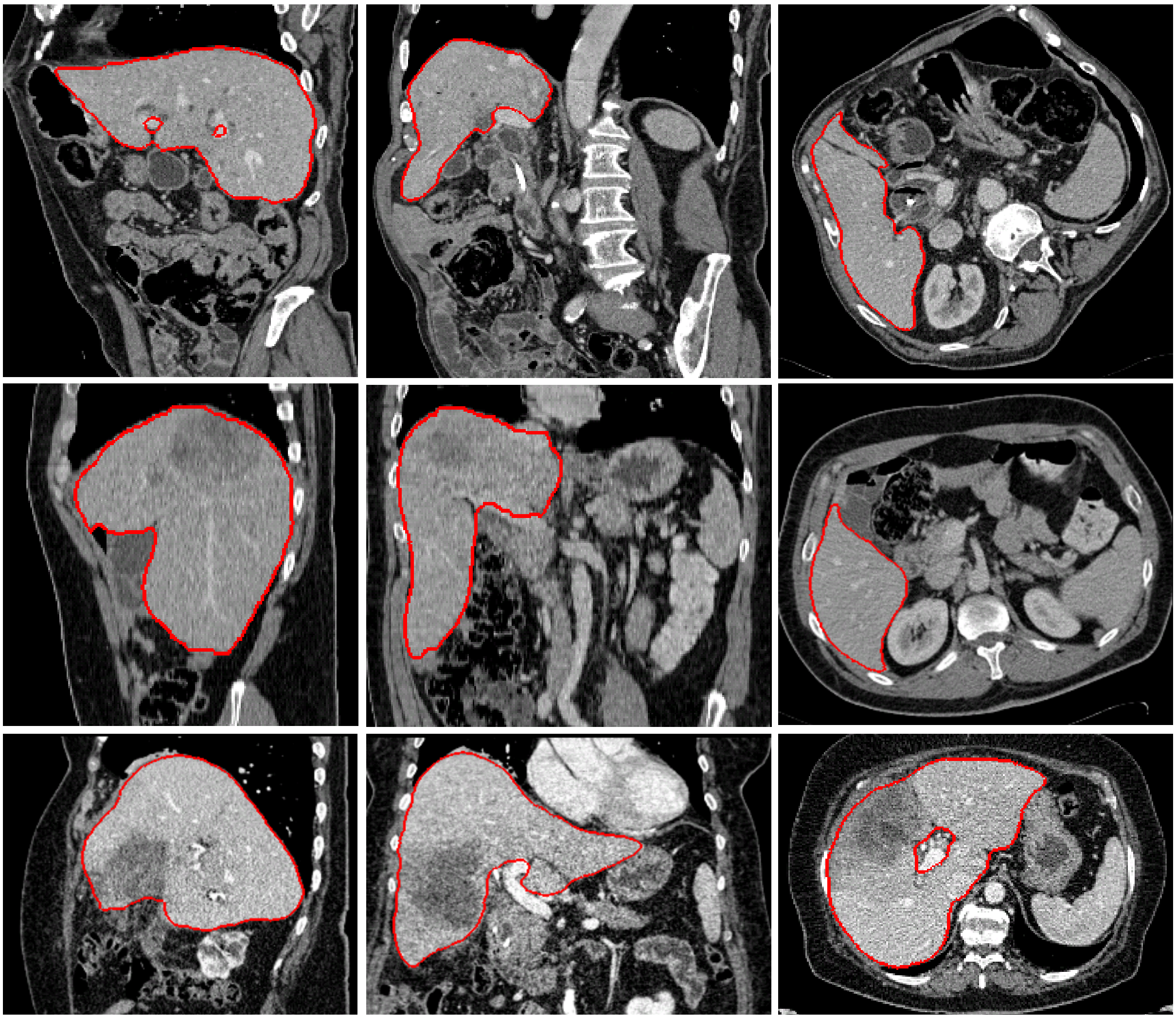

Figure 4.11. Segmentation results of the hybrid method for the onsite competition data from MICCAI 2007 workshop: from left to right, sagittal, coronal, and transversal slices from a relatively easy case (top), an average case (middle), and a relatively difficult case (bottom).

Chapter 5. DEVELOPMENT OF AN INTERACTIVE PROCEDURE FOR EFFICIENT SEGMENTATION OF LIVER VESSELS

5.1. Interactive Segmentation Method Development

An interactive vessel segmentation method was developed in the present study consisting of six steps: (1) pre-processing of CT images, (2) selection of multiple seed points, (3) identification of multiple threshold intervals, (4) vessel segmentation with identified threshold intervals using region growing method, (5) display of multiple segmentation results and selection of an appropriate segmentation result, and (6) interactive editing of the extracted vessel trees.

5.1.1. Preprocessing of CT images

CT images from arterial, portal venous, and hepatic venous phases were denoised, registered, and masked (Figure 5.1) for extraction of hepatic artery, portal vein, and hepatic vein respectively. An anisotropic diffusion filter (Perona and Malik, 1990), implemented in ITK (Ibáñez et al., 2005), was performed in the present study to reduce the effect of noise while preserving the boundaries and fine details of the organs and tissues on a CT image. The parameters of the anisotropic diffusion method used in the present study were the number of iterations = 4, time step = 0.125, and conductance parameter = 3 (Ibáñez et al., 2005). A non-rigid registration procedure based on Thirion's Demons algorithm (Thirion, 1995; 1998), implemented in ITK (Ibáñez et al., 2005), was employed to register arterial and hepatic venous phases to portal venous phase in order to avoid misalignment among the extracted hepatic artery, portal vein, and hepatic vein due to patient movements during CT scanning procedure. CT images were masked using the extracted liver in Chapter 4 to remove surroundings of the liver. The roots of the hepatic artery, portal vein, and hepatic vein outside of the extracted liver were interactively added to the liver mask.

5.1.2. Selection of Multiple Seed Points

Multiple points were interactively selected as seed points over the vascular region at different CT slices. More than 30 seed points were randomly selected at two or three CT slices in order to obtain the intensity distribution information of vessel structures to be extracted (Figure 5.2).

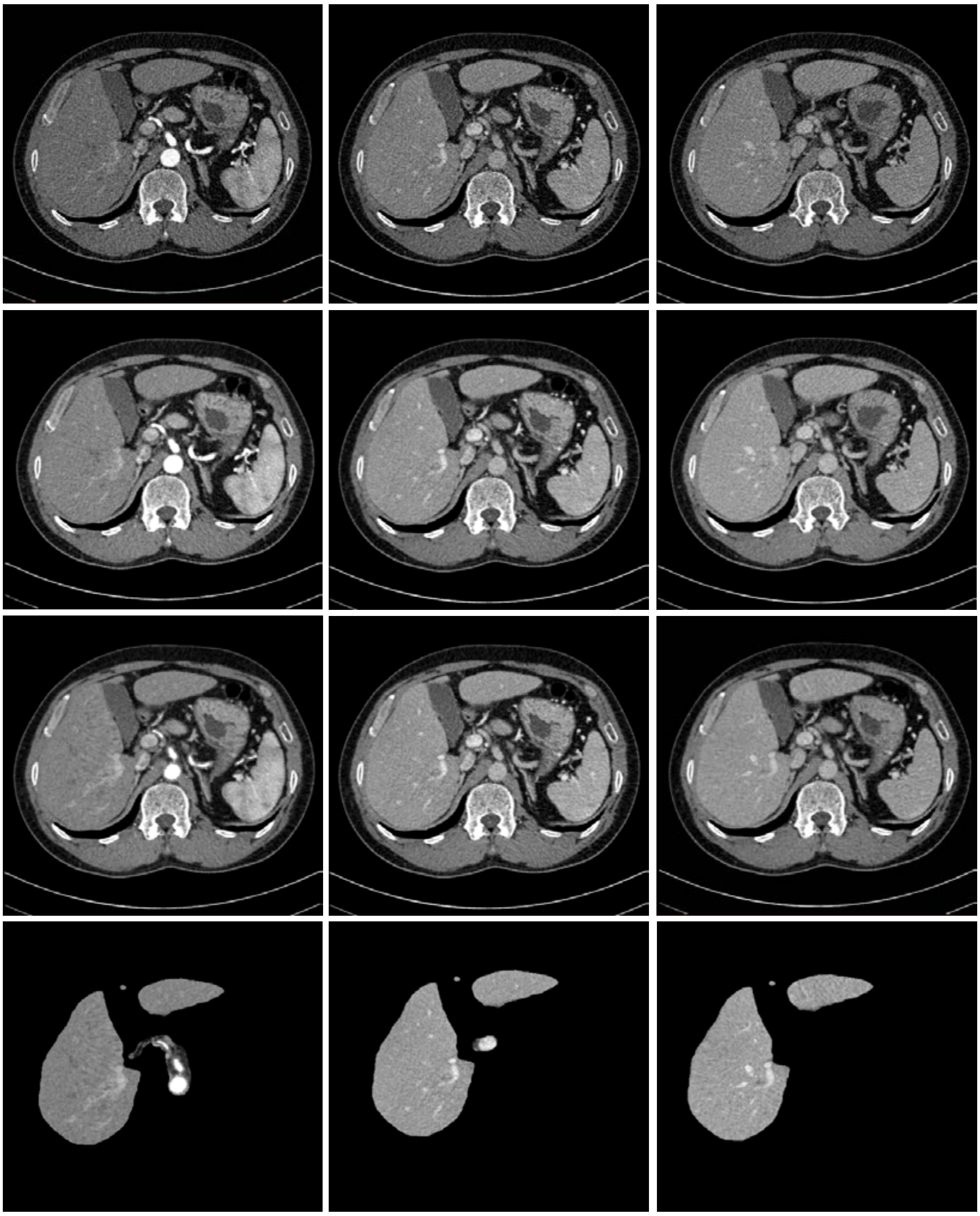

Figure 5.1. Pre-processing of CT images of arterial (left column), portal venous (middle column), and hepatic venous (right column) phases for vessel extraction. First the top row to bottom row are original CT images, denoised CT images, registered CT images to portal venous phase, and masked CT images.

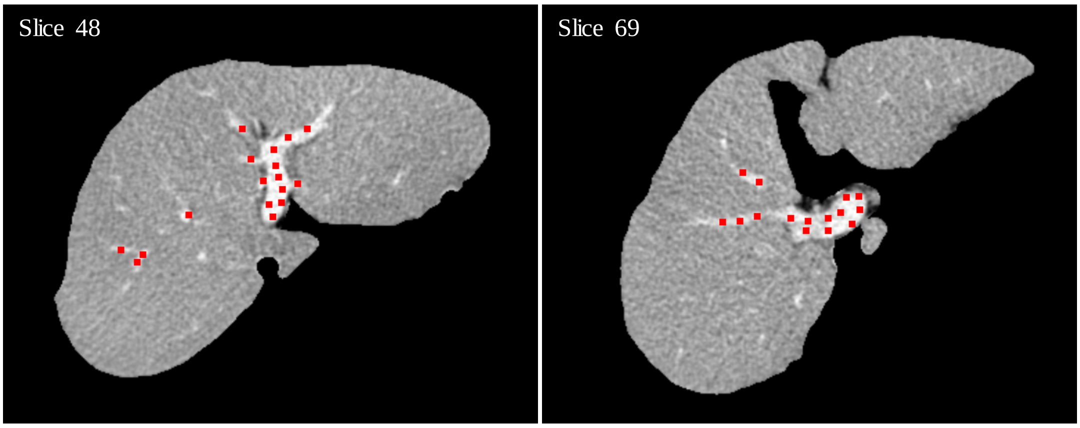

Figure 5.2. Selection of seed points (17 points at the left slice and 15 at the right slice) over portal vein region at two slices in a CT volume of 160 slices for portal vein extraction

5.1.3. Identification of Threshold Intervals

Multiple threshold intervals were determined by the average value (μ) and standard deviation (σ) of the intensity values of the selected multiple seed points as $[\mu - a\sigma, \mu + b\sigma]$, where a and b are parameters to be determined. An experiment was conducted to find appropriate values for a and b which maximize the accuracy of vessel extraction. Thirty training CT data sets (10 from Chonbuk National University Medical School, South Korea with a slice thickness of 1 mm, 20 from MICCAI 2007 workshop with a slice thickness from 0.7 to 5.0 mm and large tumors in most cases) were used in the experiment. The accuracy of vessel extraction was assessed by an expert radiologist. The space for finding appropriate parameter values was narrowed down after exhaustive experiments due to computational expense. The narrowed space consisted of 5 × 5 × 30 trials of vessel extraction (a and b: 1.0 ~ 3.0 with an interval of 0.5). As shown in Table 5.1, the average values (± S.D.) for a (ranged from 1.0 to 2.0) and b were 1.4 (± 0.4) and 3.0 (± 0.0), based on which, six threshold intervals, $[\mu - 1.0\sigma, \mu + 3.0\sigma]$, $[\mu - 1.2\sigma, \mu + 3.0\sigma]$, $[\mu - 1.4\sigma, \mu + 3.0\sigma]$, $[\mu - 1.6\sigma, \mu + 3.0\sigma]$, $[\mu - 1.8\sigma, \mu + 3.0\sigma]$, and $[\mu - 2.0\sigma, \mu + 3.0\sigma]$ were determined as candidates for vessel extraction.

Table 5.1. Appropriate parameter values for identification of threshold intervals for vessel extraction based on 30 training data sets

Training Case	*a*	*b*
1	1.5	3.0
2	2.0	3.0
3	1.5	3.0
4	1.5	3.0
5	1.0	3.0
6	1.0	3.0
7	2.0	3.0
8	1.0	3.0
9	1.0	3.0
10	1.0	3.0
11	1.5	3.0
12	2.0	3.0
13	1.5	3.0
14	1.0	3.0
15	1.5	3.0
16	1.5	3.0
17	2.0	3.0
18	1.0	3.0
19	1.5	3.0
20	1.5	3.0
21	1.0	3.0
22	2.0	3.0
23	1.5	3.0
24	1.0	3.0
25	1.5	3.0
26	2.0	3.0
27	1.0	3.0
28	1.5	3.0
29	1.0	3.0
30	1.5	3.0
Average	1.4	3.0
S.D.	0.4	0.0

5.1.4. Vessel Extraction Based on Multiple Threshold Intervals

The vessel trees were extracted using a connected threshold region growing method in ITK (Ibáñez et al., 2005) based on selected multiple seed points in Section 5.1.2 and identified six threshold intervals in Section 5.1.3. Starting from multiple seed points, the region growing method searches neighbouring voxels and adds voxels to the extracted vessel trees if the voxels are within a given threshold interval. In the present study, six vessel trees were extracted based on the six threshold intervals identified in Section 5.1.3.

5.1.5. Selection of an Appropriate Segmentation Result

A user-friendly interface (Figure 5.3) was designed for the user to verify and select an appropriate vessel extraction result. The six extracted vessel trees in Section 5.1.4 with volume information were sequentially shown to the user from the smallest to the largest threshold intervals. Checkboxes were provided for interactive selection of an appropriate segmentation result.

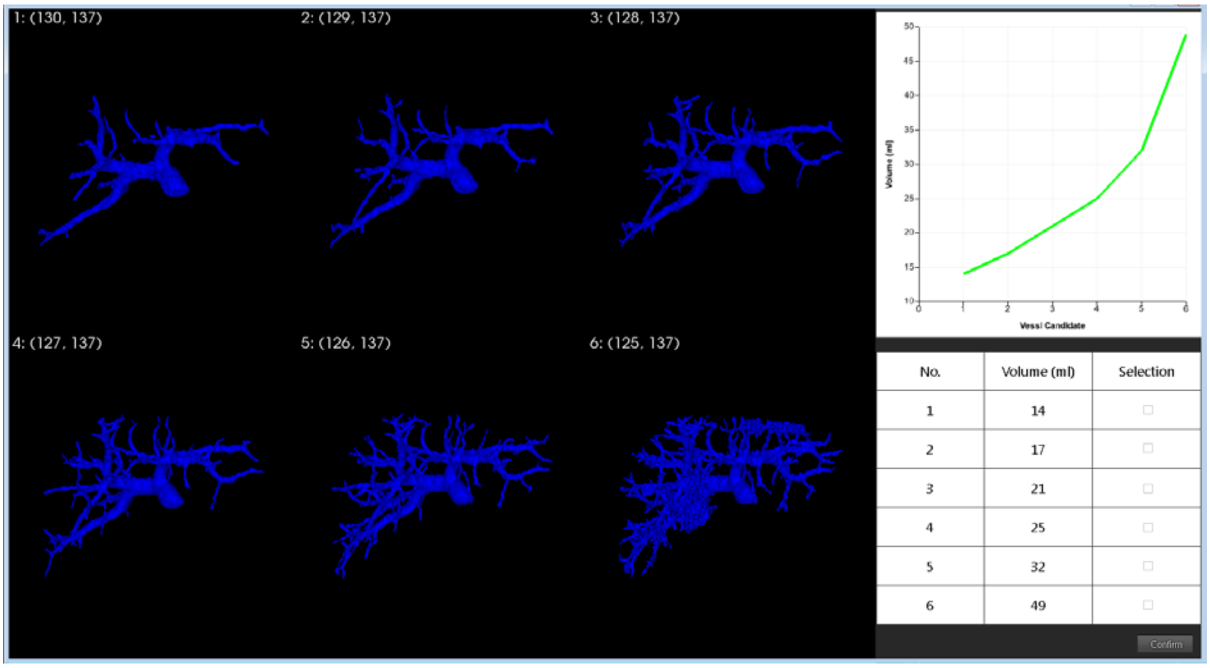

Figure 5.3. An interface for the user to verify and select an appropriate vessel extraction result from six candidates

5.1.6. Editing of Extracted Vessel Trees

The extracted vessel trees were edited using a scalable editing sphere to improve extraction accuracy if necessary. CT images of a patient were overlaid with the extracted vessel mask and the user can interactively remove a falsely extracted part or add a missing vessel part while visually verifying the segmentation result.

5.2. Interactive Segmentation Method Evaluation

5.2.1. Patient Datasets

CT images of 15 patients (4 females and 11 males; average ± SD of age = 36 ± 8; average ± SD of LV = 1377.0 ± 243.6 ml), different from the 12 training datasets, provided by Chonbuk National University Medical School were used for performance evaluation of the hybrid liver extraction method in the present study. Each abdominal CT dataset consisted of 12-bit DICOM images captured from the portal phase with a resolution of 512 × 512 pixels with a thickness of 1 mm. The CT images were obtained with a 16-row multidetector CT scanner (Somatom Sensation 16, Siemens Medical Solutions, Erlangen, Germany). The potential donors fasted for more than 6 hours before CT scanning. CT scanning was performed with a breath hold at the end of inspiration. After obtaining CT images without a contrast medium, 130 mL of iopromide (Ultravist 370; Schering, Berlin, Germany) was administered at a flow rate of 3 ml/sec using a mechanical injector, followed by triphasic CT scanning during the arterial phase (AP), the portal phase (PP), and the delayed phase (DP). With use of the bolus-tracking methods (CARE Bolus, Siemens Medical Solutions), AP scanning was initiated 30 sec after enhancement of the descending aorta reached 100 HU, followed by PP scanning 40 sec after AP scanning and finally DP scanning 100 sec after PP scanning. The scanning and reconstitution parameters were as follows: detector collimation with detector thickness × number of detector rows = 1.5 mm × 16 for unenhanced scanning and 0.75 mm × 16 for enhanced scanning; table feed per gantry rotation = 24 mm for unenhanced scanning and 12 mm for enhanced scanning; gantry rotation time = 0.5 sec; slice thickness = 5 mm for unenhanced scanning and 3 mm for enhanced scanning; and reconstruction interval = 5 mm for unenhanced scanning and 1 mm for enhanced scanning.

5.2.2. Segmentation Accuracy Evaluation

The correctness of vessel branches, connections between different vessel trees, and suitability for liver surgery planning were assessed by an expert radiologist for evaluation of segmentation accuracy.

Correctness of Vessel Branches

The radiologist was asked to detect false positive and false negative errors in extracted vessel branches. No false positive errors were found by the radiologist. False negative errors were identified at some distal branches due to small diameter and low contrast (Figure 5.4).

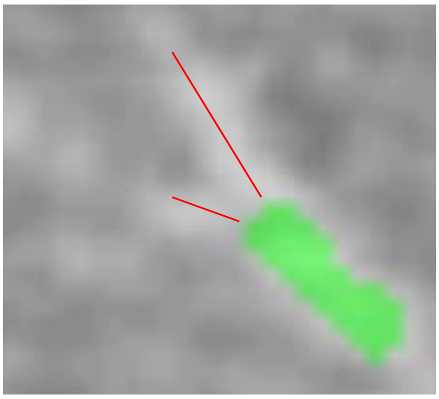

Figure 5.4. A missing branch (red) at the distal part of an extracted vessel tree (green)

Connections between Vessel Trees

The three vessel trees, hepatic artery, portal vein, and hepatic vein should be separately extracted without connections between each other for clinical application such as surgery planning. No connections among the three vessel trees (Figure 5.5) were found in the 15 segmented data sets.

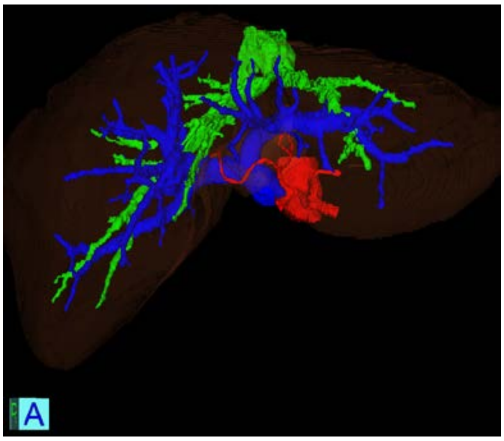

Figure 5.5. Extracted hepatic artery (red), portal vein (blue), and hepatic vein (green)

Suitability for Liver Surgery Planning

A 7-point Likert scale was used for assessment of suitability for liver surgery planning, ‘1’ for very poor and ‘7’ for very good. The average (± S.D.) score of suitability for liver surgery planning was 6.4 (± 0.7).

5.2.3. Segmentation Efficiency Evaluation

User interaction time and total vessel extraction time were measured for evaluation of segmentation efficiency. The average (± S.D.) user interaction time was 33 (± 4) sec. The average (± S.D.) total vessel extraction time was 75 (± 8) sec.

Chapter 6. USABILITY TEST OF THE DEVELOPED VIRTUAL LIVER SURGERY PLANNING SYSTEM

The usability tests of the developed virtual liver surgery planning system *Dr. Liver* consisting of (1) preliminary test and (2) main test were conducted under the same test protocol at different system development stages. To identify potential usability problems at an early system development stage, a preliminary test was conducted with three male medical doctors (aged from 30s to 40s; experienced in liver anatomy and liver surgery) from a medical center. As shown in Table 6.1, improvements have been made for the five modules (Liver Extraction, Vessel Extraction, Tumor Extraction, Liver Segmentation, and Liver Surgery Planning) of *Dr. Liver* based on the preliminary usability test results. Then a main test was conducted with 10 male medical doctors (aged from 30s to 60s; experienced in liver anatomy and liver surgery; three of them participated in the preliminary test) from five different medical centers to verify the improvements and identify new usability problems.

6.1. Test Procedures

The usability test was performed in a secure room for each individual participant, administered by a test monitor. The usability test consisted of three sessions, pre-test, test, and post-test sessions, which lasted about two hours in total. At the pre-test session, paper manual and video demonstrations of the developed surgery planning system were provided to teach a participant how to use the system. Then the usability testing was introduced by reading an orientation script. Exhaustive practice was allowed for a participant to be familiar with the system. After that, an informed consent was obtained.
In the test session, five modules of usability evaluation were conducted in sequence: (1) liver extraction, (2) vessel extraction, (3) tumor extraction, (4) liver segmentation, and (5) liver surgery planning. The order of the five modules followed the use scenario of the developed virtual liver surgery planning system for pre-operative liver surgery planning. During each test module, the performance of a participant was evaluated using various measures including accuracy measures, task completion times, number of mouse clicks, and number of keystrokes. After each module, a questionnaire was provided to survey a participant’s subjective usability assessment, likes, dislikes, and open suggestions. A 10-min. break was offered after every two modules.

Lastly, in the post-test session, debriefing was performed to learn more details. Questions raised from observations during the test session such as tasks not completed and critical comments were addressed and discussed.

Table 6.1. Improvements made based on a preliminary usability test of *Dr. Liver*

<table>
<tr><th colspan="2">Modules</th><th>Improvements</th></tr>
<tr><td colspan="2">Liver Extraction</td><td>1. Synchronization between 2D CT and 3D model views for liver contour editing
2. Providing hotkey menus on 2D CT screen for CT image manipulation such as seed point selection, CT image zooming in/out, window/level adjustment, contour editing, CT image translation, undo function, and transparency adjustment</td></tr>
<tr><td colspan="2">Vessel Extraction</td><td>1. Synchronization between 2D CT and 3D model views for vessel contour editing
2. Providing hotkey menus on 2D CT screen for CT image manipulation
3. Using masked CT images with the extracted liver region to remove surroundings of the liver
4. Automatic thresholding, instead of manual adjustment of thresholds
5. Providing multiple candidates of extracted vessel trees for the user to select an appropriate result</td></tr>
<tr><td colspan="2">Tumor Extraction</td><td>1. Synchronization between 2D CT and 3D model views for tumor contour editing
2. Providing hotkey menus on 2D CT screen for CT image manipulation
3. Automatic thresholding, instead of manual adjustment of thresholds</td></tr>
<tr><td rowspan="2">Liver Segmentation</td><td>Plane-based</td><td>1. Point selection step eliminated
2. Automatic generation of the segmentation plane</td></tr>
<tr><td>Sphere-based</td><td>1. Synchronization between 2D CT and 3D model views for liver segmentation
2. Providing hotkey menus on 2D CT screen for CT image manipulation
3. Providing a large sphere instead of a small sphere for liver segmentation</td></tr>
<tr><td rowspan="3">Liver Surgery Planning</td><td>Plane-based</td><td>1. Providing a cube box around the resection plane to indicate location and orientation of the resection plane</td></tr>
<tr><td>Segment-based</td><td>None</td></tr>
<tr><td>Sphere-based</td><td>1. Synchronization between 2D CT and 3D model views for liver surgery planning
2. Providing hotkey menus on 2D CT screen for CT image manipulation
3. Providing a large sphere instead of a small sphere for liver surgery planning</td></tr>
</table>

6.2. Usability Assessment Measures and Questionnaires

Six performance (time, similarity index, false positive error, false negative error, number of mouse clicks, and number of keystrokes) and seven preference (usefulness, ease of use, learnability, informativeness, clarity, tolerance, and overall satisfaction) measures were incorporated into the usability test. Different sets of performance and preference measures were applied to each test module (see Table 6.2) by considering the task of each test module. As an example, in Module 1: liver extraction, the time to finish the liver extraction task, number of mouse clicks, and number of

Table 6.2. Usability test measures for the developed virtual liver surgery planning system*

Modules		Performance Measures						Preference Measures						
		Completion time	Number of mouse clicks	Number of keystrokes	Similarity index	False positive error	False negative error	Usefulness	Ease of use	Learnability	Informa-tiveness	Clarity	Tolerance	Satisfaction
Liver extraction		○	○	○	○	○	○	○	○	○	○	○	○	○
Vessel extraction	Portal vein	○	○	○				○	○	○	○	○	○	○
	Hepatic artery	○	○	○				○	○	○	○	○	○	○
	Hepatic vein	○	○	○				○	○	○	○	○	○	○
	IVC	○	○	○				○	○	○	○	○	○	○
Tumor extraction		○	○	○	○	○	○	○	○	○	○	○	○	○
Liver segmentation	Plane-based	○	○	○				○	○	○	○	○	○	○
	Sphere-based	○	○	○				○	○	○	○	○	○	○
Liver surgery planning	Plane-based	○	○	○				○	○	○	○	○	○	○
	Segment-based	○	○	○				○	○	○	○	○	○	○
	Sphere-based	○	○	○				○	○	○	○	○	○	○

* ○: Applied measure

keystrokes were automatically measured by *Dr. Liver*. Similarity index, false positive error and false negative error of the extracted liver regions were measured by comparing to a golden standard (manually traced liver regions by a radiologist). Seven criteria (usefulness, ease of use, learnability, informativeness, clarity, tolerance, and overall satisfaction) were used to evaluate the participants' preference with *Dr. Liver*. Based on the evaluation measure matrix table, usability assessment questionnaires were designed for each test module. Table 6.3 shows sample questions for subjective assessment of Module 1 (liver extraction).

6.3. Test Results

Module 1: Liver Extraction

Time, number of mouse clicks, and number of keystrokes to extract the liver were automatically recorded by *Dr. Liver* system. The average (S.D.) time (unit: min) to extract the liver was 3.0 (0.5). The average (S.D.) number of mouse clicks was 78 (9). The average (S.D.) of keystrokes was 17 (3).

Similarity index, false positive error, and false negative error were measured by comparing the extracted liver region to the golden standard. The average (S.D.) similarity index (unit: %) was 96.8 (0.4). The average (S.D.) false positive error (unit: %) was 2.4 (0.3). The average (S.D.) false positive error (unit: %) was 2.8 (0.3).

Consistently high evaluation scores were given for the usability of the liver extraction module (see Module 1 in Table 6.4). The average (S.D.) of the assessments of the liver extraction module was 6.3 (0.6).

Module 2: Vessel Extraction

The average (S.D.) time (unit: min) to extract the portal vein was 1.4 (0.2). The average (S.D.) number of mouse clicks was 21 (5). The average (S.D.) of keystrokes was 10 (3). High evaluation scores were given for the usability of the portal vein extraction module (see Module 2 in Table 6.4). The average (S.D.) of the assessments of the portal vein extraction module was 6.2 (0.8).

The average (S.D.) time (unit: min) to extract the hepatic artery was 2.3 (0.3). The average (S.D.) number of mouse clicks was 46 (7). The average (S.D.) of keystrokes was 17 (4). The average (S.D.) of the assessments of the hepatic artery extraction module was 6.1 (0.8).

Table 6.3. Preference assessment questions (selected)

No	Questions	Very Poor	Poor	Slightly Poor	Fair	Slightly Good	Good	Very Good
1	How useful is it for extracting the liver from DICOM images?	①	②	③	④	⑤	⑥	⑦
2	How easy is it to use?	①	②	③	④	⑤	⑥	⑦
3	How easy is it to learn the steps of liver extraction?	①	②	③	④	⑤	⑥	⑦
4	How adequate is the information provided?	①	②	③	④	⑤	⑥	⑦
5	How clear are the step names?	①	②	③	④	⑤	⑥	⑦
6	How adequate is the tolerance to allow you make mistakes?	①	②	③	④	⑤	⑥	⑦
No	**Questions**	**Very Dissatisfied**	**Dissatisfied**	**Slightly Dissatisfied**	**Neutral**	**Slightly Satisfied**	**Satisfied**	**Very Satisfied**
7	What is your overall satisfaction with the liver extraction module?	①	②	③	④	⑤	⑥	⑦

Table 6.4. Average (S.D.s) of preference assessments

Modules		Preference Measures						
		Usefulness	**Ease of use**	**Learnability**	**Informa-tiveness**	**Clarity**	**Tolerance**	**Satisfaction**
Liver extraction		6.4 (0.5)	6.4 (0.5)	6.4 (0.5)	6.4 (0.5)	6.6 (0.5)	5.6 (0.8)	6.3 (0.5)
Vessel extraction	Portal vein	6.4 (0.5)	6.1 (0.7)	6.3 (0.8)	6.1 (0.7)	6.6 (0.5)	5.6 (1.3)	6.0 (0.6)
	Hepatic artery	6.0 (0.9)	5.7 (1.0)	6.0 (1.1)	5.8 (1.0)	6.3 (0.5)	5.5 (0.5)	6.0 (0.6)
	Hepatic vein	6.4 (0.5)	6.3 (0.5)	6.4 (0.8)	6.1 (0.7)	6.4 (0.5)	5.7 (1.0)	6.1 (0.4)
	IVC	6.4 (0.5)	6.2 (0.4)	6.4 (0.5)	6.0 (0.7)	6.4 (0.5)	5.8 (0.4)	6.0 (0.0)
Tumor extraction		6.0 (0.0)	6.3 (0.5)	6.0 (0.8)	6.0 (0.8)	6.3 (0.5)	6.5 (0.6)	6.3 (0.5)
Liver segmentation	Plane-based	6.0 (0.0)	4.5 (2.1)	4.5 (2.1)	5.5 (0.7)	6.0 (0.0)	5.0 (1.4)	5.5 (2.1)
	Sphere-based	6.5 (0.7)	6.5 (0.7)	6.0 (1.4)	6.5 (0.7)	6.5 (0.7)	6.5 (0.7)	6.5 (0.7)
Liver surgery planning	Plane-based	6.3 (0.5)	6.3 (0.8)	6.0 (1.1)	6.3 (0.5)	6.5 (0.5)	5.5 (1.0)	6.2 (1.0)
	Segment-based	5.7 (0.6)	7.0 (0.0)	6.0 (0.0)	6.0 (0.0)	6.3 (0.6)	6.0 (0.0)	6.0 (0.0)
	Sphere-based	6.7 (0.5)	6.3 (1.0)	6.3 (0.8)	6.4 (0.5)	6.7 (0.5)	6.0 (0.8)	6.1 (0.7)

* Used a 7-point Likert scale, ‘1’ for very poor or very dissatisfied and ‘7’ for very good or very satisfied

The average (S.D.) time (unit: min) to extract the hepatic vein was 1.4 (0.2). The average (S.D.) number of mouse clicks was 19 (7). The average (S.D.) of keystrokes was 5 (2). The average (S.D.) of the assessments of the hepatic vein extraction module was 6.2 (0.7).

The average (S.D.) time (unit: min) to extract the IVC was 1.5 (0.2). The average (S.D.) number of mouse clicks was 19 (4). The average (S.D.) of keystrokes was 7 (3). The average (S.D.) of the assessments of the IVC extraction module was 6.2 (0.5).

Module 3: Tumor Extraction

The average (S.D.) time (unit: min) to extract the tumor was 2.9 (0.1). The average (S.D.) number of mouse clicks was 22 (4). The average (S.D.) of keystrokes was 5 (1). The average (S.D.) similarity index (unit: %) was 97.3 (0.8). The average (S.D.) false positive error (unit: %) was 1.9 (0.2). The average (S.D.) false positive error (unit: %) was 2.3 (0.2). The average (S.D.) of the assessments of the tumor extraction module was 6.2 (0.5).

Module 4: Liver Segmentation

The average (S.D.) time (unit: min) to segment the liver with segmentation plane was 5.0 (0.6). The average (S.D.) number of mouse clicks was 44 (13). The average (S.D.) of keystrokes was 0 (0). The average (S.D.) of the assessments of the plane-based liver segmentation module was 5.3 (1.3). The low score was due to hard control of the segmentation plane.

The average (S.D.) time (unit: min) to segment the liver with segmentation sphere was 4.6 (0.4). The average (S.D.) number of mouse clicks was 21 (4). The average (S.D.) of keystrokes was 5 (2). The average (S.D.) of the assessments of the sphere-based liver segmentation module was 6.5 (0.6).

Module 5: Liver Surgery Planning

The average (S.D.) time (unit: min) to plan the liver surgery using a resection plane was 2.1(0.4). The average (S.D.) number of mouse clicks was 28 (6). The average (S.D.) of keystrokes was 4 (1). The average (S.D.) of the assessments of the liver surgery planning using a resection plane module was 6.2 (0.8).

The average (S.D.) time (unit: min) to plan the liver surgery using liver segments was1.1 (0.2). The average (S.D.) number of mouse clicks was 6 (1). The average (S.D.) of keystrokes was 0 (0). The average (S.D.) of the assessments of the liver surgery planning using liver segments module was 6.1 (0.5).

The average (S.D.) time (unit: min) to plan the liver surgery using resection sphere was 1.6 (0.2). The average (S.D.) number of mouse clicks was 12 (3). The average (S.D.) of keystrokes was 5 (2). The average (S.D.) of the assessments of the liver surgery planning using resection sphere module was 6.4 (0.7).

Chapter 7. DISCUSSION

7.1. Use Scenario and User Interface Development

This study developed *Dr. Liver*, a user-centered virtual liver surgery system, to support liver surgery. Use scenarios, user interfaces, and image processing algorithms customized to liver surgery planning were developed and implemented in the study to provide good usability and accurate information for preoperative liver surgery planning within an acceptable time for surgeons.

The use scenarios are user-centered and clinically practical, developed based on interviews with surgeons, benchmarking of existing systems, literature survey, and questionnaires. Unlike other systems such as Osrix, LiverAnalyzer, Synapse Vincent, and Mint Liver, the use scenarios of *Dr. Liver* are hierarchical and sequential, consisting of high level tasks including liver extraction, vessel extraction, tumor extraction, liver segmentation, and liver surgery planning and low level tasks to accomplish the high level tasks. Accordingly, hierarchical, sequential, and intuitive user interfaces were designed to facilitate the fulfillment of various tasks for liver surgery planning with various user-friendly features such as procedure status indication and color coding, 3D view indication box and resetting buttons for easier 3D object manipulation, and hotkey menus on the screen to decrease users' cognitive workload. The entire processing time of *Dr. Liver* (20 ~ 30 min) for liver surgery planning is significantly less than those of other systems such as OsiriX (> 2 hours) and Synapse Vincent (> 1 hour).

Various advanced image processing algorithms and procedures were developed and applied to *Dr. Liver* for better usability by minimizing user interaction time and providing easier user interaction interfaces. For example, an efficient interactive vessel extraction procedure was developed, consisting of (1) automatic masking of CT images with the extracted liver region, (2) interactive selection of multiple seed points by mouse clicking, (3) automatic identification of multiple threshold intervals, (4) automatic vessel segmentation with identified threshold intervals using region growing method, (5) automatic display of multiple segmentation results and interactive selection of an appropriate segmentation result, and (6) interactive editing of the extracted vessel trees. An interface was designed to display multiple segmentation results for users to verify the results and select an appropriate result using checkboxes. The average time to extract the portal vein by *Dr. Liver* (1.4 min) was significantly less than that of Synapse Vincent (10 min due to manual editing).

The clinical usability testing of *Dr. Liver* has been undergoing and updates have been made to *Dr. Liver*. Surgeons with a specialty of liver surgery from various medical centers in South Korea have tried *Dr. Liver* and provided suggestions for better usability and clinical applicability.

7.2. Hybrid Semi-Automatic Liver Segmentation Method

The proposed hybrid semi-automatic method sequentially incorporates a fast-marching level-set method and a threshold-based level-set method to achieve better accuracy and time efficiency in liver extraction. Extraction of the liver using the fast-marching level-set method alone would be time efficient but significantly sacrifice accuracy. In contrast, extraction of the liver using the threshold-based level-set method alone would produce accurate results (SI = 96.2%) but take a long time (more than 30 min) with the same seed points as used for the fast-marching level-set method. Through optimal incorporation of the fast-marching level-set method and the threshold-based level-set method, the proposed hybrid method in this study was found segmenting the liver from CT data with high accuracy (SI = 97.6%) as well as time efficiency (77 sec/ CT dataset). The fast-marching level-set method customized in this study was able to generate an optimal initial liver region which is quite close to the true liver boundary in less than 10 sec for a CT dataset with a thickness of 1 mm from multiple seed points selected by the user. The threshold-based level-set method propagated the initial liver region to reach the liver boundary for better accuracy in less than 40 sec.

The proposed novel hybrid semi-automatic method in this study showed high accuracy and time efficiency in liver extraction. The extraction accuracy of the hybrid method was improved by 3.6% for SI, 3.1% for FPE, 4.0% for FNE, and 5.3 mm for ASD compared with the 2D region growing method. The total liver extraction time of the hybrid method was seven times faster than the 2D region growing method. The user interaction time of the hybrid method during liver extraction for a CT dataset was 28 sec on average, which was 17 times shorter than the 2D region growing method (8 min/CT dataset).

The hybrid semi-automatic method overcomes the weaknesses of the 2D region growing method in terms of accuracy and user interaction time. The liver extraction results of the 2D region growing method are determined based on the threshold interval of intensity. In the 2D region growing method, if the intensity value of a pixel is in the threshold interval, then the pixel will be added to the extraction result no matter whether the pixel belongs to the liver or not. At an ambiguous boundary of the liver where an intensity overlap between the liver and its neighboring tissues and organs exists, a false extraction of the neighboring tissues and organs easily occurs in the 2D region growing method. In contrast, the hybrid method magnifies the difference between the liver and its neighboring tissues and organs at an ambiguous boundary and therefore prevents a false extraction to achieve high segmentation accuracy. Furthermore, the 2D region growing method requires a continual user interaction for selection of seed points and segmentation of the liver slice by slice, while the hybrid method only requires a short user interaction period (less than 30 sec) for selection of multiple seed points from 4 to 5 slices.

The hybrid semi-automatic method was found superior (onsite competition score: 78.9) to most of semi-automatic methods at the onsite competition SLIVER07 of MICCAI 2007 workshop. The score of the hybrid method can be improved if large branches of the portal vein are included into our segmentation results. In general, the hybrid method is a competitive semi-automatic liver segmentation method since it takes about 1 min on average to process one case, while others required about 10 ~ 60 min (Heimann et al., 2009).

The proposed hybrid semi-automatic method for liver segmentation is also applicable to tumor extraction in the liver since the intensities of a tumor region are quite different from its neighboring liver region. The hybrid semi-automatic method can be implemented in a preoperative virtual liver surgery planning system to assist a surgeon to make an optimal treatment plan for a patient. An interactive editing function will be useful for surgeons to improve the extracted liver contours if necessary. CT images of a patient are overlaid with the extracted liver mask and the user can interactively remove a non-liver part or add a missing liver part while visually verifying the segmentation result.

7.3. Interactive Vessel Segmentation Method

The interactive vessel segmentation method showed high accuracy and time efficiency in liver vessel extraction and high suitability for liver surgery planning. In all 15 cases, no false positive errors were found in the extracted vessel branches. False negative errors were identified at some distal branches of the vessel trees due to small diameter and low contrast. No connections among the extracted portal vein, hepatic vein, and hepatic artery were found in the 15 segmented datasets. The interaction time and total vessel extraction time were 33 (± 4) sec and 75 (± 8) sec respectively. The average (± S.D.) score of suitability for liver surgery planning was 6.4 (± 0.7).

The interactive vessel segmentation method overcomes the weaknesses of a traditional region growing method in terms of time efficiency and usability. In the traditional region growing method, users need to manually define thresholds without knowing any information about the intensity distribution of the vessel region to be extracted. To find appropriate thresholds in the traditional region growing method, users need to repeat vessel extraction procedure many times which requires a lot of user interaction and therefore time demanding and frustrating for users. In contrast, the proposed method in this study automatically identifies multiple thresholds based on average value and standard deviation of the randomly sampled multiple seed points. Multiple segmentation results from the multiple thresholds were provided to users for selection of an appropriate result using checkboxes. Therefore no repetition of vessel extraction procedure is needed and user interaction is little required in the proposed interactive vessel extraction method.

The proposed interactive vessel extraction method is intended to extract liver vessels in order to facilitate liver surgery planning. The proposed method has been proved to be highly suitable for liver surgery planning by an expert radiologist. The proposed method is also generally applicable to segmentation of other vessels such as lung vasculature and airway trees.

7.4. Virtual Liver Surgery Planning System Usability Evaluation

During the preliminary usability test conducted at an early system development stage, potential usability problems of *Dr. Liver* were identified and solved. The main usability test verified the improvement of the usability of *Dr. Liver*. The usability of *Dr. Liver* was evaluated using a comprehensive set of performance (completion time, similarity index, false positive error, false negative error, number of mouse clicks, and number of keystrokes) and preference (usefulness, ease of use, learnability, informativeness, clarity, tolerance, and overall satisfaction) measures. The usability testing is an analytical and comprehensive way to identify usability problems of *Dr. Liver* and develop recommendations for improving usability of *Dr. Liver* in a systematic manner.

This study demonstrated the application of usability testing as an effective tool throughout the development process of a liver surgery planning system *Dr. Liver*. By applying concepts and techniques of usability testing, the liver surgery planning system *Dr. Liver* with various user-friendly features was developed, problems of the system were screened, recommendations on the system for usability improvement were produced, and verification of the usability improvement was accomplished in an effective, systematic manner. The improvement of usability would contribute to a greater overall consumer satisfaction with *Dr. Liver*.

7.5. Applications

The developed 3D liver surgery planning system, called *Dr. Liver*, is applicable to preoperative liver surgery planning for a safe and rational liver surgery. By providing not only visual information of the location and size of a tumor(s), the structures of the liver vasculatures, the liver segments, the shape, location, and orientation of the resection surface, but also quantitative information of the volumes of the liver, tumor(s), liver segments, the graft, and the remnant, *Dr. Liver* supports surgeons to make an optimal preoperative liver surgery plan. Furthermore, as part of our future work, *Dr. Liver* will be applied to intraoperative navigation of open liver surgery.

Chapter 8. CONCLUSION

The main objectives of this study were development and evaluation of a 3D liver surgery planning system, *Dr. Liver*. First, Use scenarios, user interfaces, and image processing algorithms customized to liver surgery planning were developed and implemented in the study to provide good usability and accurate information for preoperative liver surgery planning within an acceptable time for surgeons. The use scenarios are user-centered and clinically practical, developed based on interviews with surgeons, benchmarking of existing systems, literature survey, and questionnaires. The use scenarios of *Dr. Liver* are hierarchical and sequential, consisting of high level tasks including liver extraction, vessel extraction, tumor extraction, liver segmentation, and liver surgery planning and low level tasks to accomplish the high level tasks. Accordingly, hierarchical, sequential, and intuitive user interfaces were designed to facilitate the fulfillment of various tasks for liver surgery planning with various user-friendly features such as procedure status indication and color coding, 3D view indication box and resetting buttons for easier 3D object manipulation, and hotkey menus on the screen to decrease users' cognitive workload. The entire processing time of *Dr. Liver* for liver surgery planning takes 20 to 30 min.

Second, a hybrid semi-automatic method was developed and evaluated for liver extraction from abdominal CT images. The hybrid semi-automatic liver segmentation method consists of (1) denoising of CT images, (2) selection of multiple seed points, (3) formation of an initial liver region with a customized fast-marching level-set method, (4) extraction of the liver based on the initial liver region with a threshold-based level-set method, and (5) smoothing of the extracted liver region. The hybrid method showed high accuracy and time efficiency in liver extraction and was found superior (onsite competition score: 78.9) to most of the semi-automatic methods at the onsite competition SLIVER07 of MICCAI 2007 workshop.

Third, an interactive procedure for efficient liver vessel extraction was developed and evaluated. The interactive vessel extraction method consists of (1) pre-processing of CT images in which multiple phases of abdominal CT images are denoised, registered, and masked with the extracted liver region, (2) selection of multiple seed points, (3) identification of multiple threshold intervals based on the intensity values of the selected seed points, (4) vessel segmentation with identified threshold intervals using region growing method, (5) display of multiple segmentation results for the user to select an appropriate segmentation result, and (6) interactive editing of the extracted vessel trees if necessary. The interactive method showed high efficiency and accuracy in liver vessel segmentation and was found suitable for clinical application such as liver surgery planning.

Lastly, the usability of *Dr. Liver* was systematically evaluated through usability testing consisting of a preliminary test and a main test conducted different system development stages. The usability of *Dr. Liver* was evaluated by using a comprehensive set of performance (completion time, similarity index, false positive error, false negative error, number of mouse clicks, and number of keystrokes) and preference (usefulness, ease of use, learnability, informativeness, clarity, tolerance, and overall satisfaction) measures. By applying concepts and techniques of usability testing, usability problems of the system were screened, recommendations on the system for usability improvement were produced, and verification of the usability improvement was accomplished in an effective, systematic manner.

The developed 3D liver surgery planning system *Dr. Liver* is applicable to preoperative liver surgery planning. *Dr. Liver* can provide not only visual information of the location and size of a tumor(s), the structures of the liver vasculatures, the liver segments, the shape, location, and orientation of the resection surface, but also quantitative information of the volumes of the liver, tumor(s), liver segments, the graft, and the remnant to support a safe and rational surgery. Furthermore, as part of our future work, *Dr. Liver* will be applicable to intraoperative navigation of open liver surgery.

REFERENCES

Abras, C., Maloney-Krichmar, D., Preece, J. (2005). User-center design. In the *Berkshire Encyclopedia of Human-Computer Interaction: When Science Fiction Becomes Science Fact* (pp. 763-768).

Bauer, C., Pock, T., Sorantin, E., et al. (2010). Segmentation of interwoven 3d tubular tree structures utilizing shape priors and graph cuts. Medical Image Analysis, 14(2010), 172-184.

Cabezas, M. et al. (2011). A review of atlas-based segmentation for magnetic resonance brain images. *Computer Methods and Programs in Biomedicine 104*(2011), e158-e177. doi: 10.1016/j.cmpb.2011.07.015

Cotran, R. S., Kumar, V., Fausto, N., Nelso, F., Robbins, S. L., Abbas, A. K. (2005). *Robbins and Cotran pathologic basis of disease* (7th ed.). St. Louis, MO: Elsevier Saunders.

Couinaud, C. (1957). *Le foie: Etudes anatomiques et chirurgicales*. Masson, Paris, France.

Dawant, B. M., Li, R., Lennon, B., Li, S. (2007). Semi-automatic segmentation of the liver and its evaluation on the MICCAI 2007 grand challenge data set. Paper presented at *the 3D Segmentation in The Clinic: A Grand Challenge*.

Debarba, H. G., Zanchet, D. J., Fracaro, D., Maciel, A., & Kalil, A. N. (2010). Efficient liver surgery planning in 3D based on functional segment classification and volumetric information. In *Proceedings of 2010 Annual International Conference of the IEEE Engineering in Medicine and Biology Society* (pp. 4797-4800). New York, NY, IEEE Engineering in Medicine and Biology Society.

Deriche, R. (1990). Fast algorithms for low level vision. *IEEE Transactions on Pattern Analysis and Machine Intelligence*, *12*(1), 78–87.

Deriche, R. (1993). Recursively implementing the gaussian and its derivatives. Technical Report 1893, Unite de recherche INRIA Sophia-Antipolis. Research Repport.

Dumas, J., and Redish, G. (1993). *A practical guide to usability testing* (1st ed.). Mahwah, NJ: Ablex Publications.

Eidheim, O. C., Aurdal, L., Jensen, T. O. et al. (2004). Segmentation of liver vessels as seen in MR and CT images. *Int. J. Comput. Assisted Radiol. Surg., 1268*, 201-206.

Esneault, S., Lafon, C., Dillenseger, J. L. (2010). Liver vessels segmentation using a hybrid geometrical moments/graph cuts method. *IEEE Transactions on Biomedical Engineering, 57*(2), 276-283.

Ferrero, A., Vigano, L., Polastri, R., Muratore, A., Eminefendic, H., Regge, D., Capussotti, L. (2007). Postoperative liver dysfunction and future remnant liver: where is the limit? Results of a prospective study. *World J Surg*, 31(8), 1643-1651.

Ghose, S. et al. (2012). A survey of prostate segmentation methodologies in ultrasound, magnetic resonance and computed tomography images. *Computer Methods and Programs in Biomedicine 108*(2012), 262-287. doi: 10.1016/j.cmpb.2012.04.006

Heimann, T. et al. (2009) Comparison and evaluation of methods for liver segmentation from CT datasets. *IEEE Transactions on Medical Imaging, 28*(8): 1251-1265.

Heinemann, A., Wischhusen, F., Püschel, K., Rogiers, X. (1999). Standard liver volume in the Caucasian population. *Liver Transplantation*, 5(5), 366-368. doi: 10.1002/lt.500050516

Hermoye, L., Laamari-Azjal, I., Cao, Z., Annet, L., Lerut, J., Dawant, B. M., Beers, B. E. V. (2005). Liver segmentation in living liver transplant donors: Comparison of semiautomatic and manual methods. *Radiology*, 234, 171-178. doi: 10.1148/radiol.2341031801

Hsu, C. Y., Yang, C. H., Wang, H. C. (2010). Multi-Threshold Level Set Model for Image Segmentation. *Journal on Advances in Signal Processing*, 2010. doi: 10.1155/2010/950438

Huang, Z.-P. et al. (2011). The segmentation of liver and vessels in CT images using 3D hierarchical seeded region growing. Paper presented at the *IEEE International Conference on Computer Science and Automation Engineering*, 2, 264-269.

Ibáñez, L. et al. (2005). *The ITK software guide*. 2nd ed. Kitware Inc.

Jiang, H., & Cheng, Q. (2009). Automatic 3D segmentation of CT images based on active contour models. Paper presented at the *11th IEEE International Conference on Computer-Aided Design and Computer Graphics*, Huangshan.

Klein, A., Andersson, J., Ardekani, B. A., Ashburner, J., Avants, B., Chiang, M. C., . . . Parsey, R. V. (2009). Evaluation of 14 nonlinear deformation algorithms applied to human brain MRI registration. *Neuroimage*, 46(3), 786-802.

Li, C. et al. (2012). Automated PET-guided liver segmentation from low-contrast CT volumes using probabilistic atlas, *Computer Methods and Programs in Biomedicine 107*(2012), 164-174. doi: 10.1016/j.cmpb.2011.07.005

Lee, J., Kim, N., Lee, H., Seo, J. B., Won, H. J., Shin, Y. M., . . . Kim, S.-H. (2007). Efficient liver segmentation using a level-set method with optimal detection of the initial liver boundary from level-set speed images. *Computer Methods and Programs in Biomedicine*, 88, 26-38. doi: 10.1016/j.cmpb.2007.07.005

Lefohn, A. E., Cates, J. E., Whitaker, R. T. (2003). Interactive, GPU-Based Level Sets for 3D Segmentation. Paper presented at the *Medical Image Computing and Computer Assisted Intervention*.

Malladi, R. et al. (1995). Shape modeling with front propagation: a level set approach. *IEEE Transactions on Pattern Analysis and Machine Intelligence 17*(1995), 158-175.

Massoptier, L., Casciaro, S. (2008). A new fully automatic and robust algorithm for fast seg mentation of liver tissue and tumors from CT scans. *European Radiology*, 18, 1658-16 65. doi: 10.1007/s00330-008-0924-y.

Meinzer, H. P., Thorn, M., and Carlos, E. (2002). Computerized planning of liver surgery-an overview. *Computers & Graphics, 26*(4), 569-576.

Muramatsu, C. et al. (2011). Automated segmentation of optic disc region on retinal fundus photographs: Comparison of contour modeling and pixel classification methods. *Computer Methods and Programs in Biomedicine 101*(2011), 23-32. doi: 10.1016/j.cmpb.2010.04.006

Nodes, T. A., Gallagher, N. C. (1982). Median filters: Some modifications and their properties. Paper presented at the *IEEE Transactions on Acoustics, Speech and Signal Processing*.

Norman, D. (1988). *The design of everyday things*. New York: Doubleday.

Nielsen, J. (1993). *Usability Engineering*. San Francisco: Morgan Kaufmann.

Nielsen, J. (2001) *Ten Usability Heuristics*, www.useit.com/papers/heuristic.

Osher, S. and Sethian, J. A. (1988). Fronts propagating with curvature-dependent speed: algorithms based on Hamilton-Jacobi formulations. *Journal of Computational Physics 79*(1988), 12-49.

Pan, S., Dawant, B. M. (2001). Automatic 3D segmentation of the liver from abdominal CT images: a level-set approach. *Proceedings of SPIE Medical Imaging: Image Processing* 4322, 128-138.

Perona, P., Malik, J. (1990). Scale-space and edge detection using anisotropic diffusion. Paper presented at the *IEEE Transactions on Pattern Analysis and Machine Intelligence*.

Preece, J., Rogers, Y., & Sharp, H. (2002). *Interaction design: Beyond human-computer interaction*. New York, NY: John Wiley & Sons.Redish 1993.

Radtke, A., Nadalin, S., Sotiropoulos, G. C. et al. (2007) Computer-assisted operative planning in adult living donor liver transplantation: a new way to resolve the dilemma of the middle hepatic vein. *World Journal of Surgery, 31*(1), 175-185.

Reitinger, B., Bornik, A., Beichel, R., & Schmalstieg, D. (2006). Liver surgery planning using virtual reality. *IEEE Computer Graphics and Applications, 26*(6), 36-47.

Ruskó, L., Bekes, G., Németh, G., Fidrich, M. (2007). Fully automatic liver segmentation for contrast-enhanced CT images. Paper presented at the *3D Segmentation in The Clinic: A Grand Challenge*.

Satou, S., Sugawara, S., Tamura, S. et al. (2007) Three dimensional computed tomography for planning donor hepatectomy. *Transplantation Proceedings, 39*(1), 145-149.

Schindl, M. J., Redhead, D. N., Fearon, K. C. H., Garden, O. J., Wigmore, S. J. (2005). The value of residual liver volume as a predictor of hepatic dysfunction and infection after major liver resection. *Gut*, 54(2), 289-296. doi: 10.1136/gut.2004.046524

Selle, D., Preim, B., and Peitgen, H. (2002). Analysis of vasculature for liver surgical planning. *IEEE Transactions on Medical Imaging, 21*(11), 1344-1357.

Sethian, J. A. (1996). A fast marching level set method for monotonically advancing fronts. Paper presented at the the *National Academy of Sciences*, USA.

Shang, Q., Clements, L., Galloway, R. L., et al. (2008). Adaptive directional region growing segmentation of the hepatic vasculature. Paper presented at *Medical Imaging 2008: Image Processing*, 6914.

Shneiderman, B. (1998). *Designing the user interface: Strategies for effective human-computer interaction* (3rd ed.). Reading, MA: Addison-Wesley.

Soler, L., Delingette, H., Malandain, G. et al. (2001). Fully automatic anatomical, pathological, and functional segmentation from CT scans for hepatic surgery. *Computer Aided Surgery 6*(3), 131-142.

Sorantin, E., Werkgartner, G., Beichel, R., Bornik, A., Reitinger, B., Popovic, N. & Sonka, M. (2008). Virtual Liver Surgery Planning. In E. Neri, D. Caramella, & C. Bartolozzi (Eds.), *Image processing in radiology – current applications* (pp. 411-418), Berlin: Springer Verlag.

Thirion, J. P. (1995). Fast non-rigid matching of 3D medical image. Technical report, Research Report RR-2547, Epidure Project, INRIA Sophia, May 1995.

Thirion, J.-P. (1998). Image matching as a diffusion process: an analogy with maxwell's demons. *Medical Image Analysis, 2*(3), 243-260.

Urata, K., Kawasaki, S., Matsunami, H., Hashikura, Y., Ikegami, T., Ishizone, S., . . . Makuu chi, M. (1995). Calculation of child and adult standard liver volume for liver transpla ntation. *Hepatology,* 21(5), 1317-1321.

Yi, J., Ra, J. B. (2003). A locally adaptive region growing algorithm for vascular segmentation. *International Journal of Imaging Systems and Technology, 13*(4), 208-214.

Yu, H. C., You, H., Lee, H., Jin, Z. W., Moon, J. I., Cho, B. H. (2004). Estimation of standard liver volume for liver transplantation in the Korean population. *Liver Transplantation*, 10(6), 779-783.

Zijdenbos, A. P., Dawant, B. M., Margolin, R. A., Palmer, A. C. (1994). Morphometric analysis of white matter lesions in MR images: method and validation. *IEEE Trans. Med. Imag*, *13*(4), 716-724.

Zohios, C. et al. (2012). Geometrical methods for level set based abdominal aortic aneurysm thrombus and outer wall 2D image segmentation. *Computer Methods and Programs in Biomedicine 107*(2012), 202-217. doi: 10.1016/j.cmpb.2011.06.009